Master Thesis

NTNU
Norwegian University of Science and Technology
Fakulty of Engineering Science and Technology
Department of Hydraulic and Environmental Engineering

Aravind Kumar Agrawal

Numerical Modelling of Sediment Flow in Tala Desilting Chamber

Trondheim June 2005

D1-2005-12

NTNU

FOREWORD

This thesis titled 'Numerical Modelling of Sediment Flow in Tala Desilting Chamber is submitted to the Department of Hydraulic and Environmental Engineering, NTNU, Trondheim, Norway in partial fullfillment of the required of the Master of science (M.Sc.) degree in Hydropower Development(HPD).

The data required & report of physical model study of Tala desilting basin is made available by CWC. The study has been carried out at NTNU, Trondheim, Norway and has been financed by NORAD.

The undesigned hereby declare that the work presented in this report is my own and any significant outside input have been duly acknowledged

Aravind Kumar Agrawal
Trondheim, Norway
June 2005

ACKNOWLEDGEMENT

I would like to thank all the individuals and organisations who have helped or provided the guidance during the course of study. Among the organisations, firstly I would like to thanks the Norwegian agency for Development and Co-operation (NORAD) who provided the opportunity to study at Norges Tekniss-Naturvitenskaplige Universitet(NTNU) under NORAD Fellowship program. I am also thankful to Central Water commission for all efforts from granting the study leave to providing all reports and drawings required for this thesis work.

I don't have words to express my thanks to Professor Nils Reider B. Olsen, in fact no words can express his generosity. He is the generator of this SSIIM programme, which has been used for this study. All through this work he has provided his guidance and help. A lot of time he has spend to reply all of my question, advice, counselling. From the inception as and whenever required, he was always ready to appease my queries. In quite simple way he made the understanding of this model easier.

Also I would like to special thanks to Dr. D.V. Thareja, Chief engineer, Central Water Commission, who encouraged and made available drawings and reports needed for it. I would also thank Director I.K.Chugh, HCD(E&NE) Dte. for make available the drawing in quite short duration of time of one or two day. Help offered to make my study possible at NTNU, by senior officers like Mr. M.E. Haque, Mr. M. S. Agrawal, V.K.Talwar is unforgettable.

Dr. Haakon, stole, with his experience and knowledge also facilitated. Mrs. Hilbjørg Sandvik, who is always eager to provide assistance in no times made study quite easy and comfortable and helped to finish the thesis work in time. I also express my gratitude to Nils. R. Ruther, who guided some times.

I am also thankful to all officers, seniors, colleges and friends who helped one or another way to make possible this study. Due to space constraint its not possible to name all.

Last but not least I would extend my word of thanks to my family, who helped me during all this duration of my study.

Aravind Kumar Agrawal

Aravind K Agrawal

Executive Summary

This thesis is about estimation of trap efficiency of desilting basin using numerical model program named as SSIIM. SSIIM is acronym for Sediment Simulation in Intakes with Multiblock Option. It is developed by Dr. Nils Reider B. Olsen, Professor at NTNU, Norway and complete software is freely available over net with user manual. The program is a stepping stone in the field of Computational Fluid Dynamics (CFD).

Study is based on desilting basin of Tala Hydropower Project (6X170 MW), an Indo Bhutan Joint venture. A physical model study of the same was done in Central Water Power Research Station (CWPRS), Pune, India,. Here this physical model and prototype both has been simulated, but with more emphasis over first one.

Three dimensional flow and sediment calculation is evaluated over three dimensional grid using Power Law Scheme (POW) with no heeding towards Second order upwind scheme (SOU).

The results are analysed, compared with physical model study and discussed. All the input data i.e. grid co-ordinates and different parameters used are appended in two files named koordina and control, using these program can be run. Number of different options were tried, but only few important has been discussed. Simulation result is found in harmony with physical model result. As real time data of sediment was not available for prototype, a relationship curve between particle size in prototype and model, as per CWPRS report, is used to get input sediment particle size for prototype.

THE NORWEGIAN UNIVERSITY OF SCIENCE AND TECHNOLOGY
DEPARTMENT OF HYDRAULIC AND ENVIRONMENTAL ENGINEERING

M Sc THESIS
in
HYDROPOWER DEVELOPMENT

Candidate: **Aravind Kumar Agrawal**

Theme: **Numerical modelling of sediment flow in Tala desilting chamber**

1. Background

Sediment transport in hydropower intakes can cause several problems. The sediments may deposit in the intake structures and channel, causing clogging and energy loss. If the sediments reach the turbines, expensive wear may result. It is important to design the intake so that the sediment problem will be minimized.

A prototype intake will usually have a complex flow field. It is then useful to the intake design process to be able to predict the flow field, and the corresponding sediment concentration. An important parameter is how much of the sediments enter the intake, and how much deposits and is taken over the spillway. This assessment can be done by physical model studies. However, such studies have problems modelling the finer sediments. The alternative is to use a CFD program. Such a program is currently being developed. One of the purposes of the present study is to test this model and assess its accuracy and reliability.

The test case for the present study is the Tala desilting basins in Bhutan. Data from this intake are available for the present study. This includes geometrical data, water flow data and sediment data. Suspended sediments has been measured in a physical model study, so this can be compared with the predictions of the CFD program.

2. Main questions for the thesis:

The thesis shall cover, but not necessarily be limited to the following main questions:

- Generation of a grid for the reservoir
- Generation of input files for the CFD model
- Computing the water flow field using the SSIIM CFD model
- Computing the sediment concentration
- Comparison of the resulting concentrations with the measurements
- Assessment of the uncertainties in the input data by a parameter sensitivity analysis
- Assessment of uncertainties in the CFD model by varying algorithms, coefficients and other input data

The thesis shall present figures of the grid, velocity vectors, concentration contour maps and tables of measured versus computed concentrations at the intake. This should be done for the different variations in input parameters and algorithms.

The conclusion shall contain the candidate's opinion on the applicability of the CFD model for assessing sedimentation problems in reservoir. It should also point to uncertainties in the model, effects of inaccurate input data and give recommendations for future work using CFD for sedimentation studies. Possible improvements in the CFD model should also be given.

All figures should conform to the note *Generation of scientific figures for CFD publications*

3. Supervision, data and information input, reporting

Prof. Nils Reidar Olsen will supervise the thesis work and make relevant information available. Discussions with colleagues and other research staff at NTNU is recommended. Significant inputs from others shall be referenced in the text or in some other convenient manner.

Professional structuring of the thesis report is important. Assume professional senior engineers as the main target group.

The report shall include a summary, giving the background of the study, together with the objectives and the main results.

4. Format and reference statements

The thesis report shall be in format A 4. It shall be typed using a word processing system on a computer.

All figures should conform to the note *Generation of scientific figures for CFD publications*

Table of content, list of figures and tables and a list of references shall be included.

The candidate is requested to include a signed statement that the work presented is his own and that significant outside input has been identified.

The thesis shall be submitted no later than **Friday 10th of June 2005**.

Department of Hydraulic and Environmental Engineering, NTNU

Nils Reidar Olsen

Nils Reidar B. Olsen
Professor

Generation of scientific figures for CFD publications

CFD results contain large amounts of numbers, presenting the classical problem for presentation. The purpose of this document is to give advice for students making figures for CFD projects, to use in papers or a thesis.

1. Types of figures

CFD programs often contains modules for presenting three-dimensional figures. These are usually difficult to understand when printed in black and white in a paper or a thesis. The three-dimensional figures are more suited for web pages and oral presentations than on paper. The figures used in a thesis or in a paper are usually a two-dimensional sections of the three-dimensional geometry. Plan views, longitudinal profiles or a cross-sections can be shown.

The most commonly used figures for a thesis are:

- Map or plan of layout of the geometry
- The grid (usually seen from above)
- Velocity vector plots
- Contour plot
- Profiles

The purpose of a scientific CFD study is usually to test how the model compares with measurements from the field or from a hydraulic laboratory. The comparison can be given in three different types of figures:

Velocity vectors

The computed and measured velocity vectors are plotted in the same figure. To distinguish between measured and computed values, the vectors are usually different. Thicker lines can be used for the measured values, or dashed/dotted lines.

Profiles

Measurements in a water body are often done in vertical profiles at several locations. The measurements can be velocities, turbulence, sediment concentrations etc. The figures usually show more than one vertical profile. The computed values are shown with lines, and the measurements with markers, for example crosses.

Contour plots

Comparisons of measured and computed values using contour plots can be done in two ways:

1. The contour lines of measured values are drawn with a different line type than the calculated results in the same figure. For example, stippled and full lines can be used.

2. Two contour plot figures can be presented beside each other, where one shows the measured values and the other shows the computed values.

2. Drawing lines

The lines in a figure should have a size similar to the line thickness of the text. If the lines are too thin, they may disappear when copied. If the lines are too thick, details of the figures may disappear.

3. Text and numbers

Text in the figures should normally be avoided. Instead, letters should be given in the figure, and the text should be given in the legend with reference to the letters.

The font should be similar to the font used in the text, or a commonly used font, for example Times or Helvetica. The font and its size should be the same for all letters, text and numbers in the figure. One should try to use as large font as possible, and then reduce the size of the figure afterwards, by copying it with size reduction.

4. Scales

The figures should contain scales, so it is possible to see the magnitude of the geometry and the variables. A line with a number in meters should be given. When the figure is seen from above, it should be non-distorted. A cross-section or a longitudinal profile can be shown a distorted. Then the scale in both the vertical and horizontal direction should be given.

If velocity vectors are given, the size should be given on one vector placed outside the geometry.

If contour plots are presented, numbers on the lines should be given. The units should be given in the legend.

5. Legends

Each figure should have a legend. It should contain the figure number and should describe two pieces of information:

- What the figure shows. This should be possible to understand without reading the text of the paper.

- Particular information about the figure. For example input parameter combinations.

Example:

Figure 4. Velocity vectors close to the water surface in Garita Hydropower Reservoir, using the SOU scheme.

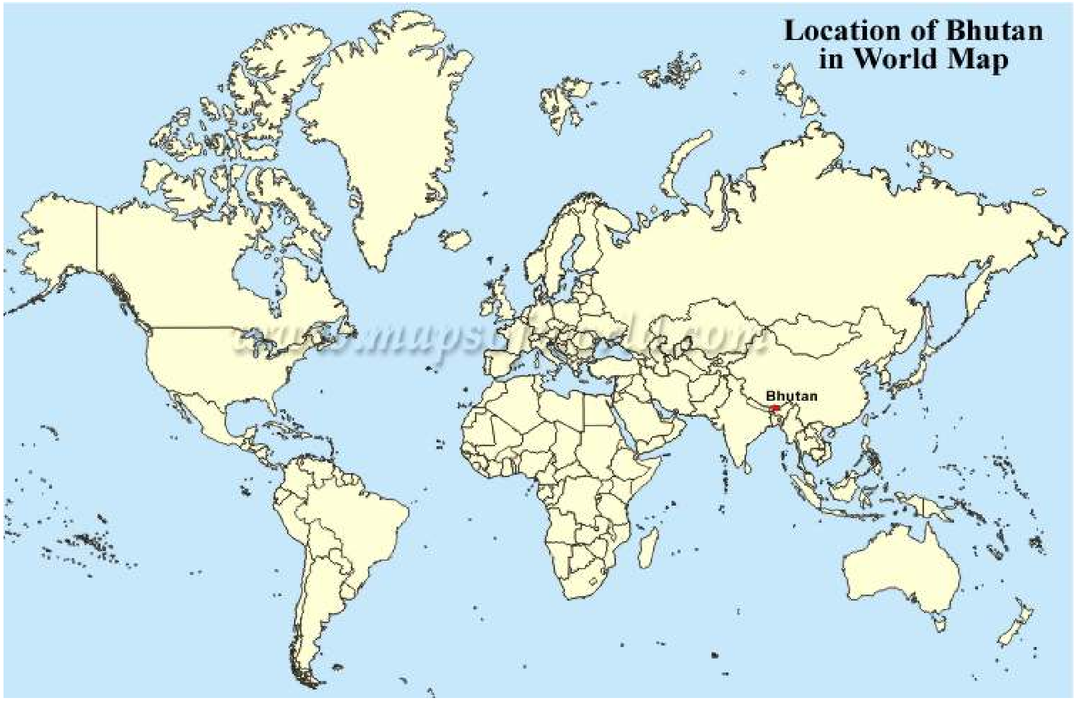

Location of Bhutan on world Map
(Ref: http://www.mapsofworld.com)

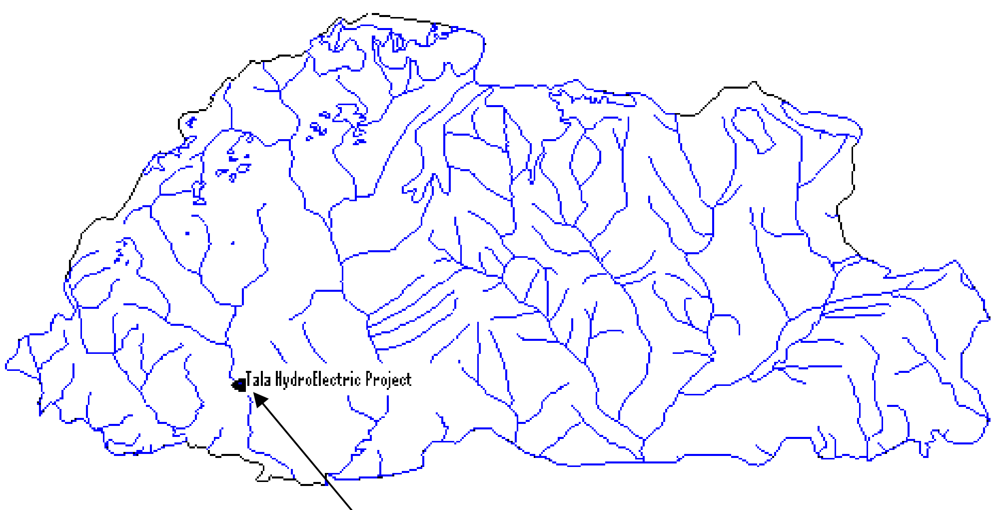

Location of Tala Hydro Electric Project in Bhutan

Table of Content

Annexure

Table

List of Figures

List of Table

LIST OF ABBREVIATIONS

CFD	Computational Fluid Dynamics
CWC	Central Water Commission, Government of India
CWPRS	Central Water and Power Research Station, Pune India
FRL	Full reservoir Level
HRT	Head Race Tunnel
MDDL	Minimum Drawdown Level
NORAD	Norwegian Agency for Development Cooperation
NTNU	Norwegian University of Science and Technology, Trondheim
PMF	Probable Maximum Flood
POW	Power Law Scheme
SPF	Standard Projection Flood
SOU	Second Order Upwind Scheme
SSIIM	Sediment Simulation in Intakes with Multiblock option
THEP	Tala Hydro Electric Project
TRT	Tail Race Tunnel
TSC	Transient Sediment Computation

LIST OF SYMBOLS

A	Area of Coss-section
i,j,k	indices
El	Elevation
g	acceleration due to gravity
hr	hour
kg	kilogram
m	metre
Nu	Ngultrum
ppm	parts per million
Rs.	Indian Currency Rupees
US$	United state currency dollar
x,y,z	Coordiantes
ϕ	Diameter
Γ	Diffusion coefficient
μ	Dynamic viscocity of water
τ	Shear stress at bed
τ_c	Critical shear stress
ν_T	Turbulent eddy viscocity
ρ_w	Specific density of water
ρ_s	Specific density of sediments
k_s	Bed roughness parameter
k	constant in wall function
ε	Dissipation rate of turbulent kinetic energy

REFERENCES

1. Techincal Report No. 3804, july 2001, Hydraluic Model studies for desilting basin, Tala Hydro electric Project, Bhutan(Report No.2), Central Water and Power Research Station, Pune
2. Technical Report no. 3827, October 2001, CWPRS
3. Salient Features & Status of Project, March 2004, Water and power consultancy service(India) Ltd., phuentsholing, Bhutan, March 2004,
4. R.S.Vashney,1986, Hydro Power Structures
5. Nils Reidar B. Olsen,2004. Hydroinformatics, Fluvial Hydraulics and Limnology
6. Nils Reidar B. Olsen,2004, User's Manual for SSIIM
7. J. Chandrashekhar, june 2004, Numerical simulation of Sediment movements in desilting basin using ssiim, Nathpa Jhakri Project, India- a case study.
8. Haakon Støle, September 2004, Hand out literature for headworks and sedimentation engineering.
9. Lysne D. K., B. Glover, H. Støle and E. Tesaker, 2003, Hydraulic Design, Hydropoer Development Volume no.8, NTNU.
10. Jain A.K., 1990, Fluid Mechanics
11. http://www.bhutannewsonline.com
12. http://www.bygg.ntnu.no/~nilsol/
13. http://www.sediment.no/
14. http://www.gto.no/

TALA HYDROELECTRIC PROJECT, BHUTAN (6 X 170MW)

SALIENT FEATURES

1. LOCATION

Project Area	Latitude 20^0 to 27.5^0 N
River	Wangchu in western Bhutan
Dam Site	Near Wangkha Village
	(3 km D/s of existing Chukha H.E. projecTail race, 60 km up from Phuntsholing, the gateway to Bhutan)

2. RESERVOIR

Full Reservoir Level	:1363 m
Maximum Reservoir Level	:1363 m
Minimum Draw-Down Level	:1352 m
Total Volume	:9.80 Mill m3
Peaking Volume	:3.20 Mill m3
Storage at MDDL	:6.60 Mill m3
Surface Area at FRL	:0.36 K m2

3. HYDROLOGY

Catchment Area	:4028 Km^2
Average flow at Dam Site	:99 m^3 / sec
Mean Annual Run-off	:3107 Mill m^3
90% dependable year flows	
Minimum 10 daily	:19.5 m^3 / sec
Mean during winter	:23.4 m^3 / sec
Annual mean	:77.6 m^3 / sec
Design Flood	SPF – 8575 m^3 / sec (For Design)
	PMF – 10600 m^3 / sec (For checking)

4. DIVERSION ARRANGEMENT

A. Diversion Tunnel

Location	:Right Bank
Length	:356 m
Design discharged	:6.8 m D-shaped
Design discharge	:350 m^3 / sec

B. U/S coffer dam

Type	:Concrete dam

Length	:94 m
Height	:14 m height

C. D/S Coffer dam

Type	:Rockfill dam
Length	:45 m
Height	:3 m height

5. DAM

Type	:Concrete gravity dam
Top of Dam	:1366m
Average river bed elevation	:1291m
Height above deepest	
Foundation level	:92 m
Length	:128.7 m,(curved), 128.5 m (straight)
Dam axis orientation	N 25^0 E

Spillways:

i) Sluice spillway	
No.	5
Size	1320 m
Crest EL	1320.0m
ii) Overflow Spillway	1360 m
No.	1
Size	4m(W) x 3m (H)
Crest EL	1360.0m
Concreting	320000 m^3
Gross Head	860 m

6. INTAKES

Location & No.	3 Nos. on Right Bank
Type	Staright intake with bell mouth
Maximum Discharge	171 m^3 / sec
Intake C/S Level	El 1343.5
Intake Tunnels	3 Nos. 4.9 m dia modified Horse shoe
Gates	3 Nos. 4m X 4.9 m Vertical lift fixed wheel gate ; 3 Nos. 4m X 4.9 m Vertical lift fixed wheel gate

7. DESILTING ARRANGEMENT

Alignment	S 17.5^oE
Size	3 Nos. 250 m X 13.965 m X 18.5 m (LxWxH)
Particle size to be removed	0.2 mm and above
Gates	3 Nos. 4.2 X 4.9 m. (WxH)
Construction Adit(Common)	36 m. 7 m D- Shaped

SILT Flushing Tunnel

Size	3.2 m X 3.95 m (WxH) D- Shaped
Flushing Discharge	20%
Gates	3 Nos. 2.85 m X 2.1 m vertical lift slide gate

GATE CHAMBER

Adit to Gate Chamber	143 m long 6 m (D – Shaped)

Gate Shaft for Desilting chamber

Size	7.1m X 2.9m (elliptical shaft)
Depth	27 m

Gate Shaft for Desilting chamber

Size	5.8m X 3.960m (elliptical shaft)
Depth	43 m

8. HEAD RACE TUNNEL (HRT)

Length	22.25 kilometre
Dia	6.8m Modified horse shoe
Sectional Area	37.611 m^2
Velocity at design discharge	3.75 m/s
Invert Level at start	1338.074 m
Invert Level at end	1257.2 m
Bed Slope(average)	1 in 280
Design discharge	141.12 m^3/S
Overloading discharge	158.52 m^3/S
Gates at adit junction	1 no., 3.1X 3.4m Flap Gate at Padechu
	1 no., 1.2X 1.5m Flap Gate at Mirchingchu
Construction Adit	5 nos.(Intermediate) and 1 no. at inlet(11 Faces)
Size	7m, D shaped

9. POWER HOUSE COMPLEX - UNDER GROUND

Power House Cavern

Alignment	N 370 W
Size of Main Cavern	240 m X 20.4 m X 44.5 m (LxWxH)

Transformer cavern

Alignment	N 370 W
Size of Main Cavern	191 m X 16 m X 25 m (LxWxH)

Rock pillar between PH/ TH	39.3 m
Installed Capacity	6X 170 MW

10. SURGE TANK

Type	Restricted Orifice
Diameter	15 m (From El. 1425 to 1310m)
	12 m (From El. 1310 to bottom)
Height	181m
Type of lining	RCC
Orific diameter	1.5m

11. PRESSURE SHAFT

No./ type	1 no. 75 / 20T
Diameter	4.0 m
Length	PS I – 1078 m
	PS II –1024 m
Alignment	N28^{0}W

Centre to Centre distance between Pressure Shafts	20m
Inclination with horizontal	52^0
Velocity flow at designed q	5.60 m/s
Maximum Design Pressure (including water hammer)	9.24 MPa

12. TAIL RACE TUNNEL

Length	3.1Km
Size	7.75m, Horse shoe
Slope	1 in 1200
Type of flow	Open channel

13. GENERATION PLANT

Turbine	
Type	Vertical Pelton,
Number	6
Capacity	173.5 MW
No. of jets	5
Design Net Head	820 m
Rated Discharge	24 m3/s
Speed	375 RPM
Gnerator	
Type	Vertical shaft, Synchronous machine
Number	6
Capacity	190 MVA
Voltage	13.8 KV
Transformer	
Type	single phase
Number	18+1(spare)
Capacity	70 MVA
Rated Voltage	13.8 KV/420/ √3 kv
Total Energy Output	3.962 GWh on the basis of 90 percent dependable

14. GENERATION TARIFF — INR 1.60 (US$ 0.036) per unit, as estimated

15. PROJECT COST — The original estimated cost of the project was Us$ 0.3 billion in 1993. The project may cost 0.93 billion (Feb 2005)

16. COMMISSIONING SCHEDULE — Project originally planned to be commissioned in June 2005, will now be commissioned in June 2006

17. BENEFICIARIES — India's Eastern Region Constituents

1 CHAPTER

INTRODUCTION

1.1 INTRODUCTION

From the hydropower point of view, all projects constructed or going to be constructed in Himalayan rivers, have a problem of sedimentation. Although this problem is not only associated with Himalayan river, many regions of the world have a problem of sedimentation. Sediment information for most of the river basins in South Asia is scant and not readily available.

The Himalayan foreland basin formed in response to the uplift of Himalaya after the collision of Indian and Asian plates that were initiated in the Palaeogene. The basin shows all the major components of a foreland system, the Himalaya, deformed foreland basin deposits adjacent to the Siwalik Hills, a depositional basin Ganga Plain and peripheral cratonic bulge Bundelkhand Plateau. The Ganga is the axial river of the basin, and originates in the Himalayan orogen, being joined by a number of major Himalayan tributaries. The mighty Brahmaputra also meets the Ganges and forms a major deltaic depo center in the Bengal basin.

Study of sediment load of any river is an essential aspect not only for assessment of sediment load for a project, it is also important for the evaluation of environmental impacts in any river basin. Monitoring of the quantity as well as the quality of sediment is important especially for the rivers of the Himalayan origin where the climatic and physical conditions are highly conducive to the erosion and sedimentation processes. Large-scale mass wasting processes, such as, landslides, landslide lake (temporary damming of river or stream by landslides) outbursts and glacial lake outburst floods bring further complications in the sedimentation process. It is felt that allocated resources for sediment sampling and analysis are less than it should be. Not only financial there are number of constraints which causes it.

Whenever a project is taken up in consideration, finance part plays an important role. So financial study for construction and as well as for operation and maintenance is done for its life time. And the life of project may be quite dependent on sedimentation. Sediment can have a detrimental effect on the life of the various component of the project. The life of electro mechanical part of the turbines reduces due to impinging of sediment on it. Also the wear and tear of these parts increases with water head applied on turbine. Not only this other parts of the project like screenings, steel liners, gates, penstock and so many other components reduces its life due to sedimentation and require more repairing, maintenance, resulting in financial loss by means of halting power supply for maintenance or other way financial loss.

Its also fact that there its practically impossible to make water sediment free, but we can check it.

1.2 OBJECTIVE

Among all the civil work associated with headworks arrangement desilting basin is one major cost item. The importance in relation to cost for this item increases when desilting basin is made underground. So optimisation of desilting basin become necessary. Usually physical model study is carried out for this, but it have also its own limitations, for example modelling of small particle size. Usually for desilting chambers it is required to remove the particles of size 0.2 mm or more. So it's hard to find the natural material to model it. To solve this problem usually plastic material of density 1050 kg/m^3 is used. This enable to overcome the problem of cohesion and boundary layer, but other problem arises.The exaggerated size of the artificial particles influence the bed roughness and the usually rounded form of plastic particles creates a very unstable bed in the model.

Nevertheless for small projects where funding is less, physical model study may not be feasible due to financial shortage or due to time shortage. In such a case numerical modelling can be idle solution.

The objective here is to use the numerical model for studying the hydraulics of an underground desilting basin. SSIIM, is acronym for Simulation of Sediment Movements in Water Intakes with Multiblock Option. The program is developed by Dr. Nils Reidar Olsen., who is a veteran in this field. He is professor at Norwegian University of science and Technology (NTNU), Trondheim. Earlier a study for Indian project named Nathpa Jhakri was also done using this program. Presently, desilting basin of a ongoing Indo-Bhutan Project, which is its in last stage of construction, has been studied, using this numerical model. There are three desilting chambers in parallel, for one of the desilting chamber this study has been made. The physical model study of desilting baisn to find out the trap efficiency has already carried out by CWPRS, Pune, India.

Here SSIIM model has been used to simulate the physical model. Simulation for prototype has also been done, but not with as many options as for physical model. Basic reason for opting the simulation of physical model not of prototype was the unavailability of grain size distribution curve for sediment of river just near the intake. On getting these data the model can be run for that also, as preliminary work for this has already been done here. Although a attempt has been made to consider the grain size distribution curve for prototype by transferring the grain distribution curve used for physical model, by means of a relation curve provided by CWPRS.

The SSIIM model has immense potential, a part of which has been used here. Various alternatives can be tested and different option can be studied by it within a short time.

1.3 STRUCTURE OF THE REPORT

It's evident that huge demand of electricity can be fulfilled by immense power potential of Himalayan river. India has been able to use only 20% of its hydropower potential. In forthcoming years in Himalayan belt no. of run of rivers will be coming up. So this type of numerical modelling will facilitate the planning and design of the hydro projects.

Chapter 2 has a brief review about the headworks and different types of traditional and innovative methods to get rid of sedimentation problem. Among these new methods few are really marvellous, not only conceptually, also from construction cost point of view.

Chapter 3 states some facts about the project for which this study has been done. Physical model study done by CWPRS is being used as a base.

Chapter 4 illustrate the theory behind the SSIIM. It's not possible to go in further detail due to dearth of space and time. Maximum reference has been made to user manual for SSIIM. Manual in itself is quite explanatory. Its readily available over net. One of the nicety of this program or the generosity of the developer is that this program is freely available over net with manual.

Chapter 5 provides the information the way the program is used herby. It illustrate that how the grid has been developed and water flow calculation has been carried out. In annexure detailed velocity report has been provided. Also velocity profiles and velocity vector with scale has been appended.

Chapter 6 includes the sedimentation study, which is the main theme of this work. It shows the different options tried here. It also discusses the results and compare the results with physical model study.

2 CHAPTER

BRIEF REVIEW OF HEAD WORKS

2.1 INTRODUCTION

The word hydropower in connection to hydropower projects is usually used to mean distinct waterway separating the intake area from the powerhouse area geographically. Sometime intake and headworks are referred to same. The objective of headwork is to diverting water for production and facilitating for safe passage of flood. So, hydraulic design of head works is different for run of river projects and storage projects. Headworks must fulfill the following task
- Safe passage to floods, even to SPF or PMF
- Passage to trash, floating debris and ice, wherever applicable
- Passage to sediments
- Bed contol at the intake
- Exclusion of suspended sediments and air.

A hydraulic model study is often needed to ensure that proposed headworks arrangement would be able to fulfill its purpose
Even when there is a systematic sediment measurement program, it may happen that peak concentrations are not observed. However, if it is recorded than also the probability would be overestimated by applying standard statistical means. So it is risky to design a headwork component where the consequences of exceeding the selected design criteria are disastrous, so headwork design should be flexible enough with respect to sediment loads and flushing capacity as well as discharging capacity.

2.2 INTAKES

Intake structures are provided on the upstream of dam block/weir for housing the trash racks, stop-log guides and the emergency intake gate of the HRT. Planning and design of intakes can not be standardized. Every river and its possible intake are unique in itself. Many new type of intakes have been innovated and are in use, e.g., Himalayan intake. In brief the traditional *intakes for Run of River schemes* are discussed below.

2.2.1 SIDE INTAKE

Its one of the most commonly used intake. As the name suggest water is drawn through intake located at riverside. So obviously its location has to be just upstream of diversion weir or dam. Main advantages of this type are:
- Gate operation, general maintenance stop-logs dropping during flood, trash handling is easier.
- Intake is constructed on dry land on the bank of river, so construction is comparatively easier and its high probability to get a good foundation conditions.

Most suitable location of this type of intake is downstream end of an outer-curve where the secondary current will be directed from the surface and down towards the river bed. The surface water will then contain less sediment than the bottom water and

as intake draws water mainly from surface, so we have less sediment, but floating debris may be a problem. In steeper river, carrying boulder, rock-outcrops etc, taking the advantage of secondary current may not be feasible. The flow pattern in the river channel will then be governed by the roughness and steepness of the local topography, not by the relatively weak secondary current.
Placing the intake at the downstream end of the outer curve may be risky as the hydraulic loss and the impact from boulders transported by the river during floods may damage the intake and its foundation. In such a scenario intake may be located in a more protected area even if more sand and gravel will follow the water course towards the intake. Bed control may be achieved by a gated bed-load sluice, which prevents deposition of bed material in front of the intake during normal operation of plant.

2.2.2 FRONTAL INTAKE

These types of intakes are used at low-head plants where the intake and powerhouse is with in the dam body. Suitability of this type of intake prevails for high, but variable flow and low head. Minimization of head loss in low head run-of-river plants can be facilitated by this type as:

- the length of the total waterways from the headworks to the tail-waters is minimized, also unnecessary bends, curves can be avoided, resulting in minimal head loss.
- parallel identical generation units can be setup
- its easy to get uniform flow distribution in the approaching flow

Where river is carrying large particles under-sluices are must in this type of intakes. As the head is low, sediment passes through turbine without much damaging it. Also when intake is built in another structure, e.g. pillar supporting a bridge frontal intake can also be used. A frontal intake located next to a overflow weir is advantageous with respect to floating debris as well as bed load.

2.2.3 DROP INTAKE

These types of intakes are located in small streams and they are adding water to either a reservoir feeder tunnel or directly to a HRT. These type of intakes are addresses by different names in different part of world. In Norway its frequently refer to brook intake. In central Europe it's called as tyrolean intake. In South Asia its refer to trench intake.

The advantages of this type are

- its simple in design
- moderate civil works required for withdrawal of relatively small amount of water

These type of intakes may be inaccessible during high floods. The intake chamber below the trash rack may be tending to be filled with gravel if the flushing system used to keep the chamber free from deposits fails.

2.3 DESILTING BASINS

2.3.1 GENERAL

It's impossible to trap all sediment but most of the sand fraction of the suspended sediments should be removed in order to maintain hydraulic transport capacity of the waterway and to reduce the abrasion of turbines. So the main aim of desilting basin is to allow suspended particles to settle out from the water body and deposit on the bottom of the basin by reducing the turbulence level in the water flow. Then deposits are removed, by different means, like flushing or by excavation. In recent years different types of desilting chambers, different methods of removal of sediments are developed and are in use.

2.3.2 DESIGN PRINCIPLE

Desilting basin (or settling basin) is guided by the fall velocity of the particles which shall be excluded. The fall velocity is function of density, size, shape and concentration of the particles which shall be excluded and to some extent water temperature. Hard minerals like quartz and feldspar causes more wear and tear to turbines than soft minerals. The material erosion rate of steel confronting water having quartz is found to be proportional to the sediment load and the velocity of the flow into the power of 3 to 4. The hydraulic design of a desilting basin should have following objectives:

- uniform flow distribution in both planes, vertical plane and horizontal plane.
- no dead pocket in basin at entrance or exit, to avoid eddies
- if there are more than one basins in parallel than even flow distribution among the basins
- ease and efficient removal of deposits

2.3.2.1 Flushing Discharge

The flushing discharge should be capable of inducing bed load movement. Usually flushing discharge range from 20 to 30 percent of the intake discharge.

2.3.2.2 Velocity in the Chamber Basin

In old basins velocities of the order of 0.2 to 0.3 m/s were realized by using large basin cross sections. In these basins a high velocity central current was observed between dead spaces and vortices, instead of the low velocity full area flow expected according to the design, phenomenon is called hydraulic short circuit. The turbulence of flow resulting in eddies keeps the particle in suspension while gravitational force thwart it. The fall velocity is affected by many parameters of which submerged weight and form are predominant. Temperature and velocity also affects it appreciably.

According to T.R. Camp the critical velocity i.e. the limiting flow through velocity can be determined by the relation

$$V = a\sqrt{d}$$

where V = flow through velocity in m/s

d = diameter of particle up to which sediment load is desired to be removed

a = constant which is
0.36 for d >1 mm
0.44 for 1mm > d> 0.1 mm
0.51 for 0.1 m > d

R. S. Vashney, India has recommended different coefficients for Himalayan rivers.

The fall velocity of the square quartz particle of different diameter and at different temperature was obtained by Hunter Rouse by experiment and is shown in following figure.

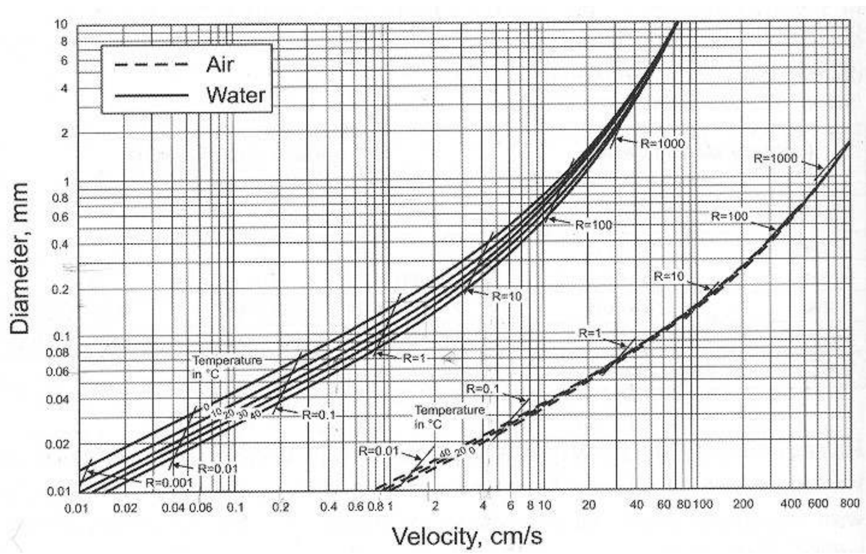

Figure 2-1 : Fall velocity of quartz sphere in water and air after Rouse

2.3.2.3 Size of sediment Load to be Removed

Earlier design criteria were to remove the particles up to 0.15 mm. The latest criteria states to eliminate sediment particles up to 0.15 mm size. In case of francis turbine, usually unaddressed one important thing is gap between the runner and cover plate. As this gap is usually 0.5 mm, so when quartz particle larger than 0.3 to 0.4 mm enter into gap, causes severe damage. This issue can be incorporated in design of desilting basin, however it may not be an optimum criteria. In Ganga valley in India it has been found that the percentage of quartz particles does not reduce rather increase with the fineness of sediment.

2.3.2.4 Desilting chamber dimensions

If depth of basin is D, width B, flow through velocity 'v', then discharge passing through the basin is Q = B.D.v …(1)

If w is the settling velocity, the settling time 't' is $t = \dfrac{D}{w}$

One important consideration is that water particle entering the basin and the sediment particles conveyed by them with equal horizontal velocity(v) should only reach the end of the basin after a period longer than the settling time. This guide the length of the basin. So basin length required is L = v.t.

Assimilating two equations we have L.w = D.v ….(2)

So from equation 1 and 2 we have six parameters, out of which we should have four known parameters to find out two unknowns. Usually Q, w, v are decided earlier and D can be selected. Different empirical equations are available to find out the length of basin.

For inlet and outlet transition zone specific care is needed, as it is main challenge from hydraulic design point of view. The velocity in the desilting chamber is low, so if uniform flow is not achieved till the end of entrance transition zone, it will be remain non uniform through out the basin and trap efficiency will reduce drastically. It’s preferable to have a good length (appx. 10-12 times width of inlet) straight before the transition zone starts at inlet. This will help to get rid-off from secondary currents. Inlet transition zone should have a gradual expansion and care should be taken that there is no separation of flow near walls. A opening angle less than 10 to 12 degree is good if possible. Guide wall can be considered to reduce the opening angle.

Depending on sediment load and flushing interval or method, there should be provision of dead space for sediment accumulating at the bottom of the basin.

2.3.2.5 Trap Efficiency

Trap efficiency of a desilting basin is mainly governed by the size and shape of the basin. As stated earlier also, the shape of the basin is important with respect to the flow distribution. A good shape will provide uniform flow distribution and thus optimum trap efficiency.

2.3.3 SEDIMENT REMOVAL TECHNIQUES

There are two approaches usually applied to remove deposits from desilting basin. Deposits can be removed from the basin while basin is in operation or while operation of basin is stopped for removal of deposits. Mechanical means or different type of tactics like flushing can be applied to remove sediments.

2.3.4 While basin is in operation

Sediment deposited at the bottom of desilting basin is continuously flushed while basin is in operation. This can be done in two way by continuous flushing, intermittent flushing.

2.3.4.1 Continuous flushing

In continuous flushing water is abstracted continuously from the bottom of desilting basin to avoid deposition. Around 20 to 30% of water is used for flushing.

One of the most common type is with longitudinal hoppers with a flushing conduit[1] running parallel to hopper. There are evenly spaced openings, oriented perpendicular to the longitudinal axis of basin, connecting the hopper to flushing conduit. Flushing conduit increase in size in the direction of flow, also some time no. of flushing conduits are provided in parallel, where every conduit carries part of flushing discharge, from a portion of desilting basin. This can be evident from the figure in **Annexure 3-5.** A constant velocity is maintained in flushing conduit. It provides a constant pressure difference between the basin & conduit, thus even abstraction of water from basin along the bottom of the hopper. A flushing gate is provided at the downstream end of flushing conduit. This gate has to be kept always open. The main problem with this system is that if deposition has occurred than flushing system can not be revitalized with normal operation of the flushing gate.

2.3.4.2 Intermittent flushing

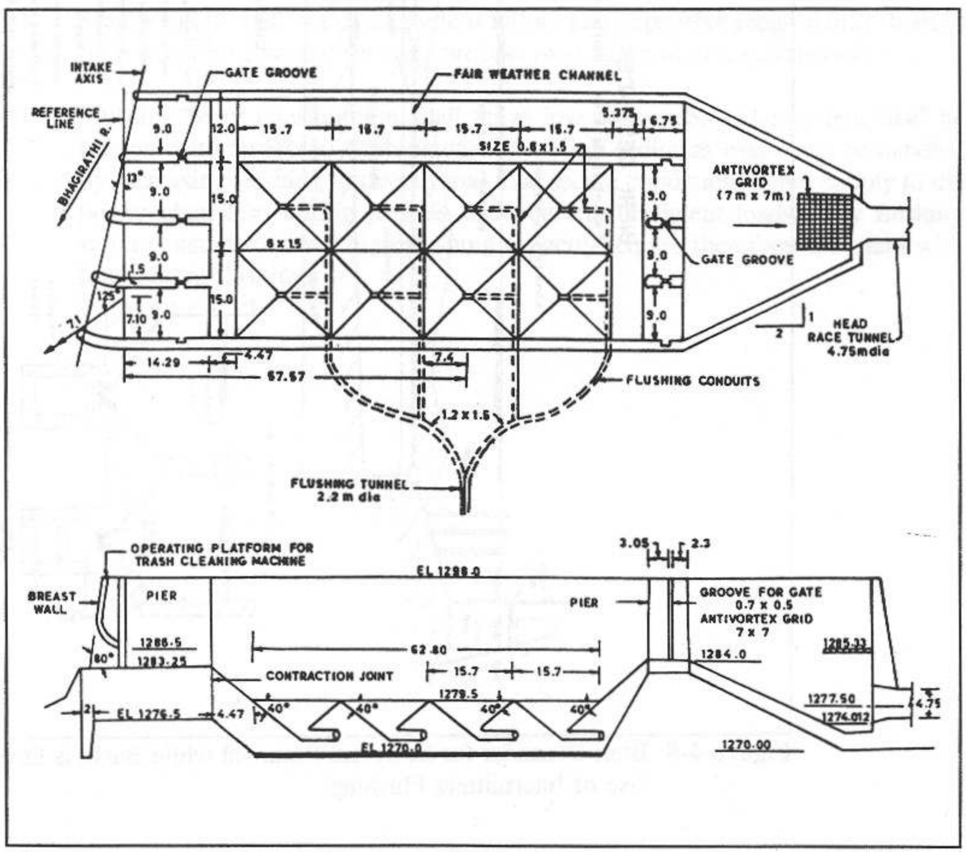

When flushing operation is intermittent there is no loss of water between two flushing operations. A hopper system with sediment ejection pipe at the bottom of each hopper is most common. Four sides of hoppers which are at bottom of desilting basin has slope of 40 to 45^{o}. The system is consist of number of valves, bends etc,. so once it is chocked, it has to be kept out of operation for some time. Gravels in sediment or mal-operation may also chock it.

[1] *Flushing conduit, flushing channel, flushing canal are terms generally used to refer the same*

Figure 2-2: Hopper system for Intermittent flushing system of desilting basin Maneri Intake works, after Haakon Støle, sept 2004, after Sharma and sing1976, from WECS 1987

Some modern system have been plasticized and patented. Bieri system, developed in Switzerland and patented one, have shutter mechanism at the bottom of the basin. Two plates one fixed and one moving with the help of servo motor opens and close the opening at the bottom of basin. When the sediment contains much quartz, wear and tear of plates are high. This system has its own limitations.

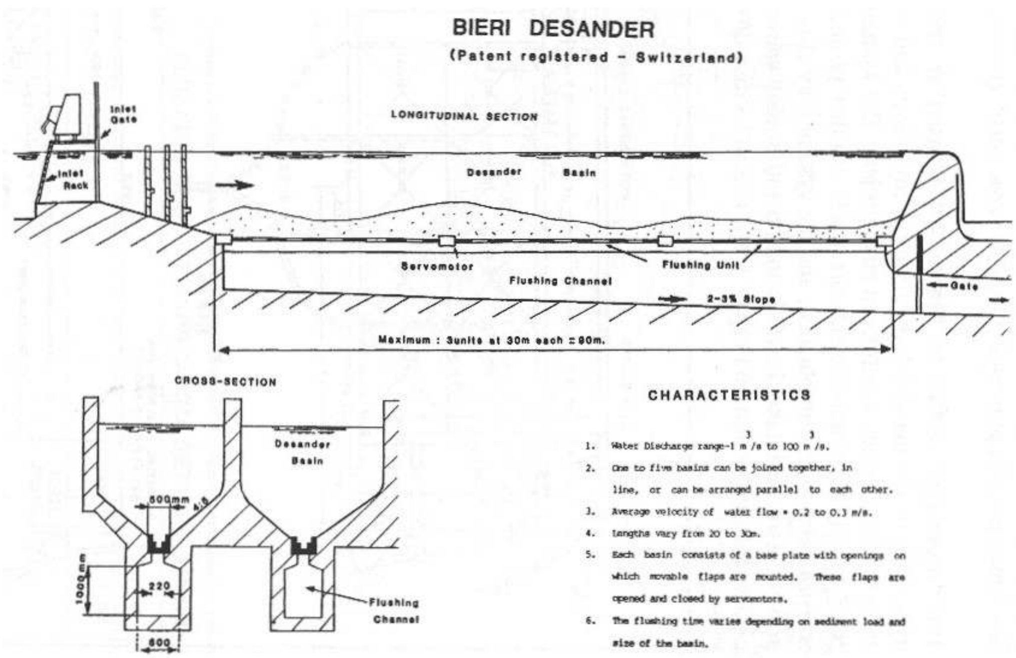

Figure 2-3: Bieri desander for sediment removal, after Haakon Støle, Sept 2004.

One other system known as Serpent Sediment Sluicing system, (usually called as S4), invented by Dr. Haakon Støle, professor NTNU and patent is with Dr. Støle and SINTEF is also been installed at many places. The serpent is a hollow heavy-duty rubber tube, which seals a longitudinal slit between the settling basin and a flushing canal along the bottom of the basin, when it is filled with water. A flushing gate at the downstream end of flushing conduit and a operational valve can fill up or empty the serpent.

Sediments can be removed in two mode one opening mode, another closing mode. In first one serpent is gradually lifted from the slit (over flushing conduit), along the bottom of the basin, over to the surface, in second mode the serpent is gradually closing the slit, when serpent is filled up with water. One advantage is that flushing water consumption is 10% only during flushing. (Ref. [6] Dr. H. Støle, sept 2004, headwork and sediment Engineering, [7] Hydraulic Design, Hydropoer Development Volume no., NTNU.)

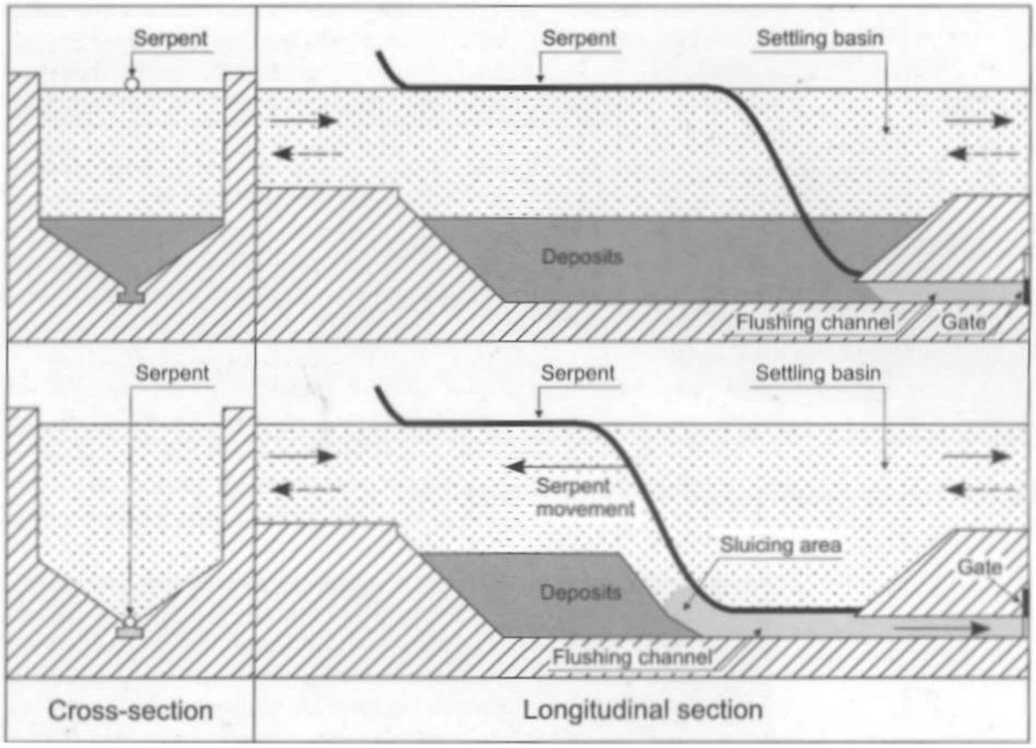

Figure 2-4: Serpent basin with the S4, from H. Støle, Sept 2004

Slotted pipe sediment excluder patented by GTO Sediments As remove sediments from open and pressurized sand traps without interrupting water supply and power production. Sediments are removed without any input of power and without any movable parts. It suck blend of sediment and water and the available head between the sand trap and the outlet is normally used as driving force, thus no external energy input is needed, and the system can operate entirely without movable parts. System has been installed at Khimati, Nepal is in use. (Ref: GTO Sediment AS, http://www.sediment.no)

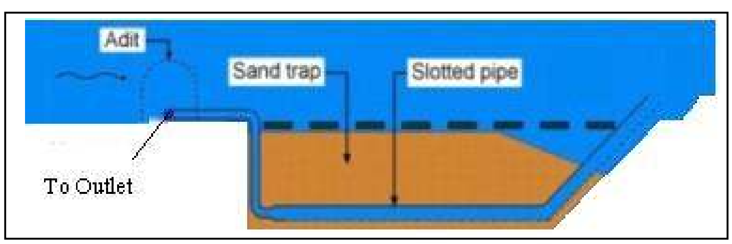

Figure 2-5: The Slotted Pipe Sediment Sluicer (SPSS), GTO Sediment AS, http://www.sediment.no)

Split and settle, a new approach, take the advantage of fact that suspended sediments are not uniform over the depth of a water conduit. The flow in the tunnel upstream of settling basin is split horizontally at the first tunnel cross. The bottom water contains relatively more sediments than the higher up. The bottom water (say 20 to 40 % of the total flow) is therefore diverted to the upstream settling tunnels running parallel to main tunnel. The settling tunnels are processing the dirtiest part of the water flow. The transit velocity is reduced in order to facilitate settling of a major part of the suspended load in relatively small caverns. The cleanest water flows in the main tunnel where the transit velocity has been reduced somewhat (60% to 80% of the velocity in the approach tunnel). Suspended sediments will therefore continue to accumulate in the lower segments of flow. The dirtiest water in the main tunnel may therefore be diverted once more in the second tunnel cross just upstream of the section where the cleaned water from the upstream settling tunnels are returned to the main tunnel. This water is then processed in the downstream desilting basin before the water in these basins are returned to the main tunnel in the third tunnel cross.

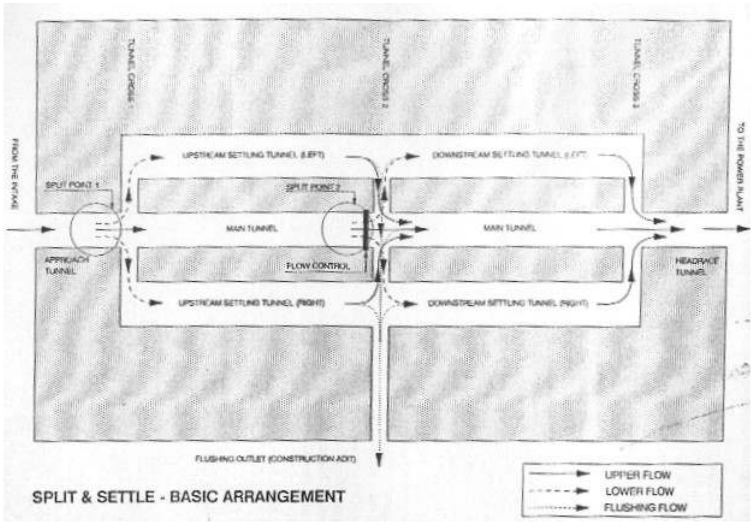

Figure 2-6: Basic Split and settle arrangement, from H. Støle, Sept 2004

This concept removes the sediments without reducing the transit velocity of the entire flow to the settling level. The settling basins are located in serial pattern compare to conventional parallel pattern. Process can be repeated several times, if necessary.(Ref. [6] Sediment Systems, Dr.ing. H. Støle AS, Trondheim, Norway). System is in use at Jhimruk, Nepal

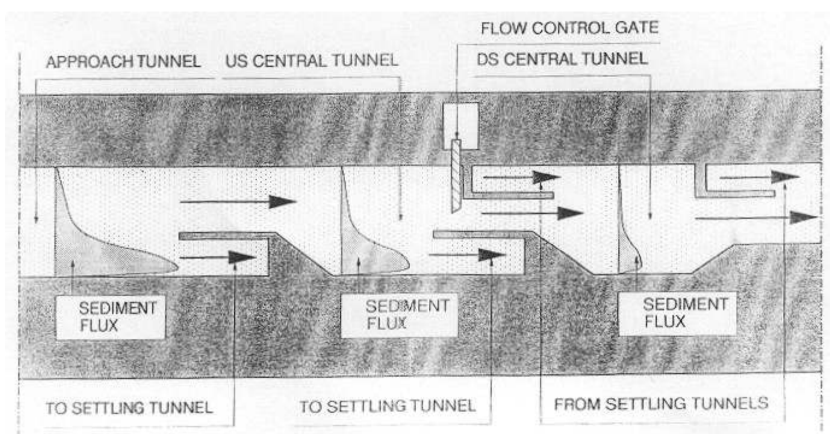

Figure 2-7: Longitudinal section through the central tunnel of Basic Split and settle arrangement, from H. Støle, Sept 2004

2.3.5 While basin is out of operation

Before removal of deposits operation of basin is stopped and it is dewatered. So to keep continuous sediment removal one spare desilting basin is required. Some times due to power requirement such a situation arise when power has to be generated without flushing, this temporarily fulfill the power requirement but in long run turbine maintenance cost increase.

Deposited sediments are removed mechanically by scrapers or by manually. Also by generating a swift current inside the basin during conventional gravity flow, scouring of deposits can be achieved. This involves operation of flushing gates in addition to the gates at the both end of the basin.

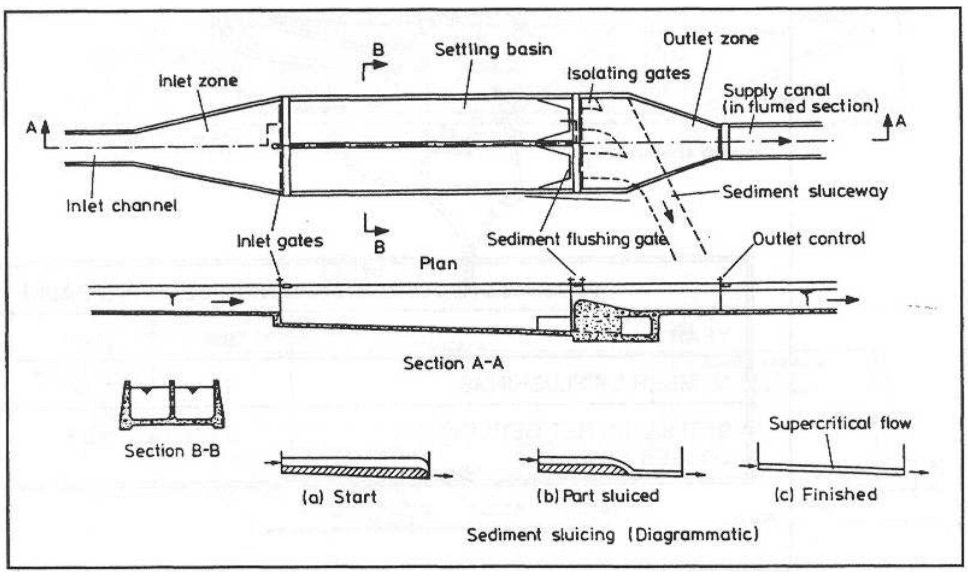

Figure 2-8: Conventional Gravity Flushing of a settling basin after Haakon stole, from Avery, P. (1989)

3 CHAPTER

TALA HYDROELECTRIC PROJECT

3.1 INTRODUCTION

Tala Hydroelectric Project, a Indo-Bhutan joint venture, is located on river 'Wangchu' in Chhukha Dzongkag of Western Bhutan. This project is 60 km up from Phuntsholing, the gateway to Bhutan and located at downstream of another Indo-Bhutan Project named Chukha. The project is a run-of-river scheme of 1020 MW installed capacity, (six units of 170 MW) with .This is the largest high-head (860m) power plant being constructed in the region. The average flow at dam site is 99 m^3/s with Mean Annual Run-off of 3107 Million m^3 and it is envisaged to generate 4865 Million units of power in an average year.

The project originally planned to be commissioned in June 2005, will now be commissioned in June 2006. The original estimated cost of the project was US $ 0.3 billion in 1993. As per reviewed estimate in February 2005 the project may cost US $ 0.93 billion

3.2 PROJECT FEATURES

3.2.1 LAYOUT

The general layout of the project is shown in **Annexure 3-1**. At Tala 92m high dam is use to divert 350 m3/s of design discharge through three intakes, which are located on the right bank. Underground desilting basin complex is consisting of three chambers. Each chamber is of oval shape with side vertical wall, 250 m long, 18.5 m high and 13.92 m wide. The water conveyance system is made of 6.8 m dia modified horse shoe channel and of 22.97 km length, which end up in two 4.0 m steel lined pressure shafts, having inclination of 52^0 with horizontal. Its have a design pressure of 9.42 Mpa. Each pressure shaft trifurcate at the end to feed three turbines.

The tail race tunnel is of length 3.1 km, 7.7m dia horse-shoe tunnel with a slope 1 in 1200 and type of flow in it is open channel type.

3.2.2 TOPOGRAPHY

The location of the project is in the foot of southern mountain range of Himalaya. The river in the area shows the topography of maturity stage characterized by the steep river gradients.

3.2.3 HYDROLOGY

At the dam site catchment area of contribution is 4028 sq. km. Ten day minimum flow is 19.5 m^3/s and average flow at dam site is 99 m^3/s. Standard Projected Flood for design has considered as 8575 m^3/s and Probable Maximum Flood for design as 10600 m^3/s.
The rain falls mainly during the summer monsoon. Precipitation is generally higher than in the Central and Western Himalaya, due to the location close to the head of the Bay of Bengal.

The limited data for rainfall on the hills (Eguchi, 1991) indicate that the middle and upper slopes are considerably more moist than the valley floors. The seasonal pattern of the river flows closely follows the summer rainfall, with the highest flows in July and August, suggesting that hydrological pathways are mostly short and direct. Local annual runoffs are in excess of two metres from high rainfall sub-catchments in the south (Wang Watershed Management Project, 2002). Also Bhutan is rarely affected by the westerly disturbances that bring significant winter rain to the Western Himalayas.

3.2.4 SEDIMENTOLOGY

Wangchu River like other Himalayan Rivers carries plenty of bed load and suspended load during mansoon period from June to September. At dam site an estimate for annual suspended load is of about 444 000 MT. Out of this, 95% load is carried only during June to October.
According to a Petrographic analysis of sediment samples, carried out by Indian Institute of Technology, New Delhi, the average percentage of quartz, feldspar, muscovite, biotite, amphibolites, pyroxenes, garnet and other minerals having low hardness values are 43.06%, 2.04%, 15.39%, 14.3%, 2.60%, 2.64%, 2.49% and 17.38% respectively. Also analysis of sediment constituents for Mohr's hardness scale showed an average of 42.76% of particles having moh's hardness greater than7. Percentage of angular/sub-angular in the total sediment concentration, having mohr's hardness more than 7, is approximately 7.65%.

3.2.5 GEOLOGY

Detailed Geological study has been taken up before the construction. Due to adverse geological situation construction of project has been delayed by one year. The area is dominated by Higher Himalayan Crystalline Complex. The type of rocks are metamorphic, Gneiss, granite quartzites, schists and marble, which are intruded with ultramafic and granitic bodies.

The geology and topography of Bhutan are shaped by the intense tectonic activity that resulted from the collision of the Indian and Eurasian continental plates, the closure of the intervening Tethys Ocean, and the uplift of the Himalayas. .

Bhutan is lithologically more homogeneous, with the gneisses underlying more than 70% of the country, and stretching southwards almost to the Indian border, except in the valley of the lower Kuri and in the southeast.

3.2.6 ENVIRONMENT AND ECOLOGY

It has a small reservoir of 9.8 million cum, i.e., virtually no reservoir, so there is no problem associated with ecology, displacement of population and deforestation. Also it is felt that major issue will not take place in relation to the natural environment, it is however necessary to monitor the EIA for long term assessment. Cost of environmental mitigation includes the cost required for implementation of the measures for mitigation and its monitoring.

3.3 PROJECT HEADWORKS

3.3.1 DIVERSION ARRANGEMENTS

It comprises of a concrete 92m gravity diversion dam near Honka for diversion of 171 m^3/s of water for generation of 1020 MW of electricity at 820m net head. There are three side intakes on right river bank, each of which feed three underground desilting chambers. The layout plan of diversion work is shown in Annexure 3-1 Also the sectional detail of the dam and intake structure is shown in Annexure 3-7
The spillway complex housed, in the central portion of dam comprises of five sluices and one overflow spillway near the left bank would be able to pass the SPF at reservoir water level(RWL) El. 1367m.The 22.25 kilometre concrete lined headrace tunnel is second longest in the Himalayas.

3.3.2 DESILTING ARRANGEMENT

Underground Desilting basin complex is consisting of three chambers. Each fed by independent inlet tunnels. The layout plan is shown in the Annexure 3-6**.** The cross sectional and longitudinal details are shown in Annexure 3 -7
The maximum width and maximum depth of basin is 18.5 m and 13.92 m respectively. Settling length is 250 m. The design is aimed to exclude particle size above 0.2 mm.

The inlet tunnel which is on right bank and have designed for 171 m^3/s and includes 20% flushing discharge. The incoming flow to basin diverse in all direction through a 39.44 m. inlet transition and vertically through 1V:2H transition. The outlet of basin converges through 17.646 m transition outlet. The outlet discharge of the desilting basin in head race tunnel is 142.5 m^3/s which fed into 22.97 km HRT.

First 18 m of desilting basin have 250mm Ø openings at the bottom @ 4.5 m centre to centre(c/c), next 25 m, 200mm Ø openings @ 5 m c/c and next middle half of the length have 150mm Ø openings @ 6 m c/c. Out of the last quarter length of desilting basin, first 18 m have 250 mm Ø openings at the bottom @ 4.5 m c/c, next 25 m possess 200 mm Ø @ 4.5 c/c and last part have 150 mm Ø @ 6 m c/c. These openings transfer flushing discharge continuously to silt flushing conduit. Mixing of different particles size is also avoided. Three separate flushing conduits are provided each for one third length of basin for flushing out coarse, medium and fine particles. Also three vertical lift slide gates each at the end of flushing conduit control the flushing operation and lead the sediment loaded water into a flushing tunnel which finally lead back to river.

3.3.3 PHYSICAL MODEL STUDIES

Physical model studies for the different components of Tala HEP has been carried out at Central Water and Power Research Station, Pune, India. One unit of desilting chamber from inlet to HRT and flushing tunnel, hydraulic model study on 1:30(G.S.) scale model, reproduced partly in fibre glass and partly in transparent Perspex, was carried out at same place. Three numbers of flushing tunnels having size of 0.5m(W) X 1.2m (H) at upstream end and 0.75 m(W) X 1.2 m (H) at the downstream end were also reproduced in the model. Openings of different size at different spacing were provided in the slab separating flushing tunnel and the desilting basin.
Initially design discharge of 57 m^3/s was run and coarse sediment with high concentration was injected from upstream of inlet and Model was also run for 10% extra discharge at inlet.
Main observations were that the settling efficiency for the material used in the model was found to be 83.25 %. These result were correlated to the material size having 2.62 as in the field and it was found that the overall size and shape of the basin is adequate for 90% settlement of material coarser than 0.2 mm diameter. It was also seen that the flushing tunnels below desilting basins were adequate for flushing of the settled sediment. Studies for efficiency of flushing tunnels beyond desilting basin are carried out on a separate model.

3.4 PROJECT FINANCE

The THEP is the biggest Indo-Bhutan joint project. This project is entirely funded by the Government of India (GOI) by way of grants and loan. India will provide a 60 percent grants and 40 percent loan at 9 percent interest. It will produce 3,962 million units (MUs) of power in a "90 percent dependable year". The project is expected to transform the Bhutan's economic health. Estimates suggest that Bhutan's annual per capita income would increase from about $700 to about $1200
The original cost for the THEP was estimated at Bhutanese (Ngultrum) Nu or Indian Rupees 14,080 million (US$ 0.3 billion) in 1993. The cost of project was then revised at Nu/Rs 30,800 million in 2001, Nu. 37,250 million (37.25 billion or app. US $ 750 million) in March 2003 and Nu. 43,000 million on January 22, 2004. The project may cost to Nu. 43,450 million, an increase by Nu. 7650 million from the initial estimation. Information is as per Managing Director of the project on February 14, 2005.

3.5 CURRENT STATUS

The construction of initial work on the dam, power tunnel, power house complex and transmission system was started in 1998. It is targeted for commissioning in the year 2004-2005. Bharat Heavy Electrical Limited of India is the supplier of the complete generating plant at a cost of Nu. 4,210 million. Tala Hydro-electric Project Authority (THPA) manages the project. M/s Hindustan Construction Company, M/s Larsen and Toubro and M/S Jaiprakash Industries are other Indian contractors.

4 CHAPTER

SSIIM MODEL

4.1 GENERAL

There are different types of numerical models available for one two and three dimensional analysis with varying degree of sophistication and reliability. The science of numerical modeling is advancing fast.

Generally there are two type of 'Computational Fluid Dynamic' (CFD)[1] programs, one are general purpose programs and other are exclusively made for River Engineering. Among the first type PHOENICS, STAR-CD, CFX, FLUENT and FLOW-3D and in second type TELEMAC, MIKE3, DELFT-3D, CH3D, TABS and SSIIM are prominent.

In recent years multi-dimensional computer programs for computing several different processes, for example water quality, sediment transport and water surface profiles etc has been developed. These multi-dimensional programs may be two-dimensional, three-dimensional with a hydrostatic pressure assumption, fully three-dimensional. There also exist width-averaged two-dimensional models, but these are mostly used mainly for research purposes.

4.2 MODEL INTRODUCTION

SSIIM is an abbreviation for Sediment Simulation In Intakes with Multiblock option. Dr. Nils Reidar B. Olsen, Professor Civil Engineering, Department of Hydraulic and Environmental Engineering at The Norwegian Institute of Technology, is developer of this program.
The program is designed to be used in teaching and research for hydraulic/river/sedimentation engineering. It solves the Navier-Stokes[2] equations using

---

[1] The Navier Stokes equations are set of coupled **differential equations** and could, in theory, be solved for a given flow problem by using methods from **calculus**. But, in practice, these equations are too difficult to solve analytically. In the past, engineers made further approximations and simplifications to the equation set until they had a group of equations that they could solve. Presently, fast computers are being used to solve approximations to the equations using a variety of techniques like finite difference, finite volume, finite element, and spectral methods. This area of study is called **Computational Fluid Dynamics** or **CFD**. SSIIM model developed by Dr. Nils is a stepping stone in this field.

[2] The **Navier-Stokes Equations** describe how the velocity, pressure, temperature, and density of a moving fluid are related. The equations were derived independently by G.G. Stokes, in England, and M. Navier, in France, in the early 1800's. The equations are extensions of the Euler Equations and include the effects of viscosity on the flow. These equations are very complex

the control volume method with the SIMPLE algorithm and the k-epsilon turbulence model. It also solves the convection-diffusion equation for sediment transport, using Van Rijn's formula for the bed boundary. Also, a water quality module is included. The program is not made for the marine environment, and it can not compute any effects of stratification due to salinity gradients

The program has an interactive graphical grid editor creating a structured grid. The post-processor includes vector graphics, contour plots, profiles etc. which can run simultaneously with the solver, enabling viewing of intermediate result. A post-processor viewing coloured surfaces in 3D is also made, as a separate program.

The flow chart of SSIIM shows the main modules of the program. At startup, the control[3] and koordina[4] files are read. The choices described

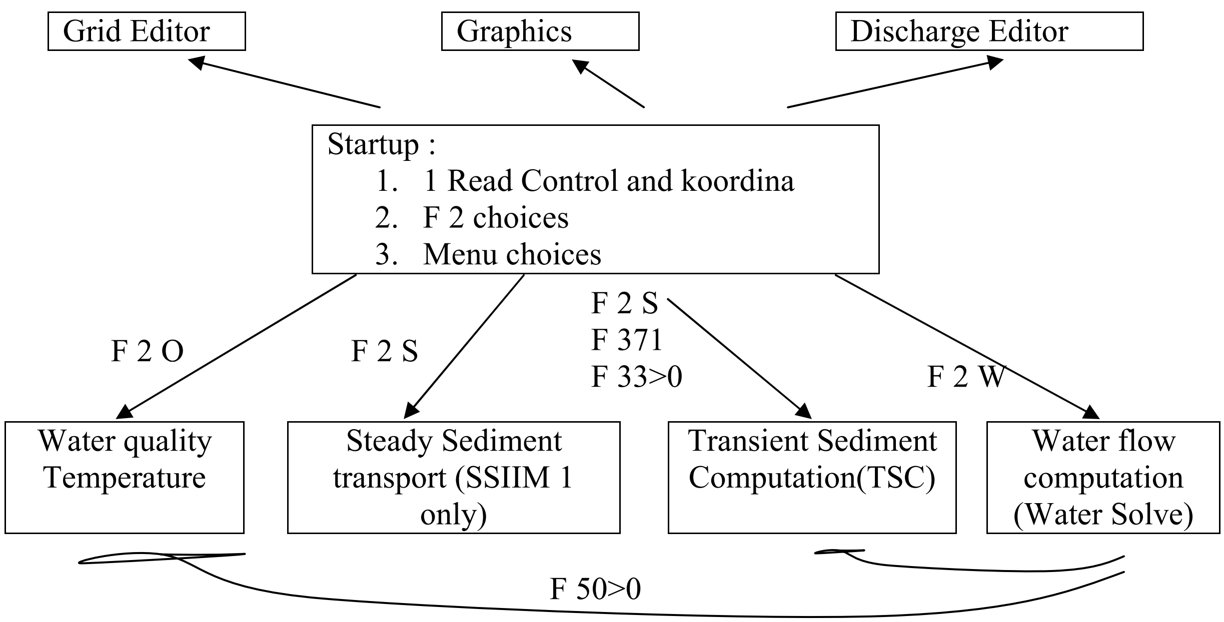

4.2.1 Different versions

The first versions of SSIIM was introduced in 1993, and ran only on OS/2. In the summer of 1999 a Windows version was made. The user interface in this version is slightly different than the OS/2 version. Only one window is showing, instead of multiple

[3] Control file control the model and it contain most of the parameters model needs. The main parameters are the size of the array used for the program. Program read each parameter one by one. Different data set contain different parameter. For example G1 data set provide the total no. of cross section longitudinal section, vertical sections and number of sediment sizes

[4] Koordina file describes the bed of the geometry with a structured grid (SSIIM 1). The grid can be made using a map, a spreadsheet or the grid editor. Details about the types of file and data set, SSIIM uses are discussed in detail in SSIIM Manual by Nils Reidar B. Olsen

windows for the OS/2 version. Also, 3D OpenGL viewer is separate, and runs only on Windows NT, WinXP, Win2000. The ssiimwin.exe program runs on Windows 95, Win 98, Win NT and Win2000. Also it has been run over Linux using wine emulator. The data must be transferred between the two programs in files. The main program makes the "result" file, which can be read by the 3D viewing program.

The version SSIIM1.0 uses a structured grid while SSIIM 2 uses an unstructured grid. In a structured 3D grid, each cell will have three indexes, which makes easy to identifying of grid location. The location of walls and inflow outflow surfaces are then specified in input files, where the grid indexes are included in the data set. Modelling of temperature-stratified flow is only possible in SSIIM 2.

4.3 THEORETICAL BASIS

A short theoretical background of the model is discussed below. Navier-Stokes equation with k- ε turbulence model for velocity and turbulence is solved for a three dimensional water body. SSIIM calculates sediment transport by Sediment transport size.

4.3.1 WATER FLOW CALCULATION

In a three dimensional geometry, Navier-Stokes equations for turbulent flow are solved to obtain the water velocity. The k-ε model is used to calculate the turbulent shear stress.

The Navier-Stokes equations for non-compressible and constant density flow can be modeled as follow:

$$\frac{\partial U_i}{\partial t} + U_j \frac{\partial U_i}{\partial x_j} = \frac{1}{\rho} \frac{\partial}{\partial x_j} (-P\delta_{ij} - \rho \overline{u_i u_j})$$

The left most term on the left side is transient term and the second term is convective term. The first term on the right hand side is pressure term and second term is the Reynolds stress term. To evaluate this term, a turbulence model is required.

The default algorithm in SSIIM neglects the transient term. By means of different data sets this term, time step, number of inner iterations can be controlled.

The k-ε turbulence model

Th eddy viscocity concept with the k-ε turbulence model is used to model the Reynolds stress term:

$$\overline{u_i u_j} = \nu_T (\frac{\partial U_i}{\partial x_i} + \frac{\partial U_i}{\partial x_j}) + \frac{2}{3} k \delta_{ij}$$

The first two terms on the right side of the equation forms the diffusive term in the Navier-Stokes equation. The third term on the right side is incorporated into the pressure. The eddy viscocity in the k-ε is as:

$$\nu_T = c_\mu \frac{k}{\varepsilon^2}$$

K is turbulent kinetic energy, defined as:

$$k = \frac{1}{2} \overline{u_i u_j}$$

k is modeled as :

$$\frac{\partial k}{\partial t} + U_j \frac{\partial k}{\partial x_j} = \frac{\partial}{\partial x_j} (\frac{\nu_T}{\sigma x_j} \frac{\partial U_i}{\partial x_j}) + P_k - \varepsilon$$

Where P_k is given by:

$$P_k = \nu_T \frac{\partial U_j}{\partial x_j} (\frac{\partial U_j}{\sigma x_i} + \frac{\partial U_i}{\sigma x_j})$$

The dissipation of k is denoted ε, and modeled as:

$$\frac{\partial \varepsilon}{\partial t} + U_j \frac{\partial \varepsilon}{\partial x_j} = \frac{\partial}{\partial x_j} (\frac{\nu_T \partial \varepsilon}{\sigma_k \partial x_j}) + C_{\varepsilon 1} \frac{\varepsilon}{k} P_k + C_{\varepsilon 2} \frac{\varepsilon^2}{k}$$

In all above equations ‘c’ are different constants. The k- ε model is the default turbulence model in SSIIM.

Wall laws

The wall law for rough boundaries is used, as given by Schlichting (1979)

$$\frac{U}{u_x} = \frac{1}{k}\ln\left(\frac{30y}{k_s}\right)$$

The roughness, k_s is equivalent to a diameter of particles on the bed.

4.3.2 SEDIMENT FLOW CALCULATION

Conventionally sediment transport is divided in bed load and sediment load. The sediment load can be calculated with help of convection-diffusion equation for the sediment concentration, c, volume fraction in SSIIM

$$\frac{\partial c}{\partial t} + U_j \frac{\partial c}{\partial x_j} + w\frac{\partial c}{\partial z} = \frac{\partial}{\partial x_j}\left(\Gamma \frac{\partial c}{\partial x_j}\right)$$

here 'w' represents the fall velocity of the sediment, and Γ diffusion coefficient, which is taken from the k-ε model.

$$\Gamma = \frac{\nu_T}{S_c}$$

Where Sc is the Scmidth number, set to 1.0 as default in model, but different value can be adopted in model.

In the above convection-diffusion equation the first term is for convection of sediments, i.e, sediments transported through walls of finite volume, because of the velocity of the water at the wall. The second term is due to the fall velocity of sediments and can be said as extra convection term added to the velocities in the vertical direction. On right hand side term is for diffusion of sediments. Γ is diffusion coefficient due to the mixing by turbulence in the water. It depicts amount of sediments transported through the walls of the finite volume because of turbulence and the difference in concentration between the two sides of the wall.

For problem involving resuspension of sediment, a boundary condition near the bed is necessary. For this in SSIIM van Rijn's formula is used.

$$c_{bed} = 0.015\frac{D_{50}}{a}\frac{\left[\dfrac{\tau-\tau_c}{\tau_c}\right]^{1.5}}{\left\{D_{50}\left[\dfrac{(\rho_s-\rho_w)g}{\rho_w \nu^2}\right]^{\frac{1}{3}}\right\}^{0.03}}$$

Where D_{50} = Sediment particle diameter
τ = bed shear stress
τ_c = critical bed shear stress for movement of sediment particles
ρ_s = density of sediment
ρ_w = density of water
ν = viscosity of the water
g = acceleration due to gravity
a = reference level set equal to the roughness height

The influence of sediment concentration on the water flow is still a matter of discussion and possess different opines.

4.4 USER INTERFACE AND INPUT/OUTPUT

USER INTERFACE

The windows version consists of only one window with one menu. At start up, the window shows text with information about convergence and the run. The content of the window can be changed by choosing different sub-options in the view option of the menu. Changing the view, will also change the main menu. The different views are

- Map graphics with contour plots or vectors
- Longitudinal/ cross-sectional profiles
- Grid Editor
- Discharge Editor (SSIIM2)

INPUT OUTPUT FILES

Normally SSIIM run start by reading input files, or generating the grid using the Grid Editor. After generating the grid, the inflow and outflow should be stated using discharge editor. Then the data should be saved in the unstruc/koordina files, before the computation are started and the results are viewed.

As a input for model three main things are needed as follow:

1. Geometry of the hydraulic structure
2. Water inflow/outflow data
3. sediment data
4. different controlling parameters

Hydraulic system is modeled by means of x, y and z co-ordinates with a structured grid(SSIIM1). Coordinates are of points where grid lines meet. Grid lines define cells between the grid lines and grid is seen from above. The variables are calculated in the centre of each cell. The geometry have six surfaces. The water surface or the roof of the basin define the sixth surface of the three dimensional water body. Also by blocking out cells geometry can be changed.

The koordina file, which has to be kept in the same folder where control file is, describes the bed of geometry with a structured grid in SSIIM1. A file named koomin with same format can be used to provide minimum bed surface elevation for bed changes. The bed level will not be lowered below this surface.

The water inflow/outflow have to be specified for all boundries where water is flowing into or out of the water body. Water velocities are given by three dimensional vector. Also the sediment concentration at inflow is required. Friction and shear stress is based on the roughness.

Control file[5] control all parameters.

A intermediate file with the name 'boogie' is generated which shows print-out of intermediate results from the calculation. It also shows parameters as average water velocity, shear stress and water depth in the initialization. Trap efficiency and sediment grain size distribution is also written in this file. If any error occur during the run of program, it is written here with explanation before the program terminates. With the help of D and F 1 options in control file additional details can be written in this file.

The result file is written when prescribed number of iterations have been calculated or when the solution has converged. The results are velocities in three dimensions, k, ε, pressure and the fluxes on all the walls of the cells. The data from this file is used as input for the sediment flow calculations.

A flow chart describing the various files[5] are given below. Many of the files mentioned in the chart are not used, they are used for specific purposes. Some of files are out put files.

---

[5] The detail and option available are explained in detail in SSIIM User Manual by Nils R. B. Olsen In the Tala desilting chamber study only few files are used. Details about how to use these input/ output files is stated in manual

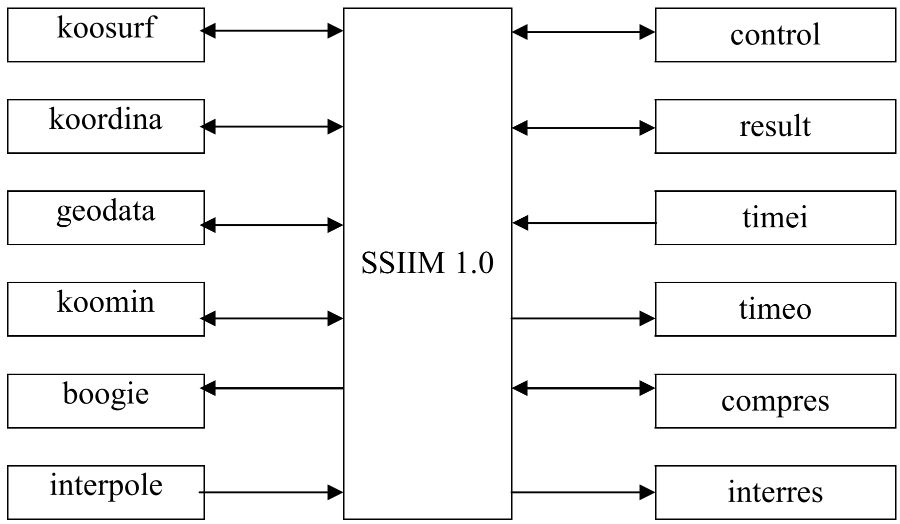

All the files are ASCII files. Also that the names of the files can not be changed. The two main input files are the control and koordina file for SSIIM 1.

5 CHAPTER

WATER FLOW SIMULATION AND RESULT DISCUSSION

5.1 GENERAL

SSIIM 1.0 is used to simulate Tala desilting basin. A physical model[7] study of one desilting basin from inlet to outlet was carried out by Central Water and Power Research Station, Pune India. The results of this studies are obtained from Central Water Commission, New Delhi, India. The physical model of desilting basin has been simulated here, as well as Prototype is also simulated here. The flushing system is modified in both of the cases. A uniform flow through out the bottom of desilting basin is considered. In place of small holes in prototype in model study a through out slot through desilting basin has been considered. This has been done due to practicality which is further discusses in article 5.2.2. However this approximation would not effect the results. The aim is to simulated hydraulic model here, as there was no real time sediment data was available for prototype. However prototype is also simulated here, using the grain size distribution curve which is a transformation of grain size distribution curve used for hydraulic model as per relationship provided by CWPRS report annexed in Annexure 5-3. In the physical model sediment of specific gravity 1.32 was used. Same has been used in simulation of hydraulic model. In simulation of prototype sediment of specific gravity 2.65 have been used. Dimension and details of basin used for simulation are as follow:

Data	Prototype	Physical model
Inlet discharge (m^3/s)	57	0.115
Outlet discharge (m^3/s)	47.5	0.009636
Flushing discharge (m^3/s)	9.5	0.001927
Depth of flow (m)	18.5	0.617
Length of basin (m)	250	8.33
width of basin (m)	13.9	0.46
Flow area (m^2)	198.316	0.22
Specific gravity	2.62	1.32

5.2 TALA DESILTING BASIN

5.2.1 GRID GENERATION

The whole desilting basin from inlet to outlet has been simulated. Longitudinal plan and sectional elevation of original and simulated are shown in Annexure. With the help of orthogonal three axis co-ordinate system grid has been generated. In the co-ordinate

1 In this chapter wherever the word ‘model’ has been used it refers to the numerical model for SSIIM. Wherever reference is made for physical model by CWPRS it has written as physical model.

system 'i' 'j' and 'k' represent stream-wise, cross stream-wise and vertical directions respectively. Mathematically X, Y and Z axis define flow direction, cross stream-wise direction and vertical direction.
The geometry of the structure has defined by six surfaces. The bed profile, inlet, outlet and two side walls are five surfaces out of it. The roof or water level is sixth surface. All gridlines in the k direction are parallel to Z axis. i.e the horizontal position of the grid line is determined from the two dimensional grid seen from above. The Z coordinate are fraction of total depth.
Firstly the grid is generated for prototype in spread sheet. As the physical model have a scale 1:30 (G.S.) the grid was transformed to 1:30 scale for SSIIM program. The prototype desilting basin has 250m length inclusive of 39.44m initial transition zone and 17.646m transition zone at the end. In simulation it has been reduced to physical model scale i.e 1/30th times of prototype. The roof and basin has 1:600 upward slope in prototype, which has been taken into account. Silt Flushing conduit at the bottom of desilting chamber has been not modelled here due to complicacy. The maximum height of prototype is 18.5 m and width is 13.927 m and it is all along the basin length of 250 m. In physical model study it was 61.67 cm and 46.42 cm respectively along the 83.33 cm length of physical model and it is kept same here in numerical model. Except the transition zones cross section is uniform all along. The outlet tunnel has a gate at a distance of 16 m from start of transition in prototype. This is not included in the model here. Initial and final section of the basin has 4.9 m horse shoe modified section in prototype which is modelled in the scaled way.

5.2.2 DEVIATIONS DUE TO PRACTICAL REASONS

In prototype there are openings of diameter from 150 to 250 mm varying @ 4.5 to 6 m c/c at bottom of desilting basin. Same was reproduced in physical model. In this numerical model a through out opening equivalent to area of one cell at bottom has been considered. Which have same flushing outflow as it is in physical model and in case of model for prototype it has same outflow as of prototype. The reason behind uniform opening for model is practicality. As the hole size is quite small, to reproduce it, we have to make cell size at least equivalent of it. This will increase the total number of cells and hence calculation time, without affecting the results.
The sides of tunnel at some places have been modified in numerical model, which are depicted in figures. For a structured grid there has to be four faces of a cell in either projection, so to avoid triangular cells original tunnel cross section has been changed a little, which neither effect the result quality nor its quantity in appreciable way.

5.2.3 DETAILS OF GEOMETRY

The details of simulated and prototype of various cross section is enclosed in **Annexure 5-1.** The simulation has been carried out on prototype and physical model, i.e.,1:30 scaled prototype. So the shapes of cross section are being same in both simulations, i.e. for prototype and as well as for physical model. It has been assumed that hydraulic model developed by CWPRS was exact replica of prototype. Orthogonality of grids are maintained to avoid false diffusion.

The geometry have 124 X 11 X 11 gridlines. It means 124 cross sections(i value) including inlet and outlet cross sections and the distance between these two section is 307.086m for prototype & 10.231m for model. In the transverse direction the geometry is divided into 11 profiles (j values) including the two end side wall. In the vertical direction the geometry is divided in 11 profiles too(k values), including top and bottom surfaces. The vertical points in a line are at equidistance, as height is divided in equal ten parts. So we have in total (124-1) X (11-1) X (11-1) number of cells. The coordinates of simulated profile for physical model is obtained by dividing the coordinates of profile for prototype by 30.

A fine mesh of geometry was also created with 247 X 21 X 21 gridlines, but it did not result appreciable changes in result, moreover simulation running time increased many fold.

The cross section areas at different chainages are shown here. In between the section no. 18 and 117 cross sectional areas are same. Cross sectional details at different sections of desilting basin are as follow:

Table 5-1: Cross sectional details at different sections:

Cross section		X Cordinate in simulation	Area (sq. m.)		
No.	Chainage(proto type)		Prototype	Physical model	Simulated
1	0	0	19.5296	0.0217	0.0215
2	2.5	0.083	22.1591	0.0246	0.0242
3	5	0.167	24.4276	0.0271	0.0268
4	7.5	0.250	26.1179	0.0290	0.0290
6	12.24	0.408	30.4931	0.0339	0.0334
18	41.94	1.398	30.4931	0.0339	0.0334
50	121.95	4.065	30.4931	0.0339	0.0334
100	246.93	8.231	30.4931	0.0339	0.0334
117	289.44	9.648	207.9607	0.2311	0.2286
124	297	9.900	106.1448	0.1179	0.1276

5.2.4 VELOCITY DISTRIBUTION

The boundary condition has to be defined to simulate velocity field. The average flow through velocity through basin in physical model is 0.048 m/s. In control file by G8 data set initial values has been given. Velocities at input are not needed to be correct by value, but should be correct in direction. The discretisation[8] of the equation is done by Power Law Scheme (POW). In POW scheme, to calculate a variable for a three dimensional particle, variable of surrounding six cells are used. The Second order upwind scheme

2 Its process to transform the partial diffusion equation for convection diffusion into a new equation where the variable in one cell is a function of the variable in the neighbouring cells.

(SOU) is based on a second-order method to calculate concentration on the cell surface. In SOU surrounding twelve cells are involved. POW scheme converges more easily compare to SOU scheme. Only POW schem has been used here.
The relaxation factor (represented by K6 data set in control file) has been lowered than default value for program. A graphical representation of velocity in all three directions is obtained by simulation.

5.2.4.1 Velocity distribution in the horizonatl plane (X-Y plane)

The velocities along the plane x-y plane, i.e., horizontal plane at different levels are given in the annexure 5-4. by means of velocity vector with scale. The upper layers have higher velocities compare to lower one, although a uniformity is maintained layerwise. The maximum velocity is 0.4888 m/s.

5.2.4.2 Velocity distribution in the longitudinal plane (Y-Z plane)

The velocities vector at the y-z plane, i.e., at different cross sections are given in the annexure 5-6. with scale. The velocity distribution in the transition zone is uniform initially. At the transition zone vertical velocity is higher at upper part than lower part. Gradually the vertical velocity takes an eccentricity. i.e on one of the corner of upper side it is higher and gradually it reduce in an oblique plane to diagonally opposite corner. The velocity vector represent this.

5.2.4.3 Velocity distribution in the longitudinal plane (X-Z plane)

The velocity vector with scale at different longitudinal plane are shown in annexure 5-7. The velocity vector with scale is shown in annexure 6-8 and velocity profile in the annexure6-9. It depicts that the velocities are higher at upper part at the end of transition zone. The Flow achieve uniformity after travelling the one third length of desiltign basin. The maximum and minimum velocity is found .0258 m/s and 0.4886 m/s

5.2.5 INLET AND OUTLET

The inlet of desilting chamber where transition zone start have a cross section of 4.9 m modified horse shoe tunnel and transition zone is 39.44m length for prototype. The velocity variance in these zones are depicted in annexures showing variation of velocities at different planes.

5.2.6 MECHANISM OF TURBULENCE

In turbulent flow small masses of water actively participate in transverse mixing. Momentum of a Water particle, moving from a lower velocity to high velocity(e.g from position A to B) increases and exerts a drag on the fluid at B. Similarly if a particle moves from higher velocity to lower velocity it will try to accelerate the water particles around it at new position. These forces are the result of turbulence cross motion of small masses of water and shear force within water mass occur.

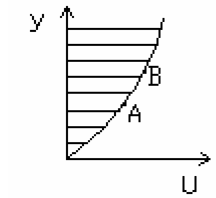

Fig Velocity distribution in turbulent flow

The total shear stress in turbulent flow consists of a laminar and turbulent part and can be stated as:

$$\tau = \tau_l + \tau_t = \mu \frac{d\bar{u}}{dy} + \eta \frac{d\bar{u}}{dy} = (\mu + \eta)\frac{d\bar{u}}{dy}$$

Here μ represents the water property and its independent of type of flow, whereas η depends on water density and turbulence and also its value changes with general conditions and from point to point in a flow.

With increase in Reynolds number beyond a critical value, eddy viscosity become prominent and can be given as $\eta / \rho = \varepsilon$ and the ratio η / ρ is known as kinematic eddy viscosity.

5.2.7 TURBULENCE CLASSIFICATION

Turbulence is present usually in the form of shear flow. It can be classified as whether it is occurring along solid surface or at the interface between water masses having different velocities. Turbulence near solid boundary is called as wall turbulence and another one is free turbulence. In details it is discussed at Article 4.3.1 of chapter-4. The model gives the values of shear stresses along the boundaries.

5.3 TALA DESILTING BASIN-THREE BASINS IN COMBINATION

An attempt has been made to find out the amount of flow passing through each of the three desilting basins, as three basins are in parallel and there is side intake and moreover the intake length of each of basin is different. So along with part of river, three desilting basins and part of HRT has been simulated. The grid plan as seen from above is shown in annexure 5-9. It have grid size of 186 X 45 X 11. Also a cross sectional grid at mid of desilting basin is shown in annexure 5-9. For a flow equal to one third of design flow, it was found that 35%, 32% and 33% flow passes through first, second and third desilting basins. Here intake of third basin is nearest to the dam. Moreover its assumed that total flow of river is going to intake of desilting basin.

6 CHAPTER

SEDIMENT FLOW SIMULATION AND RESULT DISCUSSION

6.1 GENERAL

For determining the trap efficiency of settling basin and determining flow pattern SSIIM model has been used. Sediment transportation can be divided in two parts: one sediment flowing close to the bed and sediment flowing in suspension. Although there can not be a definite demarcation between these two. Number of formulas, approaches and theories are available to deal these. In SSIIM its assumed that a negligible amount of sediment is flowing close to bed or rather to say moving by rolling on bed. Most of the sediment is moving in suspension. For the side walls symmetric boundary condition for the sediment are used. For upstream sediment input concentration has been provided. Maximum concentration of sediment is 2000 ppm. In fact 2000 ppm concentration in the river would be only for a few days in a year, rest of the year it is likely to be much less. For the suspended load computation is done as described in article 4.3.2 of chapter 4 and process of discretization is followed.

In this study particle diameter of 0.063 mm to 0.210 mm is used for physical model simulations. For prototype simulation it is .07 mm to 0.27 mm. The specific gravity of the sediment particle for prototype is 2.65 and for physical model it is 1.32. It is considered in the simulation. The fall velocity of the sediment particles, for physical model with a density 1.32, is given in the CWPRS report and it is used in the simulation. For prototype it is taken from Rouse diagram.

The bed concentration is recalculated as simulation proceeds. In SSIIM different option can be used. The results obtained by using different options are tabulated.

The evaluation of changes in bed elevation is obtained by satisfying continuity of the sediment fluxes on the bed boundaries. For each particle size same process is followed. For total change a summation of changes for each particle size is summed up.

In SSIIM, the convection diffusion equation for sediment flow by POW scheme is used, no SOU scheme is used.

Number of different options has been applied for simulation of physical model of desilting basin, out of which few has been discussed here. For prototype as there was no particle size distribution curve, only one simulation has been carried out.

6.2 TALA HYDROPOWER DESILTING BASIN

6.2.1 SEDIMENT CONCENTRATION PROFILES

In this study coarser material are not considered in both of simulations. From the *Technical Report no. 3804 for hydraulic model studies for desilting basin for Tala hydro electric project, CWPRS, Pune, India*, obtained from *Central Water Commission*, grain size distribution curve is taken and it is used for simulation of physical model. From the report sample No.1 is chosen for study and first four particles sizes are simulated, as this report states 100% removal of particles having size greater than this. It has also seen from simulation study that particles of size 0.230 and more will be removed 100%. So, particles having diameter 0.210 mm or less has been studied. In report the particles size distribution curve shows ten different grain sizes and each sizes is 10% by weight. The corresponding fall velocities are given. It is shown in table 6-1.

For simulation of prototype grain size distribution curve is obtained on the basis of curve for physical model. The particles diameter for prototype is obtained by converting the diameter for physical model with help of curve showing the relationship between particle size in prototype and model, as given in Annexure 6-3

6.2.2 TRAP EFFICIENCY CALCULATION FOR PHYSICAL MODEL

6.2.2.1 SIMULATION OF PHYSICAL MODEL

Different options and different parameters has been considered while simulating the physical model. Simulation has been run varying different parameters one at a time to analyse the affect of parameter. Simulation was run with and without openings at the bottom of basin, i.e. with and without flushing discharge, trap efficiency was evaluated. Later option provides conservative results. The results with flushing flow are discussed only. Transient sediment computation(TSC) algorithm has been used.
An inflow sediment concentration of 0.0222 kg/second is taken for simulation. This is based on the CWPRS report as annexure 5-2, where 400 litres of sediment was injected during model run. So to maintain 2000 ppm sediment concentration, the amount of flow required is $(10^6 X400)/2000$ litres. In physical model inlet discharge was 0.115 m^3/s. so time of model run was $(10^6 X400)/2000/11.5$ seconds or 4.8 hours. Based on it concentration of inflow sediment comes up as: 400 kgs/4.8 hrs ≅ 0.022 kg/s. Assuming sediment (mix of sediment particles and water) has density 1000kg/m^3. As each particle size has 10% representation of total sediment. So sediment inflow of each particle size is 0.0022 kg/s. As per the physical model study report from CWPRS the trapping of different particle size, calculated analytically is shown in table below along with results from numerical model SSIIM :

Table 6-1: Comparison of Theoretical and SSIIM evaluated Trap efficiency (with design discharge in physical model)

As per CWPRS hydraulic model study Report							Total removal percentage on taking in account the flushing channel too(%)	
Sl. No.	% finer	mean dia(mm) from gradation curve	Fall velocity	122 W/V	W/Vo	Removal ratio for flow passing through desilting basin	Theoretically calculated	Simulation of physical model
1	5	0.063	7.16E-04	1.930	0.20	0.20	36	41
2	15	0.11	2.10E-03	5.330	0.59	0.57	66	75
3	25	0.16	4.26E-03	10.827	1.19	0.88	90	96
4	35	0.21	6.97E-03	17.710	1.96	1.00	100	100
5	45	0.23	8.16E-03	20.740	2.29	1.00	100	100
6	55	0.26	1.00E-02	25.410	2.81	1.00	100	100
7	65	0.28	1.14E-02	28.970	3.20	1.00	100	100
8	75	0.31	1.35E-02	34.310	3.79	1.00	100	100
9	85	0.34	1.57E-02	39.900	4.41	1.00	100	100
10	95	0.45	2.50E-02	63.540	7.03	1.00	100	100
		Trap efficiency in %					89.2	91.2

where V = Average Forward velocity = 0.048 m/s

V_0 =Required Forward velocity = 3.555 X 10^{-3} m/s

In table above, on adding the part of sediment removed through flushing flow, removal percentage is find out. It is assumed that flushing flow, which is 20% of inflow, has same representation of sediment as it is in inflow. Also, whatsoever amount of sediment is contained by flushing fluid at the time of intake is flushed i.e. 100% removal of sediment of the part of flow passing through flushing channel. The comparison between trap efficiency evaluated by different methods is as follow:

Table 6-2: Trap efficiency evaluation by different methods

Methods	Trap efficiency (%)
Analytical	89.2
Physical model study	83.3
Simulation of physical model	91.2
Simulation of prototype	92.2

SSIIM has been run only for first four particle sizes, so analytically percent removal of sediment consisting of only these four particle size is :

$$= \frac{(100 + 90 + 66 + 36)}{4} = 73\%$$

When the model was run for 18000 seconds with a time step of 5 seconds following results were obtained. Also minimum elevation surface for bed change was given as bed surface, i.e. no bed erosion of bed was allowed. Size no. 1 represent coarsest particle size and size 4 represent finest particle size of sediment. The control file as a example is appended in annexure 6-4.

Table 6-3: Comparison of Removal percentage for four finest particle sizes.

Size no.	Size (mm)	Inflow	Outflow	LayerActive	LayerInac.	Suspended	Defect	% Defect	% Removal	
									SSIIM	analytical
1	0.210	0.0303	0.00007	0.000111	0.031408	0.000081	-0.001369	-4.5%	100%	100%
2	0.160	0.0303	0.001311	0.00014	0.030172	0.000129	-0.001452	-4.8%	96%	90%
3	0.110	0.0303	0.007979	0.000127	0.023655	0.000205	-0.001666	-5.5%	74%	66%
4	0.063	0.0303	0.018913	0.000066	0.013589	0.000279	-0.002547	-8.4%	38%	36%
	Flux	0.008898	0.002077					Overall removal	77%	73%

On increasing the simulation running time, trapping percentages were same. Although trapping percentages of each particle reached a stable condition around 1300 seconds i.e. around 260 iterations, but there was an impact on defect percentage. Defect reduces slowly with higher number of iterations, but rate of reduction reduces as iteration nuber increases.

The simulation has been run only for lower four grain size and it is evident that particles having diameter more than 0.210 mm are removed 100%. As trapping is not a function of concentration, we can extend our calculation to find out total trap efficiency of desilting basin. On adding the percentage removal of the particles having diameter more than 0.210 mm we have trap efficiency of desilting basin as 90.8%, whereas analytically established trap efficiency is 89.2%. The calculation is shown in following table:

Table 6-4 : Trap efficiency of desilting basin based on the trapping percent of four smallest grain sizes

Sl. No.	Particle dia (mm)	% of total sediment	Sediment removal	
			% of fraction	% of total
1	0.063	10	38%	3.8
2	0.110	10	74%	7.4
3	0.160	10	96%	9.6
4	0.210	10	100%	10
5	Dia> 0.210	10	100%	10
6	Dia> 0.210	10	100%	10
7	Dia> 0.210	10	100%	10
8	Dia> 0.210	10	100%	10
9	Dia> 0.210	10	100%	10
10	Dia> 0.210	10	100%	10
			Total	90.8

6.2.2.2 SIMULATION OF PHYSICAL MODEL WITH OTHER OPTIONS

To reduce the defect, SSIIM was also run with some other options like different sediment pick up for re-suspension, different thickness of upper active layer of sediment, different bed roughness etc. To study a comparative effect of each of the parameter simulation was run with a time step of 5 seconds and equal number of iterations. Few of results are analyzed and tabulated here:

a) Effect of Sediment pick-up rate, F 37 2

SSIIM was run with different sediment pick up rates by changing F 37 data set. When F 37 1 data set is used re-suspension of sediment is at a fixed rate and when F 37 2 data set is used re-suspension becomes a function of flux. In both of the cases all other parameters are same. In following both of the tables, result are placed only varying the sediment pick up rate after 500 no. of iterations.

Table 6-5: Removal percentage with F 37 2

Size no.	Size (mm)	Inflow	Outflow	LayerActive	LayerInac.	Suspended	Defect	% Defect	% Removal	
									SSIIM	analytical
1	0.210	0.004208	0.000009	0.00012	0.003732	0.000083	0.000264	6.3%	100%	100%
2	0.160	0.004208	0.000173	0.000145	0.003356	0.00013	0.000403	9.6%	96%	90%
3	0.110	0.004208	0.001052	0.000128	0.002336	0.000202	0.00049	11.6%	75%	66%
4	0.063	0.004208	0.002526	0.000057	0.00097	0.000267	0.000388	9.2%	40%	36%
	Flux	0.008888	0.002006					Overall removal	77%	73%

Table 6-6: Removal percent with F 37 1

Size no.	Size (mm)	Inflow	Outflow	LayerActive	LayerInac.	Suspended	Defect	% Defect	% Removal SSIIM	% Removal analytical
1	0.210	0.004208	0.000009	0.000521	0.003814	0.000081	-0.000217	-5.2%	100%	100%
2	0.160	0.004208	0.000174	0.00065	0.003511	0.000129	-0.000256	-6.1%	96%	90%
3	0.110	0.004208	0.001069	0.000601	0.002688	0.000204	-0.000354	-8.4%	75%	66%
4	0.063	0.004208	0.002627	0.000317	0.001634	0.000278	-0.000648	-15.4%	38%	36%
	Flux	0.008888	0.002006					Overall removal	77%	73%

Although total trap efficiency did not change, but trapping percentage of finest particle is higher in first case by 5 % . Also its evident that defect percentages has been changed. As re-suspension is calculated only at bottom cell and by convection diffusion its impact goes on upper cells, so particles which are in active layer near the bottom will mostly affect by the method re-suspension is calculated. Its also evident from Van Rijn formula that particles of smaller size will have smaller equilibrium sediment concentration than that of bigger size. So, finer particles are sensitive to this data set.
Moreover based on this, trap efficiency of desilting basin is 90.8 % as evaluated by SSIIM and analytically it is 89.2%

b) Effect of bed roughness

Keeping all parameters constant, inclusive of sediment pick up rate too, bed roughness was varied. In SSIIM bed roughness to individual cells can be provided by writing a file named ‘bedrough’. The roughness height provided to individual bed cells in ‘bedrough’ file overrule the value calculated from manning-Strickler’s coefficient and this file named is kept in the operating folder.
It is assumed that sediment deposited at the bottom of desilting basin makes a slope of 45^0. i.e., angle of repose for sediment deposited is 1:1. So a bed roughness equal to half of the distance in between the openings at the bottom of desilting basin is provided. In prototype distance between openings for flushing is 4.5 m to 6 m. So a deposition height of 2 m is considered. Hence for 1:30 scale model bed roughness equal to $2/30 \cong 0.06$ m is set.

Table 6-7 : Trap efficiency with and without bedrough file

Size no.	Size (mm)	Inflow	Outflow	Without bedrough			With bedrough			analytical
				Suspended	% Reomval	Defect	suspended	% reomoval	Defect	
1	0.210	0.004208	0.000009	0.000081	100%	-5%	0.000081	100%	-5%	100%
2	0.160	0.004208	0.000174	0.000129	96%	-6%	0.000129	96%	-6%	90%
3	0.110	0.004208	0.001069	0.000204	75%	-8%	0.000206	75%	-8%	66%
4	0.063	0.004208	0.002627	0.000278	38%	-15%	0.000281	37%	-15%	36%
	Flux				77%			77%		73%

From the table its evident that there is no particle impact of changing bed roughness, except variation of 1%. In removal of finest particle. Extending our calculation further as earlier done in table 6-3, trap efficiency of desilting basin is 90.8 % as evaluated by SSIIM and analytically it is 89.2%

Also model was run varying with bed roughness equal to three times of d90. This trial also strengthened the earlier inference, except a re-arrangement of active and inactive layer, i.e. combination of deposition and re-suspension is constant.

c) Effect of shield's coefficient

By varying F 11 data set shield coefficient of bed shear for movement of a sediment particle for a average velocity can be calculated according to parameterization of the original curve. Keeping all parameters constant F11 1.32 -0.045 data used, the result is tabulated below:

Table 6-8 : Effect of shield's coefficient over Trap efficiency

Size no.	Size (mm)	Inflow	Outflow	LayerActive	LayerInac.	Suspended	Defect	% Defect	% Removal	
									SSIIM	analytical
1	0.210	0.004208	0.000009	0.000112	0.004244	0.000079	-0.000235	-5.6%	99.8%	100%
2	0.160	0.004208	0.000166	0.000141	0.004051	0.000127	-0.000276	-6.6%	96.1%	90%
3	0.110	0.004208	0.001033	0.000129	0.0032	0.000201	-0.000354	-8.4%	75.5%	66%
4	0.063	0.004208	0.002465	0.000067	0.001903	0.000272	-0.000499	-11.9%	41.4%	36%
	Flux	0.008898	0.002006					Overall removal	77.5%	73%

Result can be compared with 'Table 6-6: (Removal percent with F 37 1)' as all of the parameters and data set are exactly same in both of the cases except the F11 data set. It can be perceived that although overall trapping is not affected due to this parameter, but trapping percentage of finest particle has been increase by 4% and defect has been reduced. As the impact is over only finest particle and which has only 10% share in total sediment, for practical purposes the effect is ignorable.

d) Effect of thickness of the upper active sediment layer

Also to achieve a reduced defect SSIIM was run providing the thickness of the upper active sediment layer. It overrides the original value which is equal to maximum grain size diameter. Thickness height of upper active sediment layer can be given by F 106 data set in control file.

Table 6-9 : Trap efficiency based on predefining upper active sediment layer

Size no.	Size (mm)	Inflow	Outflow	LayerActive	LayerInac.	Suspended	Defect	% Defect	% Removal	
									SSIIM	analytical
1	0.210	0.004208	0.000009	0.000521	0.003814	0.000081	-0.000217	-5.2%	99.8%	100%
2	0.160	0.004208	0.000174	0.00065	0.003511	0.000129	-0.000256	-6.1%	95.9%	90%
3	0.110	0.004208	0.001069	0.000601	0.002688	0.000204	-0.000354	-8.4%	74.6%	66%
4	0.063	0.004208	0.002627	0.000317	0.001634	0.000278	-0.000648	-15.4%	37.6%	36%
	Flux	0.008898	0.00207					Overall removal	76.7%	73%

Extending our calculation further as earlier done in table 6-3, trap efficiency of desilting basin is 91.7 %. There is little impact of this data set over trapping percentage and also defect remains unchanged. It can be compared with Table 6-6.. In both of the cases each and every parameter is same except the thickness of upper active sediment layer. In table 6-6 it is equal to maximum grain size and intable 6-7 it is 001 m. As the flow velocity is quite low and as seen from velocity vector from water flow calculation that after inlet zone there is no eddies, so even by varying upper active sediment layer there is no impact over amount of re-suspension or deposition.

e) Applying correction for sloping bed

The bottom of desilting basin have slope in longitudinal and transverse direction. while performing sediment flow calculation Critical shear stress obtained from shield's curve can be modified by using F 7 B data set.

Table 6-10 : Effect of sloping bed over Trap efficiency

Size no.	Size (mm)	Inflow	Outflow	LayerActive	LayerInac.	Suspended	Defect	% Defect	% Removal	
									SSIIM	analytical
1	0.210	0.004208	0.000013	0.000099	0.004235	0.000098	-0.000237	-5.6%	99.7%	100%
2	0.160	0.004208	0.000215	0.000126	0.004044	0.000152	-0.000328	-7.8%	94.9%	90%
3	0.110	0.004208	0.001304	0.000112	0.003126	0.000232	-0.000566	-13.5%	69.0%	66%
4	0.063	0.004208	0.003405	0.000053	0.001713	0.00031	-0.001273	-30.3%	19.1%	36%
	Flux	0.0089	0.002415					Overall removal	72.9%	73%

It is seen that there is good impact of this data set. The trap efficiency of two finest particles have been reduced and defect percentage has been increased by 50% and 150% for size no. 3 and 4 respectively. So a trial was made with higher number of iterations and it was observed that trap efficiency increases and defect percent reduces as number of iterations goes on higher, and reach a steady condition slowly. As one fourth of height of settling basin has a sloping face toward centre. The correction imparted over critical shear stress due to it for finest particle is considerable.

In general the trapping percentage obtained from SSIIM is in harmony with analytical results. The deviations can be explained as follow:
In SSIIM the trapping percentage of each individual particle is calculated and to get total trap efficiency it is summed up and fall velocity of individual particle is given as input. In practice sediment is consistent of varying particle size and not a mixture of few particular sizes of particles. So each particle as given in SSIIM is a representative of group of particles having size around it. We have divided sediment grain size distribution curve in equal ten parts and each fraction is represented by a particular size.
Also in practice when finer particles settle they settle in a group and settling velocity is more than settling velocity of individual particle.
All above approximations may result in small deviations, which is also evident here.

6.2.3 Simulation of prototype

With 20 % of the flow as flushing flow, prototype desilting basin is simulated. In simulation Flushing flow is passed through uniform opening at the bottom of basin. The area of opening is equal to area of one middle cell in plan.

Analytically by Vetters method trap efficiency is calculated. By vetters method trap efficiency is $\eta = 1 - e^{-(wA_s/Q)}$

Where A_s = surface area (m^2)
Q = flow (m^3/s)

As out of 57 m^3/s inflow 11.4 m^3/s is passing uniformly through flushing channel so average inflow is 51.3 m^3/s. Its assumed that 20% of the flow which passes through flushing channel, also carries the amount of sediment load which it was carrying before entering into the basin. Based on this we have theoretical trap efficiency as in following Table. Also particle sizes are not based on real observation. Its obtained from the relationship curve between sediment particle diameter for prototype and physical model as shown in annexure 6-3.:

Table 6-11 : Trap efficiency for prototype by Vetters method

Size no.	Fall Diameter (mm)	Fall Velocity (m/s)	w.As/Q	η (%)	η (%) Including flushing flow
1	0.266	0.0420	2.85	94.2	96
2	0.172	0.0180	1.22	70.5	76
3	0.110	0.0083	0.56	43.0	55
4	0.070	0.0043	0.29	25.3	41

Table 6-12 : Trap efficiency for Prototype by SSIIM

Size no.	Size (mm)	Inflow	Outflow	LayerActive	LayerInac.	Suspended	Defect	% Defect	% Removal	
									SSIIM	Analytical
1	0.266	10.754717	0.053427	0.002274	9.131689	0.918531	0.648796	6.0%	100%	96%
2	0.172	10.754717	0.719874	0.050483	6.852262	2.14647	0.985629	9.2%	93 %	76%
3	0.110	10.754717	2.83977	0.000458	3.962376	3.239306	0.712807	6.6%	74 %	55%
4	0.070	10.754717	4.798149	-0.053214	2.177985	3.808952	0.022846	0.2%	55 %	41%
	Flux	45.853806	12.429546					Overall removal	78%	67%

As the simulation has been run only for lower four grain size and it is evident that particles having diameter more than 0.2658 mm are removed 100%. On this basis if we extend our calculation to find out total trap efficiency of desilting basin as done earlier, we have trap efficiency desilting basin is 92.20 %. As per the theoretical calculation it is 86.6%

Table 6-13 : Trap efficiency based on the trapping percent of four smallest grain sizes for prototype

Sl. No.	Particle dia (mm)	% of total sediment	Sediment removal	
			% of fraction	% of total
1	0.063	10	55%	5.5
2	0.11	10	74%	7.4
3	0.16	10	93%	9.3
4	0.21	10	100%	10
5	Dia> 0.210	10	100%	10
6	Dia> 0.210	10	100%	10
7	Dia> 0.210	10	100%	10
8	Dia> 0.210	10	100%	10
9	Dia> 0.210	10	100%	10
10	Dia> 0.210	10	100%	10
			Total	92.20

7 CHAPTER

CONCLUSION AND RECOMMENDATION

7.1 CONCLUSION

In water resource sector science of CFD modeling of sediment transport is in research stage. SSIIM is freely available powerful software to evaluate many problems associated with fluid dynamics. The results and its interpretation included in this thesis work are carried out in five months. Trap efficiency and deposition pattern for a physical model and prototype of a desilting basin has been determined and compared with physical model study. Full desilting basin plan, i.e., three desilting basins in parallel with part of HRT was in study but due to time constraints it can be added here. The conclusion of study is as follow:

7.1.1 SSIIM SCOPE

SSIIM has plenty of scope. It can be used for desilting basin, reservoirs, local scour, intakes, bends, meandering channels etc and has given satisfactory results. In this thesis work a fraction of it has been used. SSIIM 1, i.e., only structured grid is used in study to evaluate trap efficiency of desilting basin.

For determining the water flow, sediment transport, trap efficiency, bed deposition and its pattern SSIIM can be used effectively at all stages of project. i.e., from project planning stage to operational stage.

Care is required to prepare grid and control file. Convergence depends on proper planning of grid and choosing the appropriate parameters. Some trials may be needed to achieve appropriate parameters, different from default value.

Results have impact of numerical approximation and obviously of input data. So results have to be interpreted and perceived carefully before using it.

With fineness of grid simulation time increase, so judicially a optimum cell size can be selected without affecting accuracy.

7.1.2 DESILTING BASIN

Desilting basin as proposed by physical model study for Tala H.E. Project is found adequate for removal of particle 0.2 mm and greater size with 2000 ppm concentration.

Recirculation has been observed near inlet zone, which changes from one side of basin to other side of basin, as we move from lowest point to highest point in a cross section.

Defects in percent is lower in case of prototype simulation than of physical model.

Effect of different parameters have been studied and its found that the finest particle is sensitive to most of them and coarser particles don't feel any impact.. The impact of side slope by varying F7 data set over finest grain size is much, it has further scope of study.

Results obtained by simulation of physical model and of prototype both are in accordance to results obtained from physical model study and analytical calculation.

7.2 RECOMMENDATION

Its strongly recommended for further study. SSIIM has great potential. The results obtained from long term simulation of deposition provide useful information. While simulation is on, results can be seen and perceived pictorially as well as in text form.

Number of geometries can be tried with SSIIM and it can be modified based on the results obtained. Nicety is that, this can be done in a very short duration. Various flow, various concentration can be applied and effect of it and efficiency can be evaluated. Different grain size curves also can be applied. All these trials can be performed with different combinations.

There was no real time based grain size distribution curve available for sediment. On getting it an enhanced study for prototype can be done. There is plenty of scope of study with varying flow and with various real time sample based grain size distribution curve.

Moreover a detailed study of flow percent passing through each of the desilting basin and impact of variance in river flow over desilting arrangement and desilting itself can be further studies.

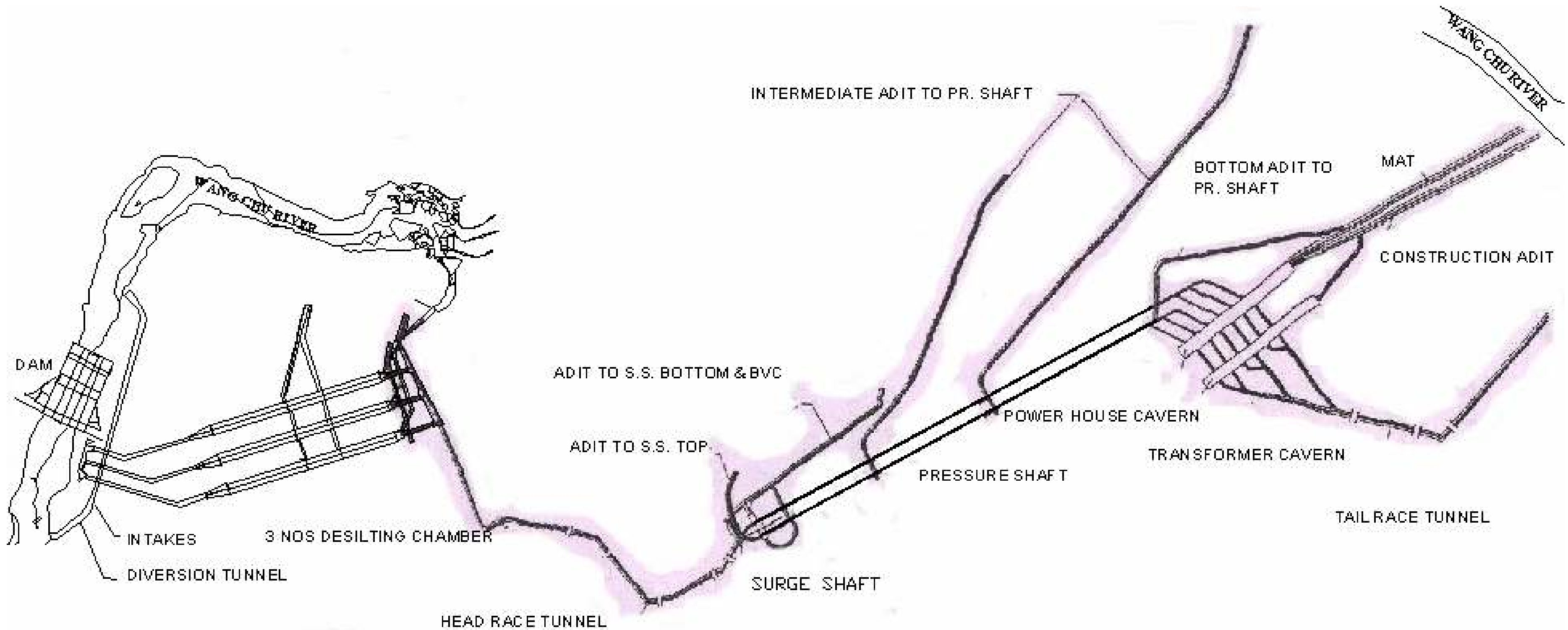

GENERAL LAYOUT PLAN

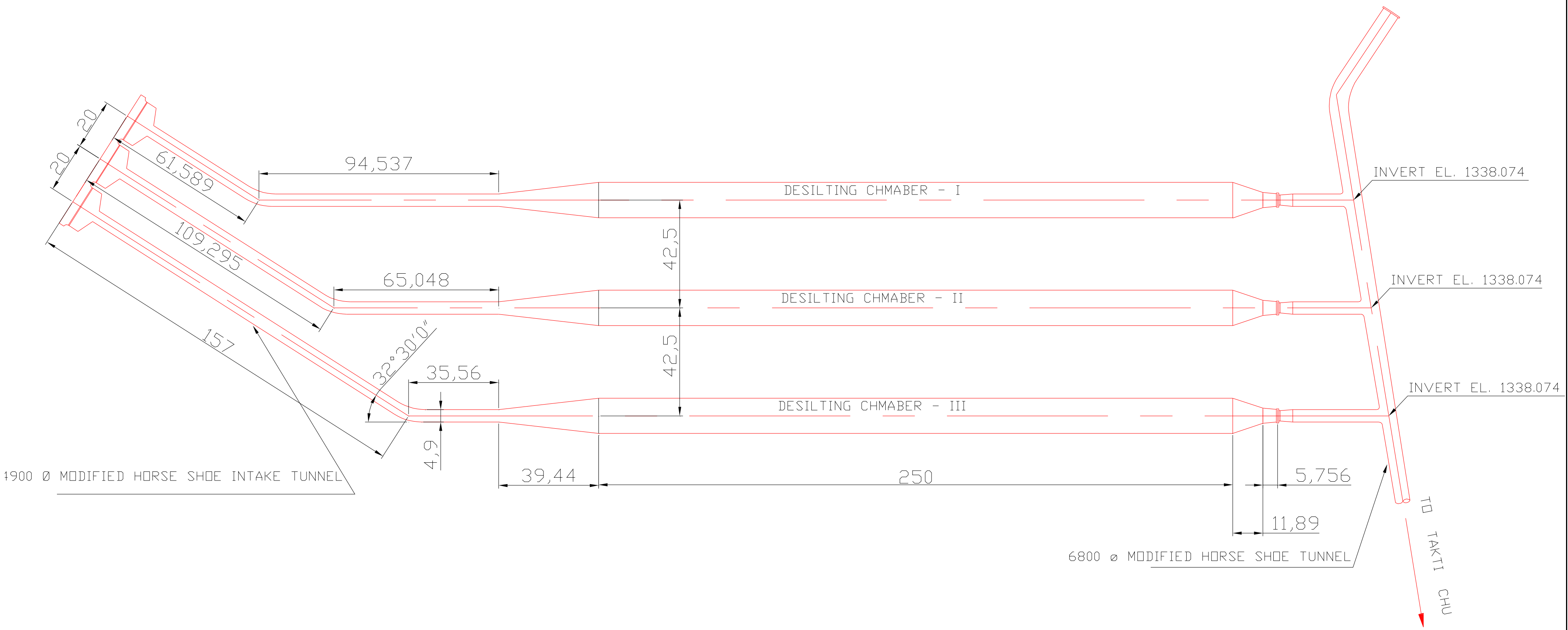

ALIGNMENT OF INTAKE AND DESILTING CHAMBER COMPLEX

NORWEGIAN UNIVERSITY OF SCIENCE AND TECHNOLOGY M.SC. HYDROPOWER DEVELOPMENT		
TALA HYDROELECTRIC PROJECT (BHUTAN), CWC DRAWING		
ALIGNMENT OF INTAKE AND DESILTING BASIN COMLEX		
MAY 2005	NOT TO SCALE	Annexure 3-2

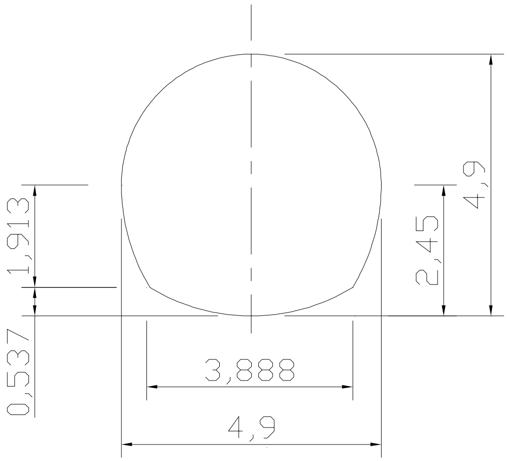

Chainage 0.0

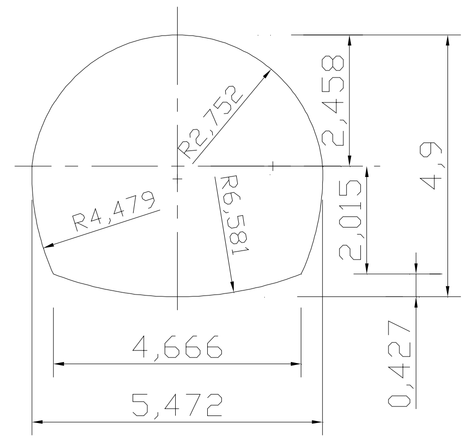

Chainage 2.5

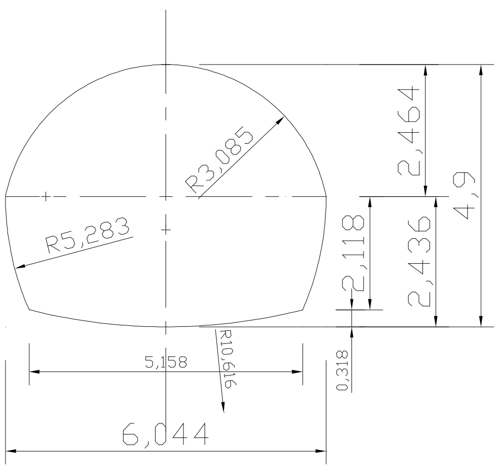

Chainage 5

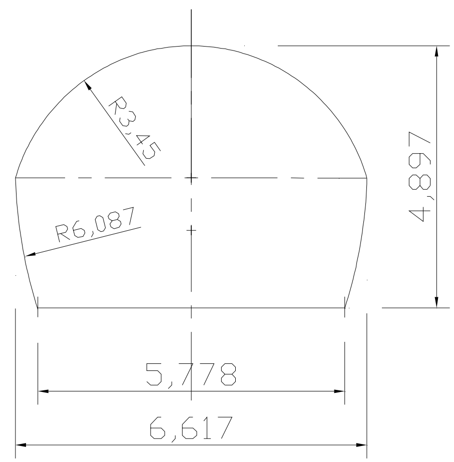

Chainage 7.5

NORWEGIAN UNIVERSITY OF SCIENCE AND TECHNOLOGY
M.SC. HYDROPOWER DEVELOPMENT

TALA HYDROELECTRIC PROJECT (BHUTAN)

Different Cross sections of Desilting Basin

MAY 2005	NOT TO SCALE	Annexure 3-3

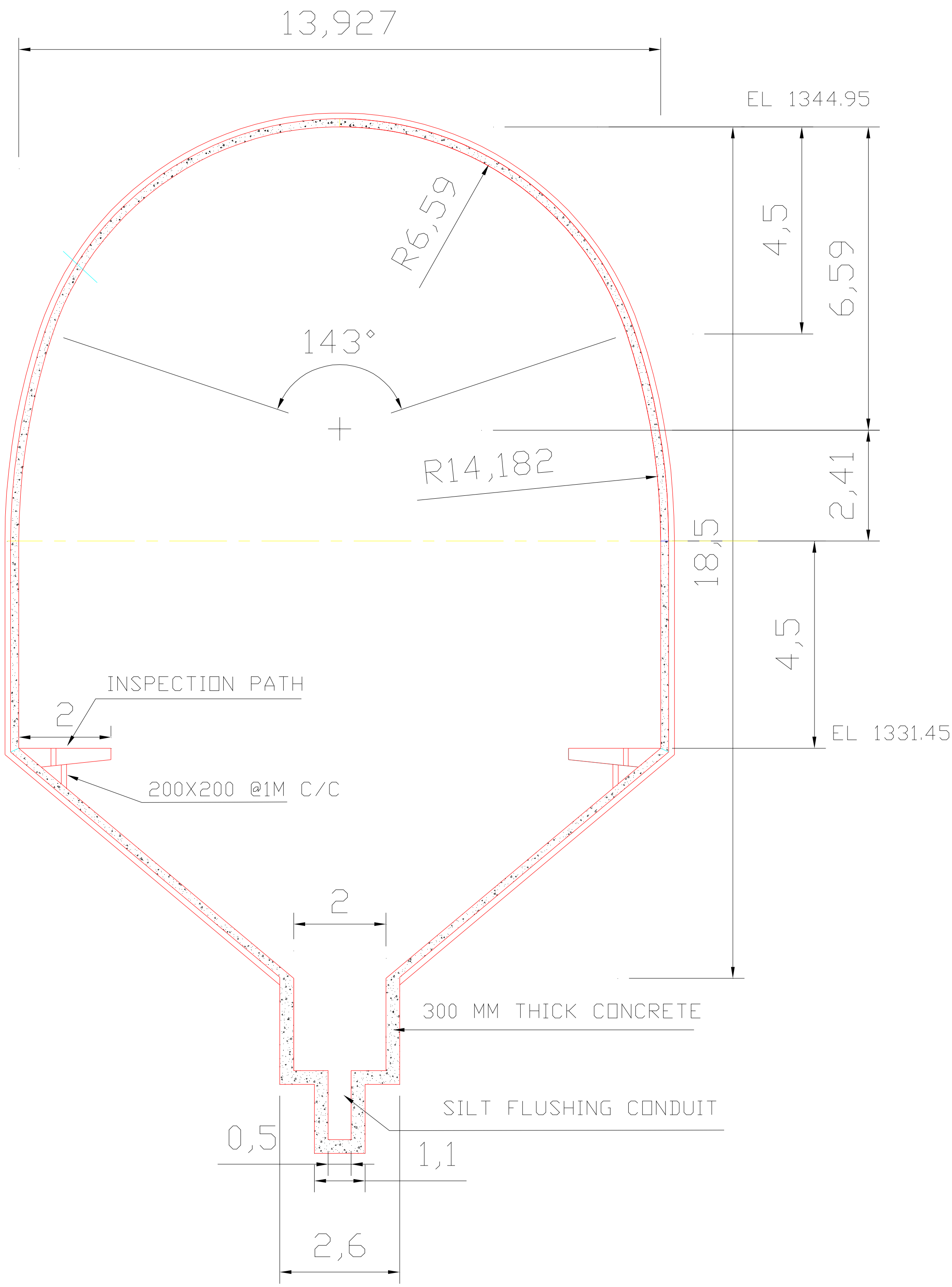

NORWEGIAN UNIVERSITY OF SCIENCE AND TECHNOLOGY
NTNU M.SC. HYDROPOWER DEVELOPMENT

TALA HYDROELECTRIC PROJECT (BHUTAN), CWC DRAWING

CROSS SECTION OF DESILTING CHAMBER

MAY 2005	NOT TO SCALE	Annexure 3-4

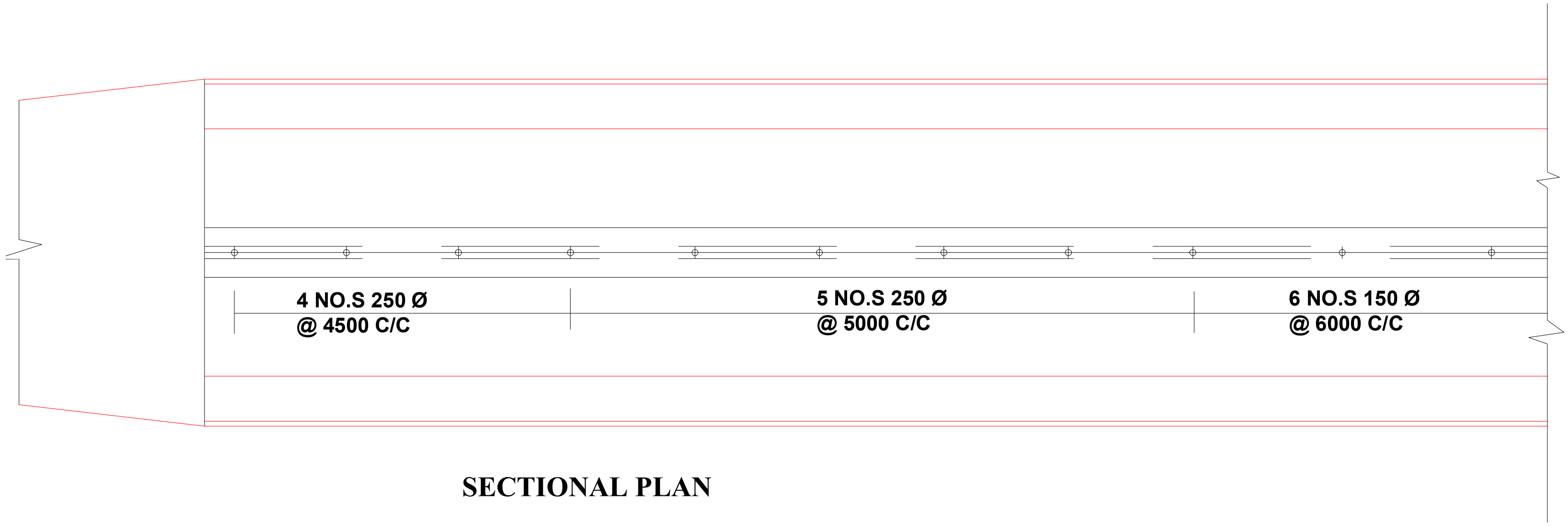

SECTIONAL PLAN

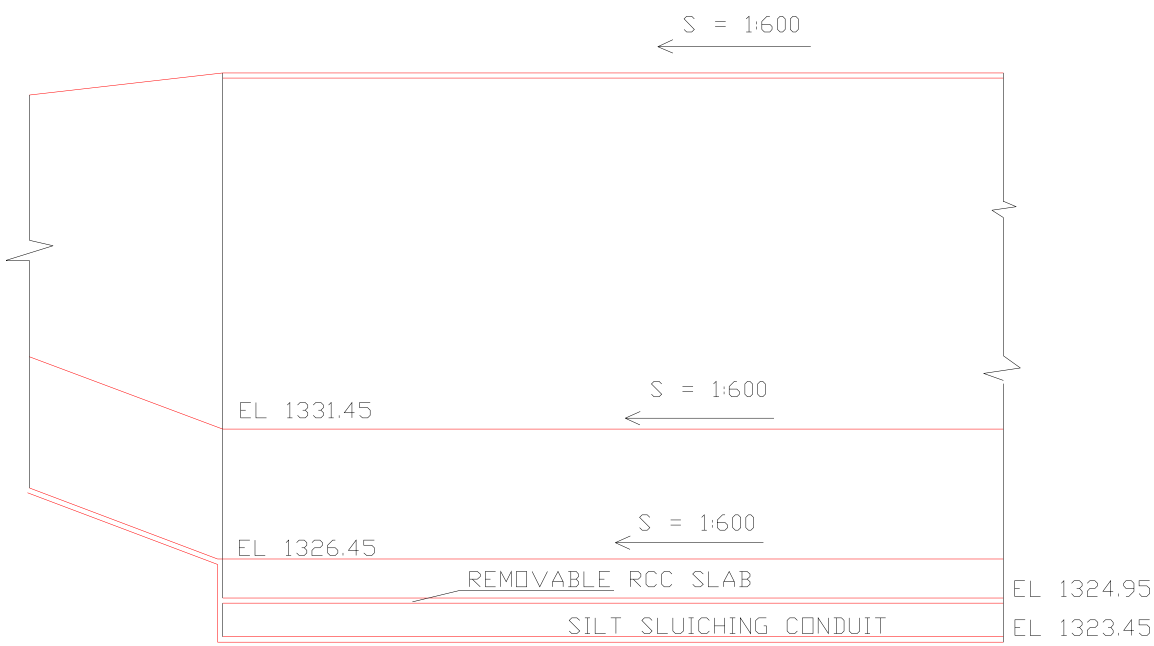

LONGITUDINAL SECTION

NORWEGIAN UNIVERSITY OF SCIENCE AND TECHNOLOGY NTNU M.SC. HYDROPOWER DEVELOPMENT		
TALA HYDROELECTRIC PROJECT (BHUTAN), CWC DRAWING		
TYPICAL PLAN AND SECTION OF DESILTING CHAMBER		
MAY 2005	NOT TO SCALE	Annexure 3-5

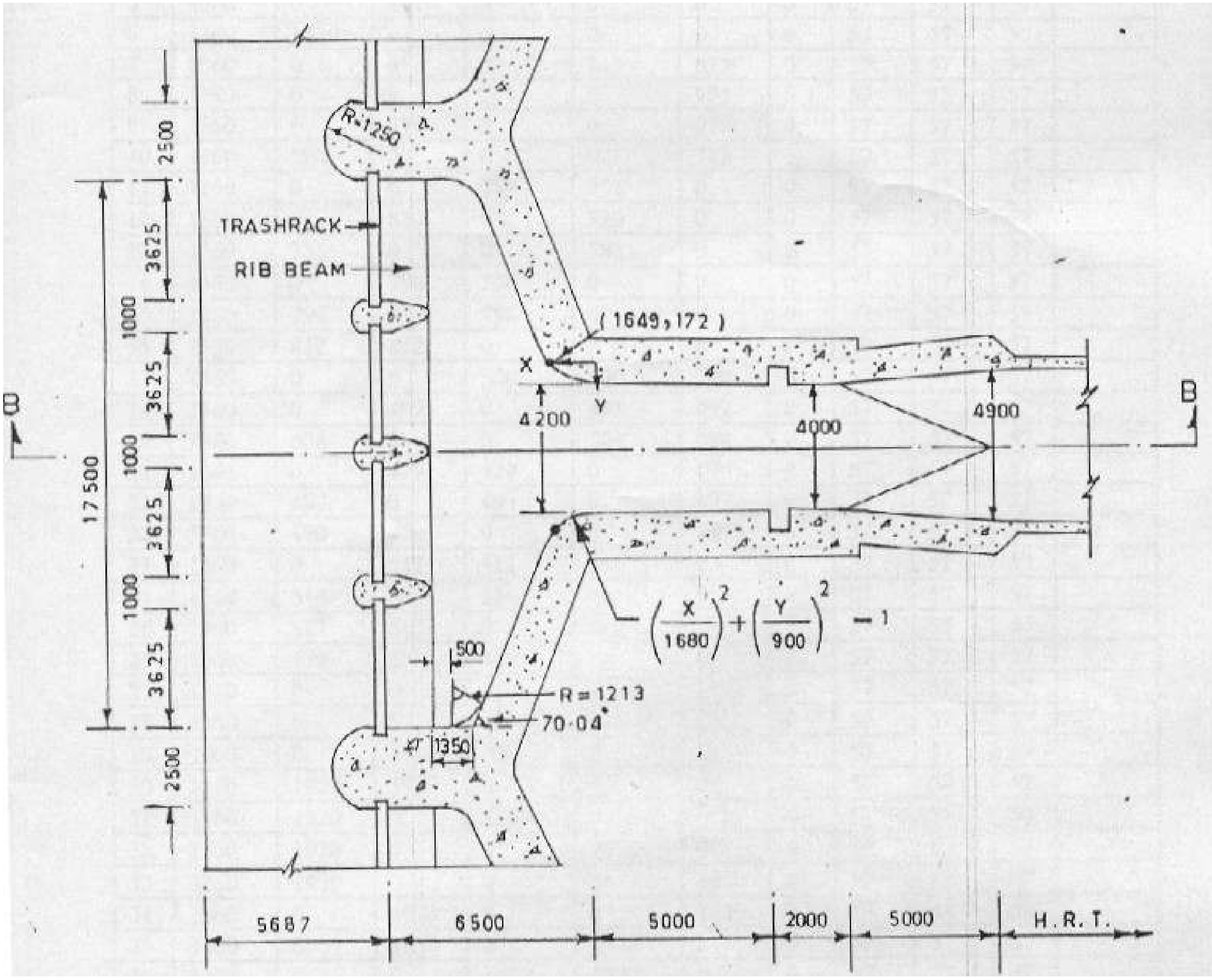

$$\left(\frac{X}{1680}\right)^2+\left(\frac{Y}{900}\right)^2=1$$

PLAN AT A-A

TYPICAL PLAN OF POWER INTAKE

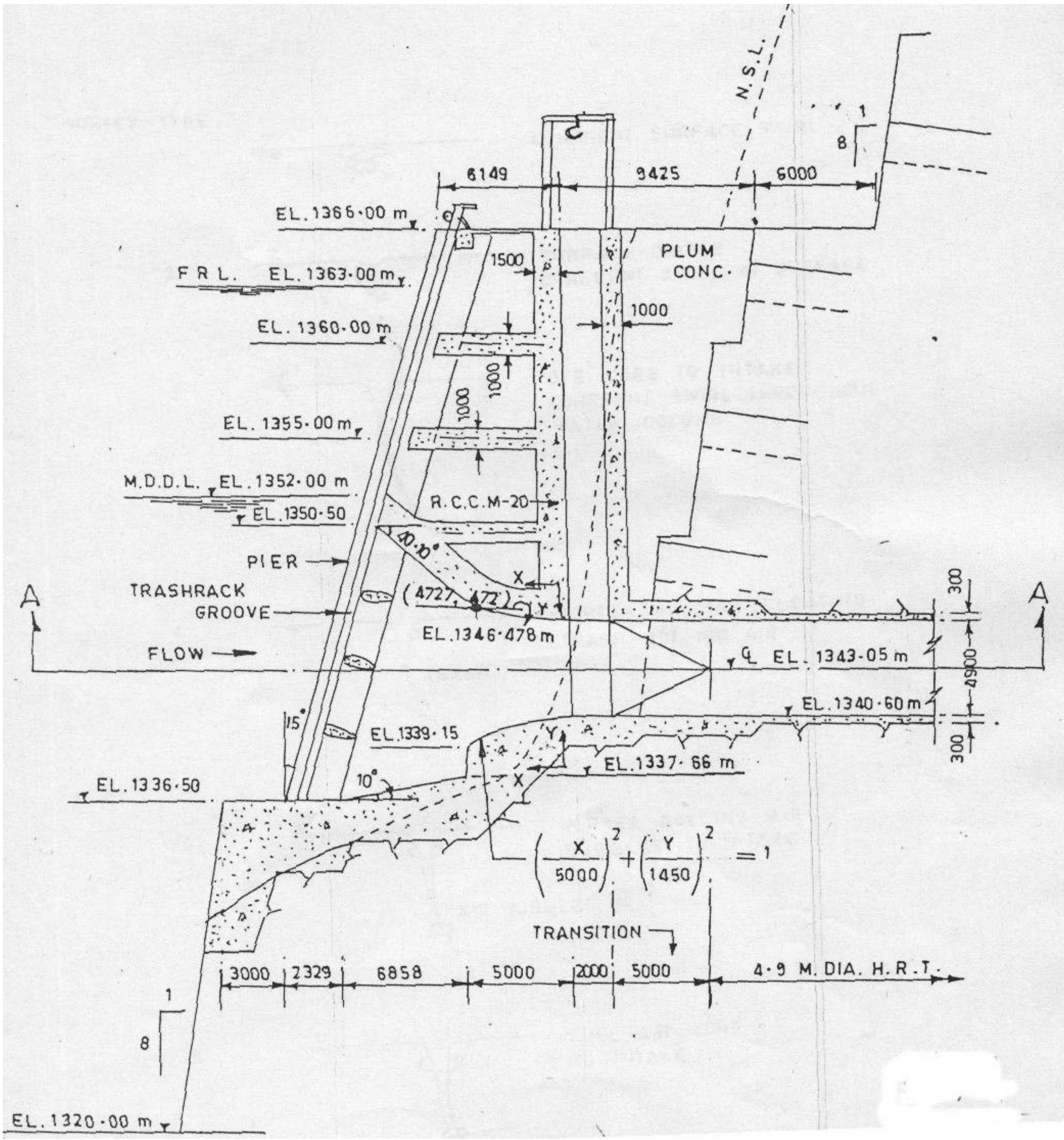

SECTION B-B

TYPICAL SECTIONAL DETAILS OF POWER INTAKE

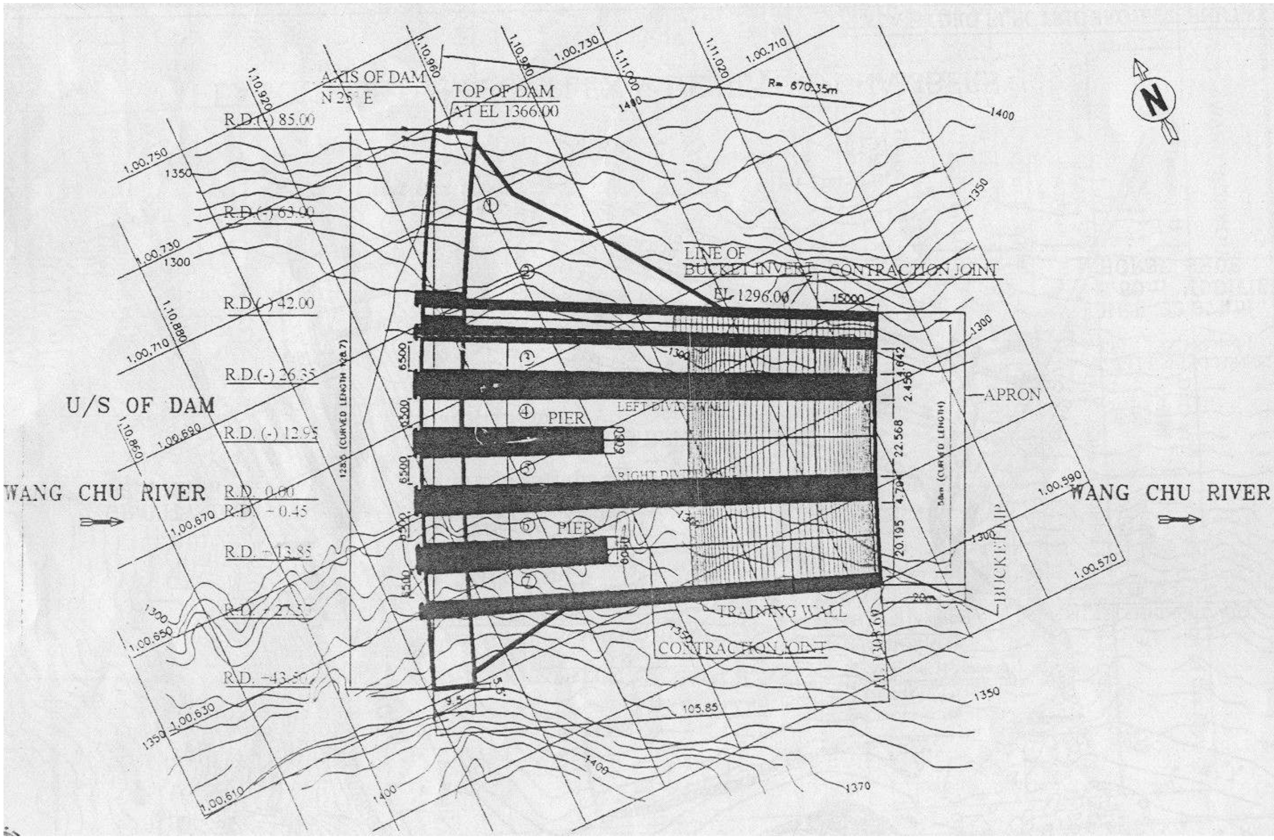

WANGKHA DAM PLAN

(From Salient features and Status of Project, WAPCOS(India, Ltd.)

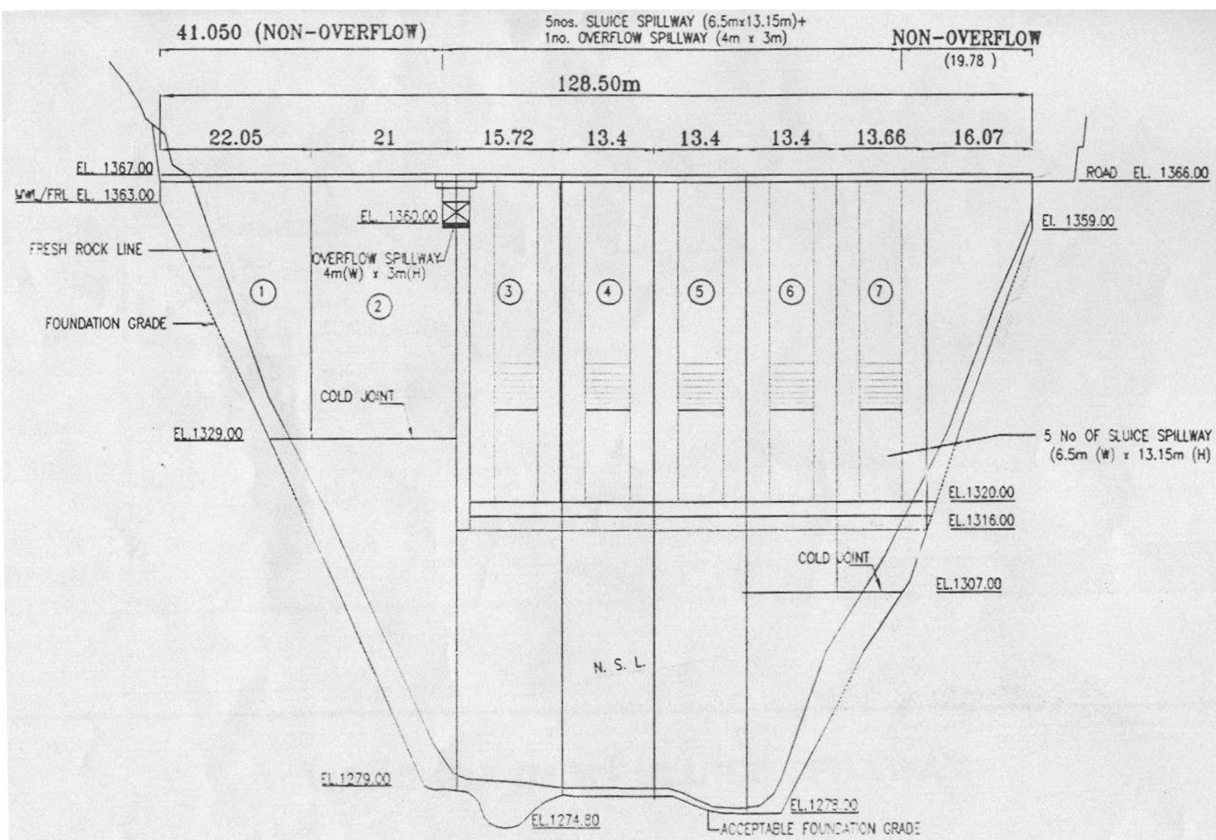

WANGKHA DAM UPSTREAM ELEVATION

(From Salient features and Status of Project, WAPCOS(India, Ltd.)

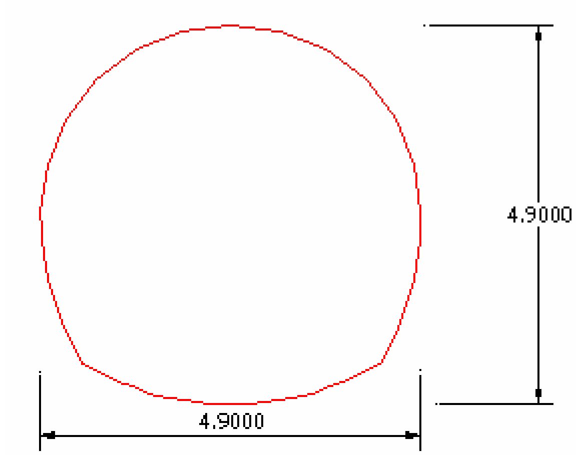

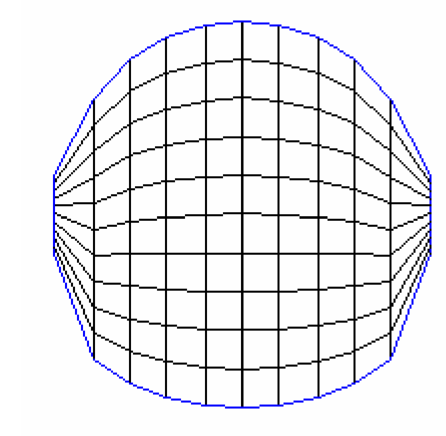

Chainage 0.00: Original cross section and Simulated Cross section

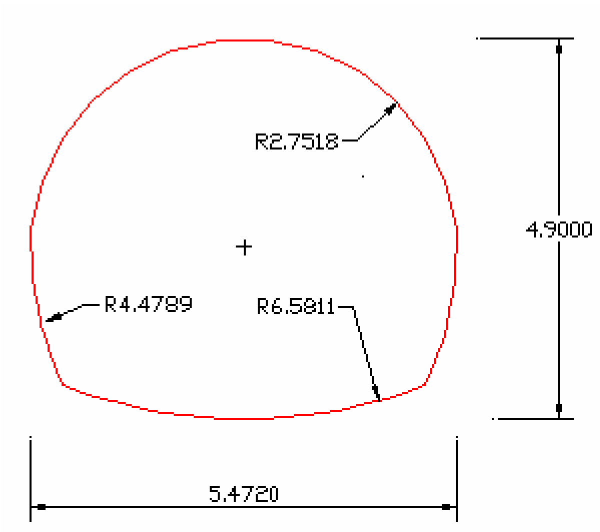

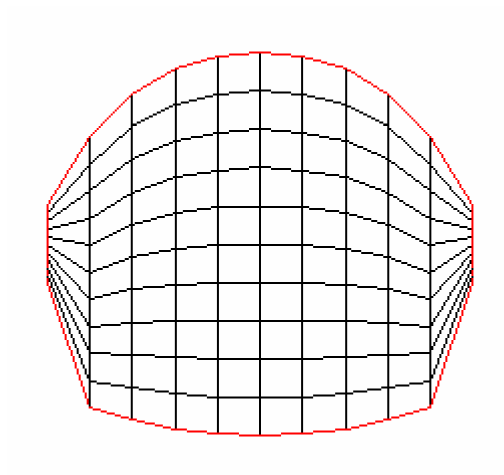

Chainage 2.50: Original cross section and Simulated Cross-section

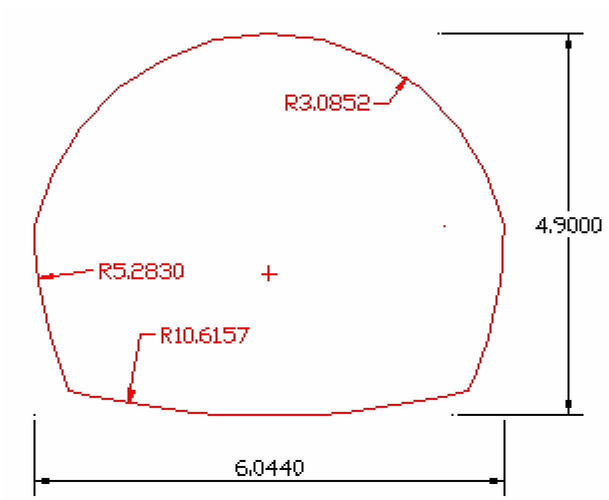

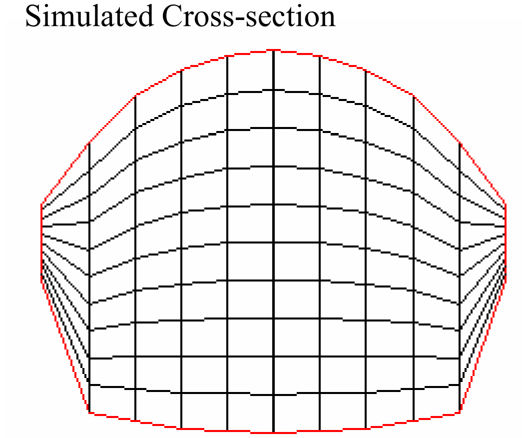

Chainage 5.0: Original cross section and Simulated Cross-section

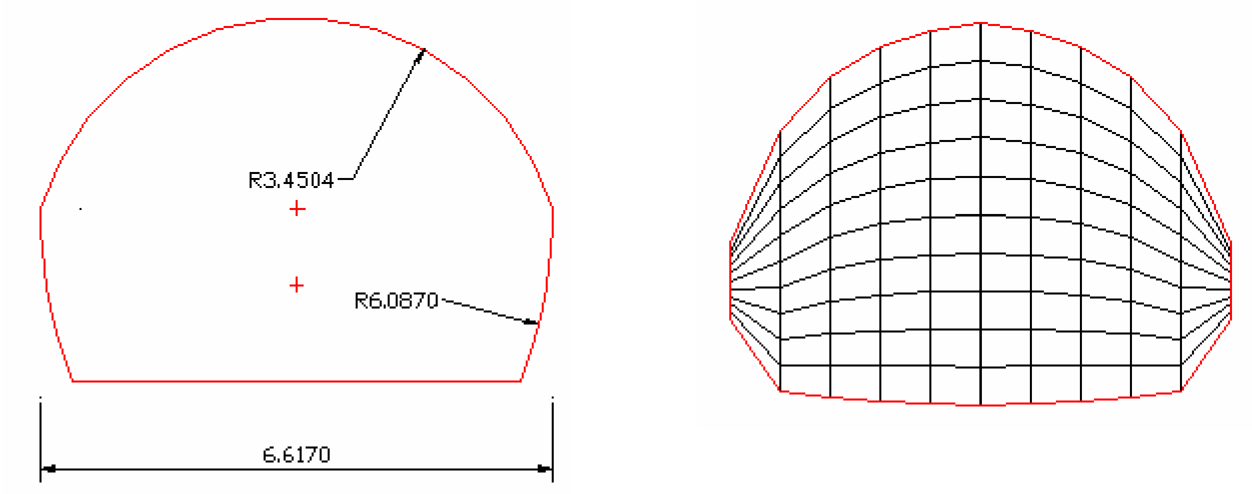

Chainage 7.5: Original cross section and Simulated Cross-section

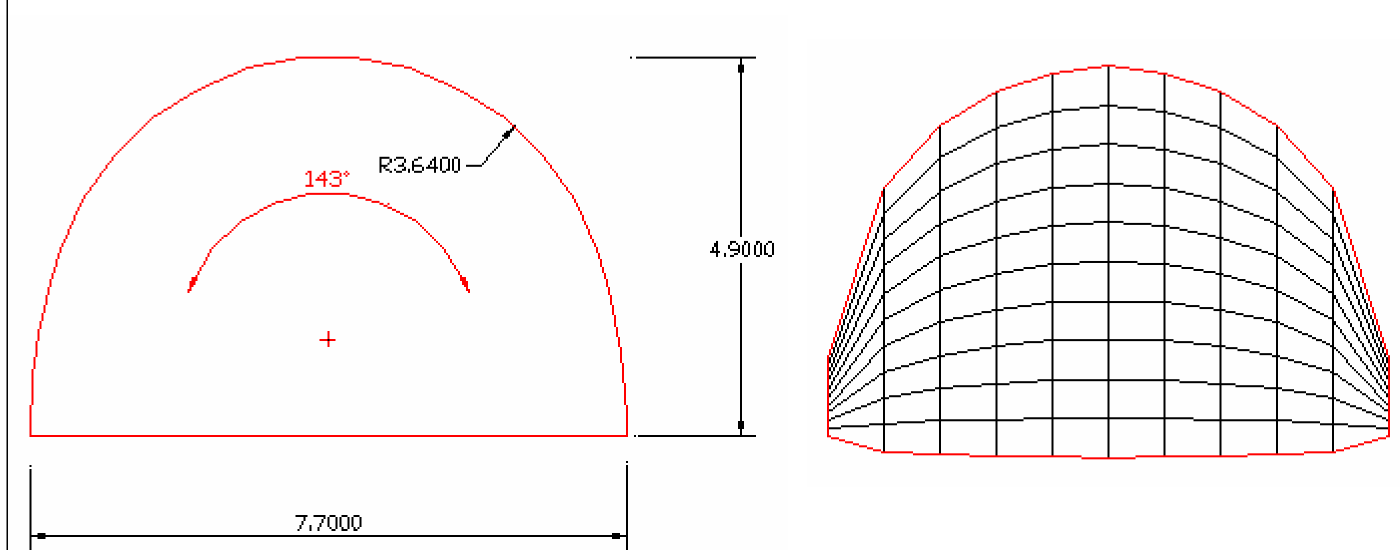

Chainage 12.24: Original cross section and Simulated Cross-section

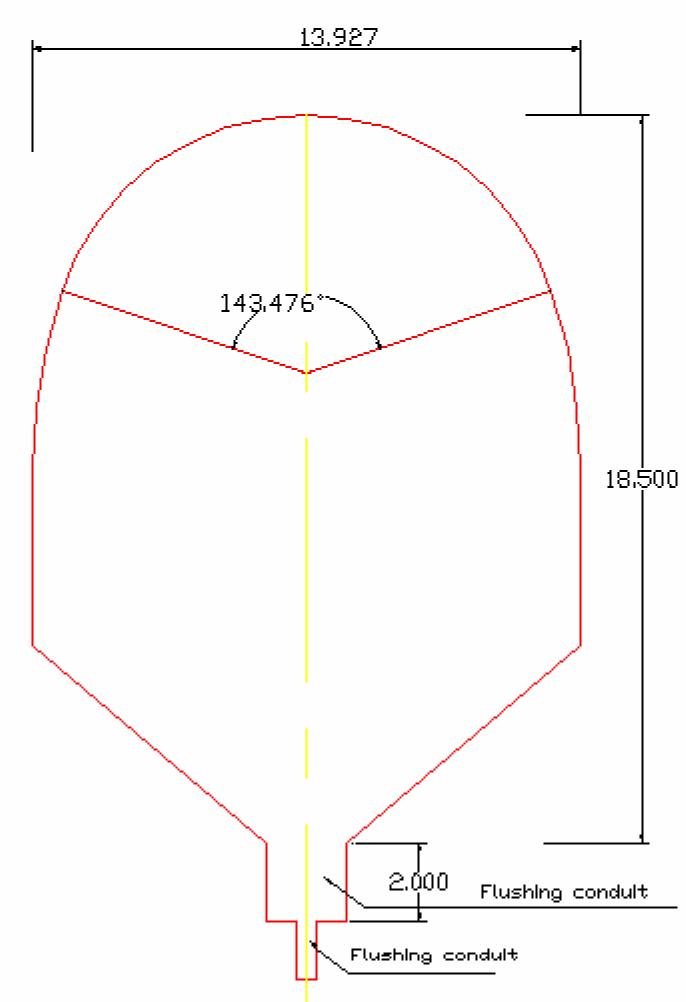

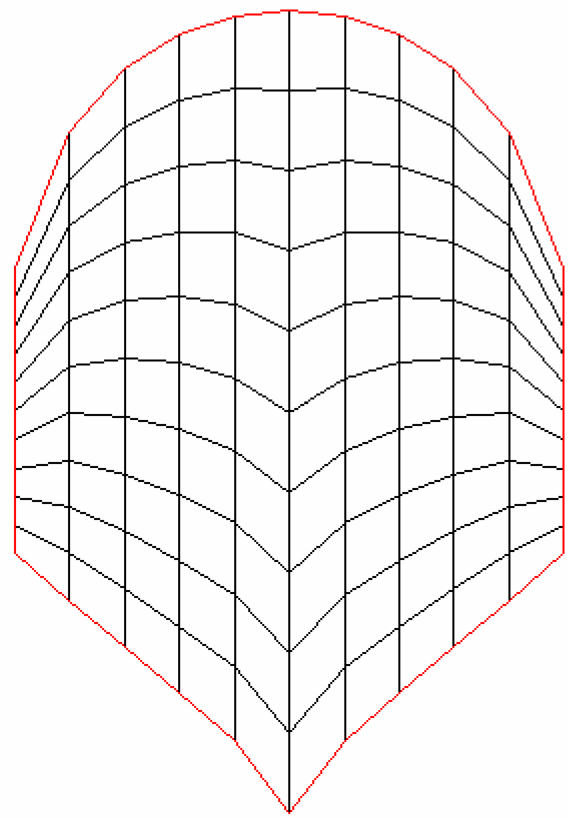

Chainage 39.44: Original cross section and Simulated Cross-section

Note: From chainage 39.44 to 289.44 m i.e. 250 length of settling basin has same cross section through out.

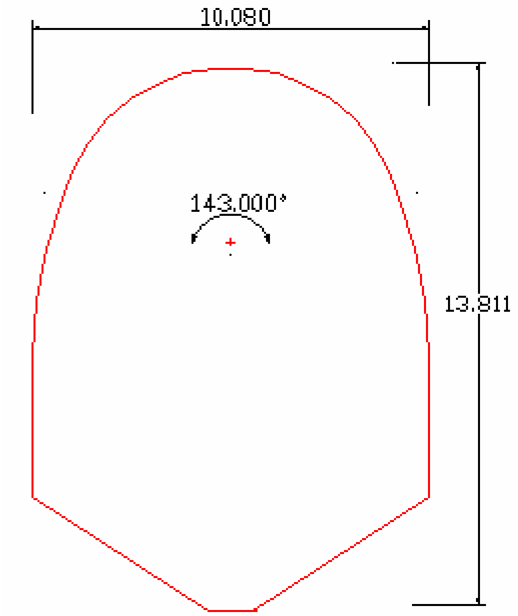

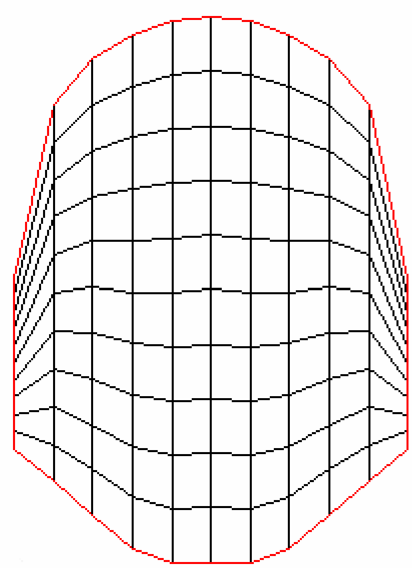

Chainage 297: Original cross section and Simulated Cross-section

TABLE-4

MODEL STUDIES FOR DESILTING BASIN - TALA H.E. PROJECT, BHUTAN

STUDIES WITH DESIGN DISCHARGE

Material injected = 400 litres

Material recovered

Flushing tunnel = 330 litres

H.R.T. = 55 litres

Material washed away = 400-330-55 = 15 litres

Distributing the material washed away in the proportion of discharge

Material washed away through flushing tunnel = 15 x 0.2 = 3 litres

Total material in flushing tunnel = 330 + 3 = 333 litres

$$\therefore \text{ \% Settling efficiency } = \frac{333}{400} \times 100 = 83.25\%$$

Average efficiency on analytical basis (Details of computations for samples 1, 2 and 3 are given in Tables 5, 6 and 7 respectively)

$$= \frac{86.50+86.20+85.20}{3} = 85.96\% = 86\%$$

From Hydraulic Modell studies for desilting Basin, THEP Bhutan (report no.2), Tech report 384, July 2001, CWPRS, Pune

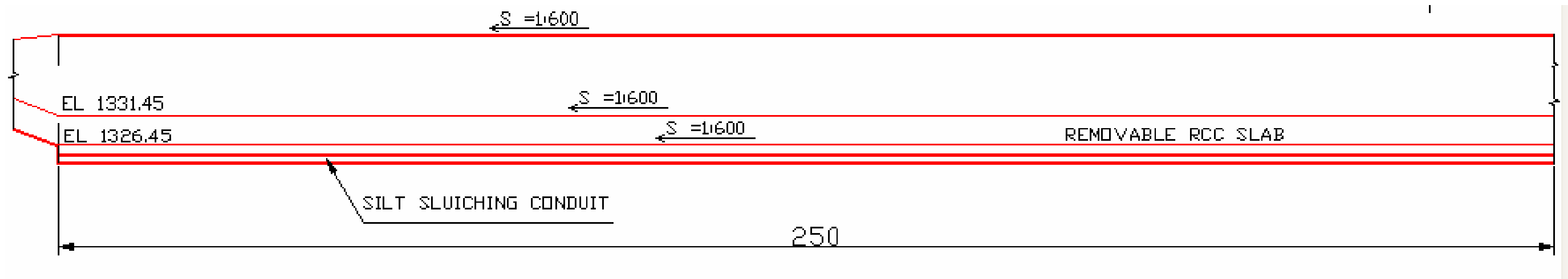

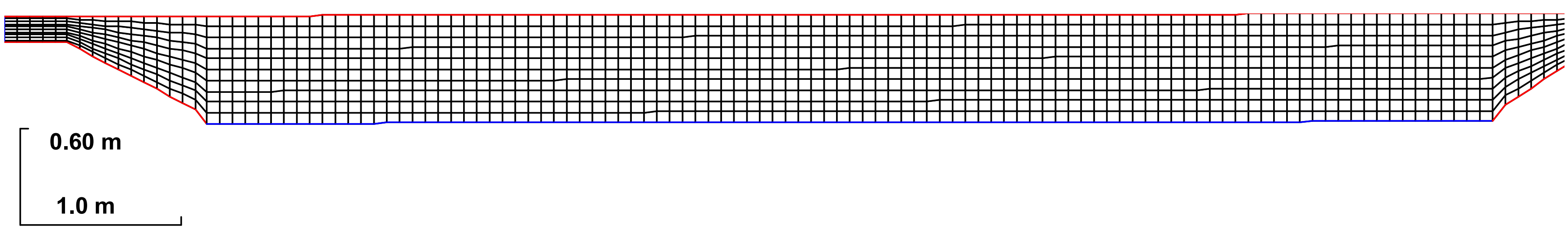

Original and simulated Longitudinal section of desilting basin

VELOCITY VECTOR AT DIFFERENT LEVEL IN X-Y PLANE

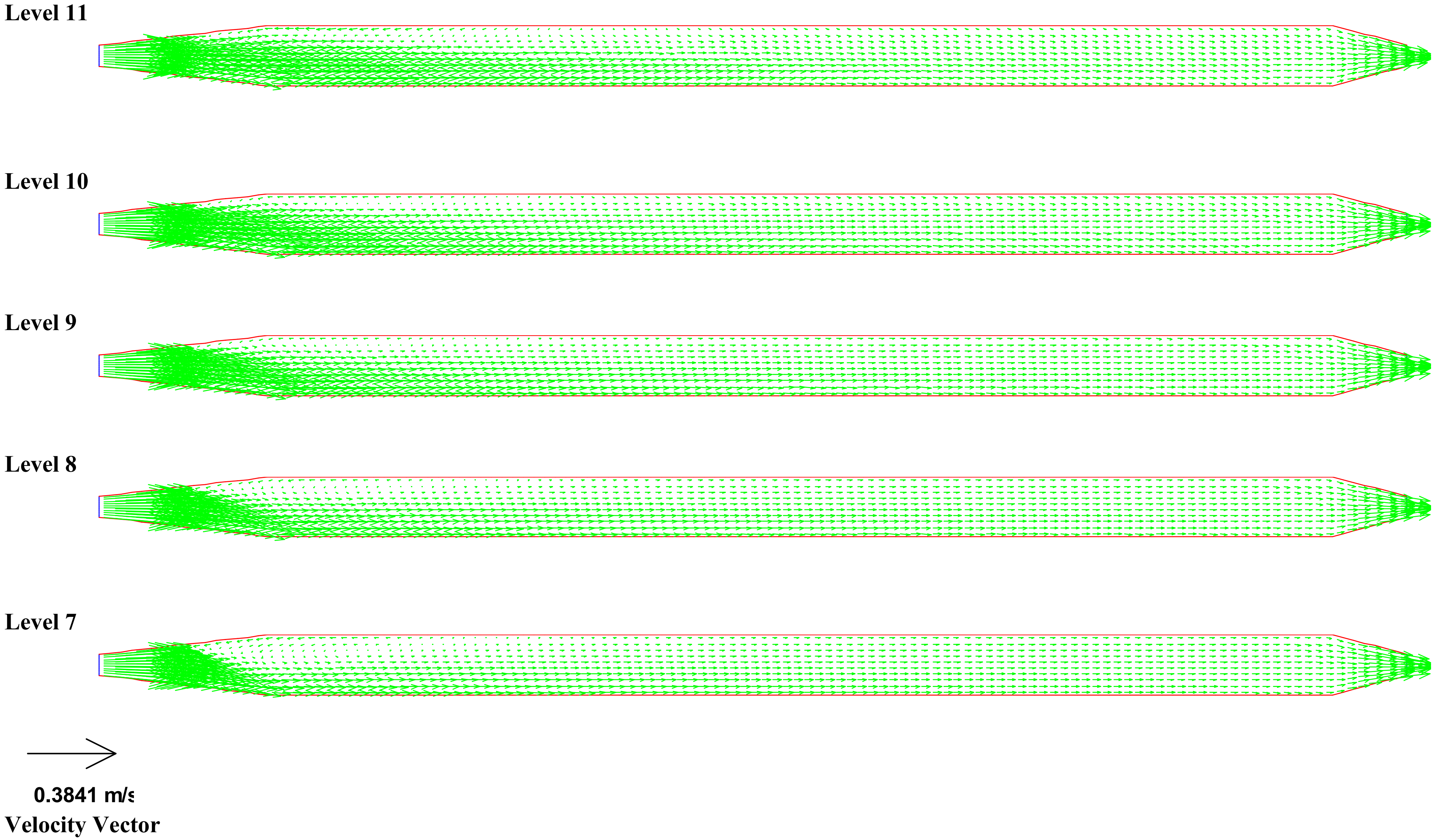

Annexure 5-4

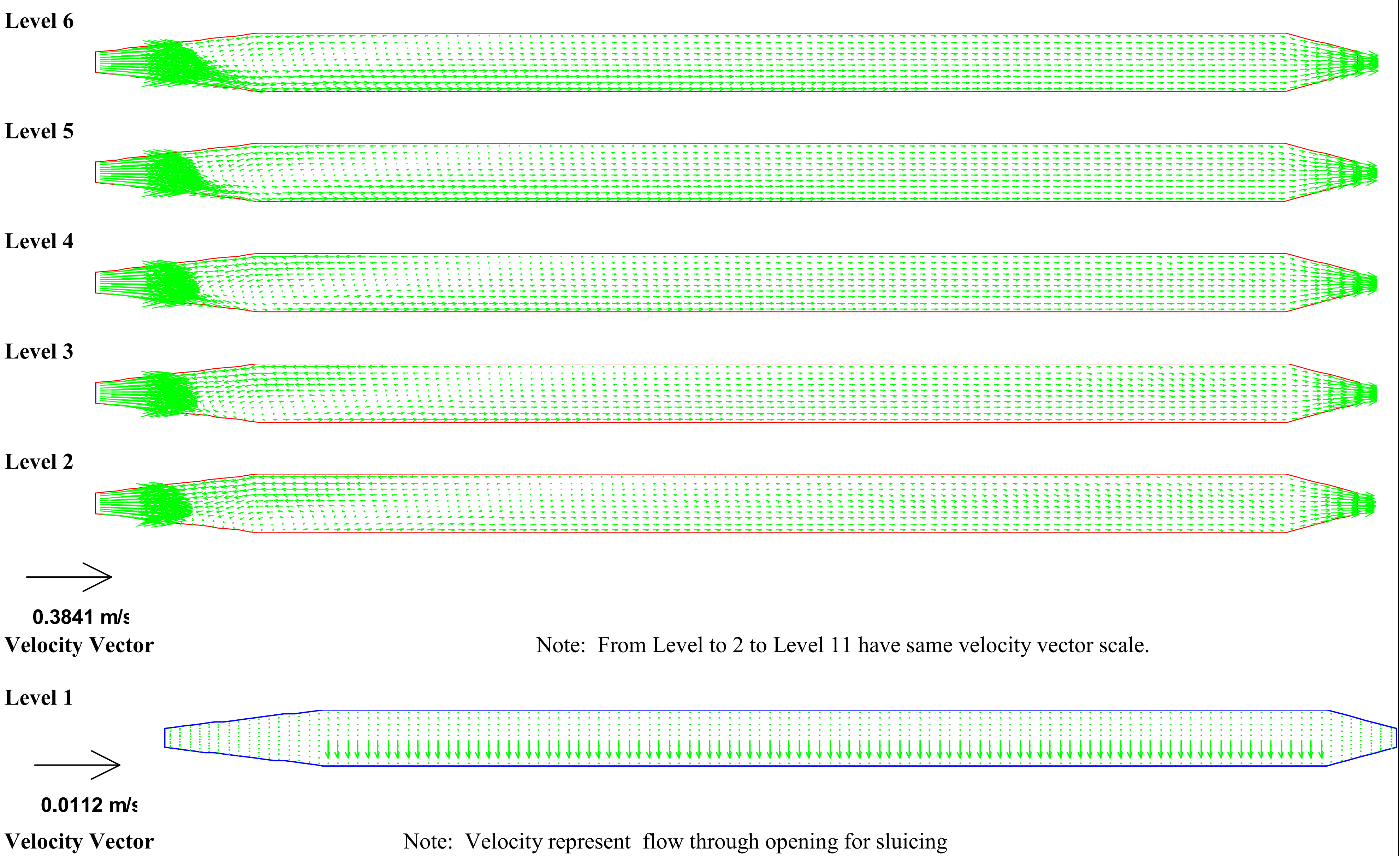

Velocity vector in X-Y Plane

Annexure 5-4

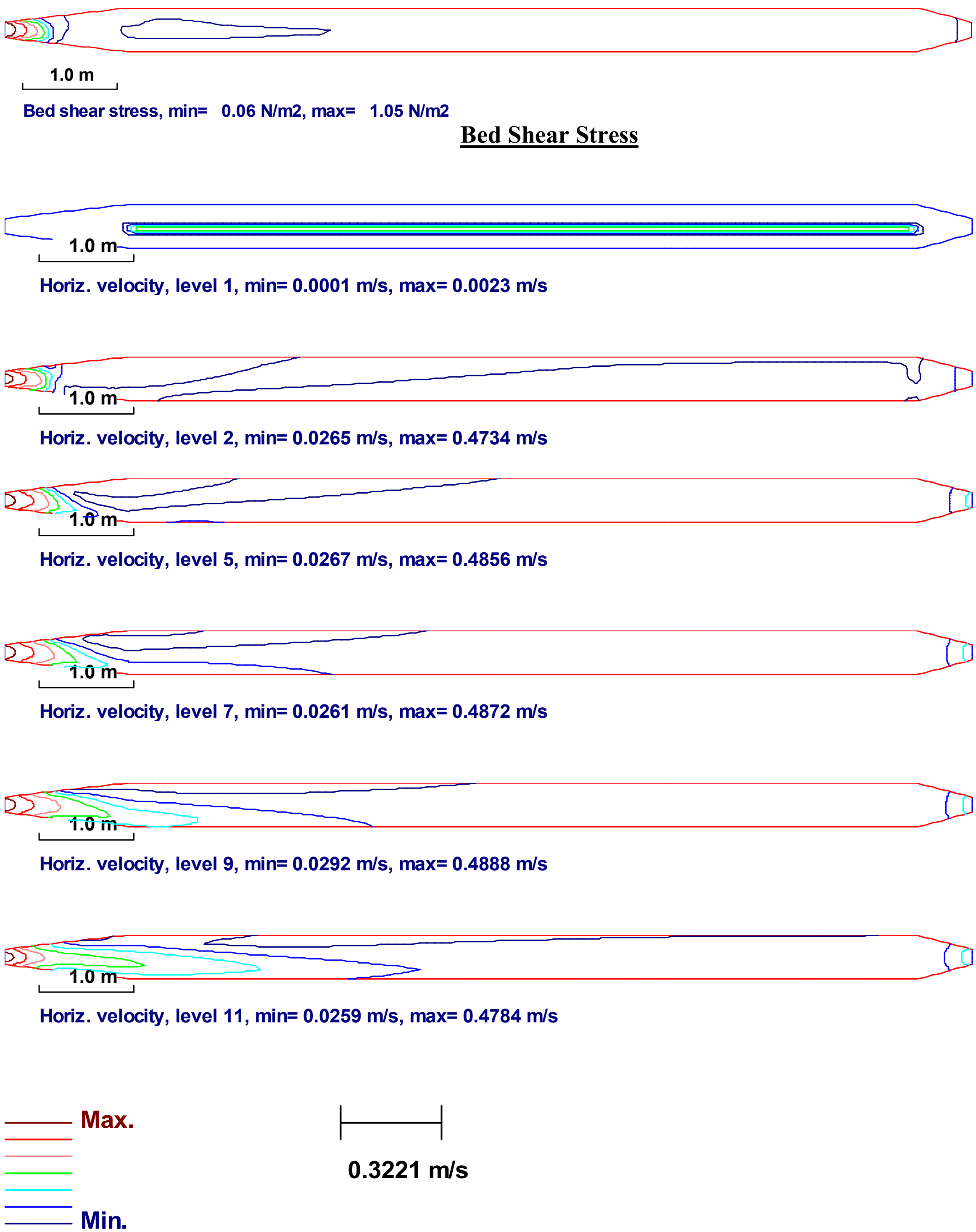

Bed Shear stress and Horizontal velocity profile at different levels (X-Y Plane)

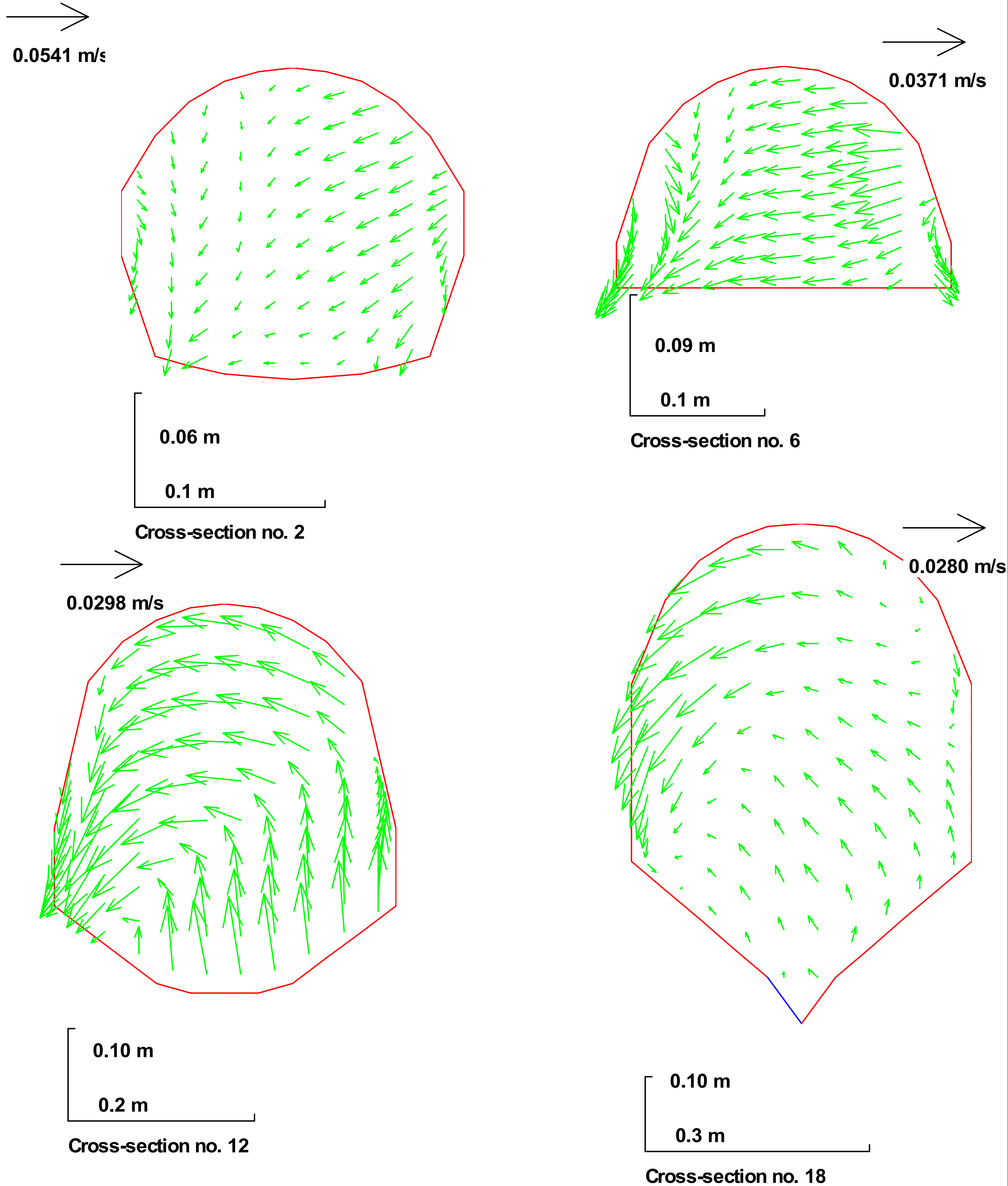

Velocity vector in Y –Z Plane (at different cross sections)

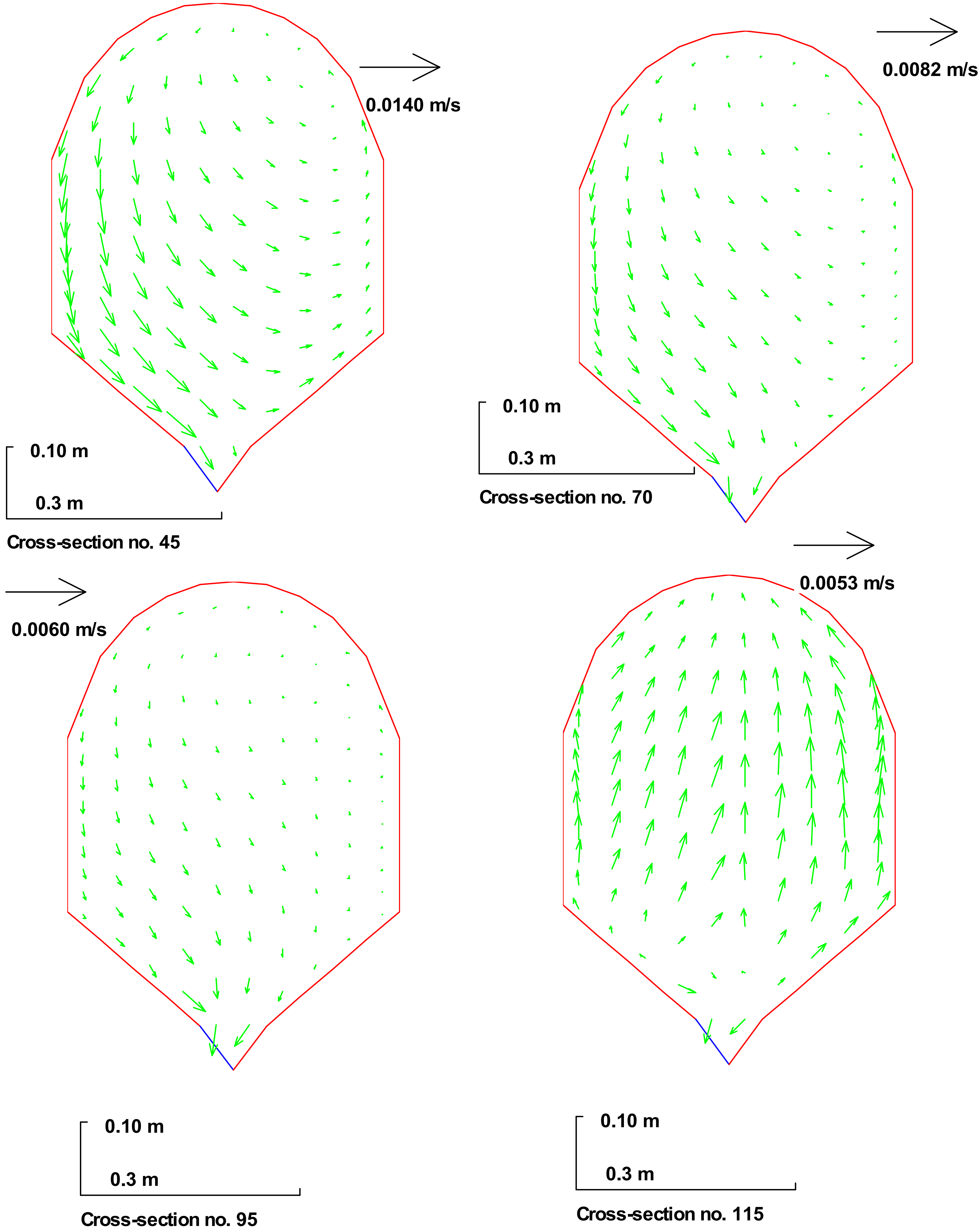

Velocity vector in Y –Z Plane (at different cross sections)

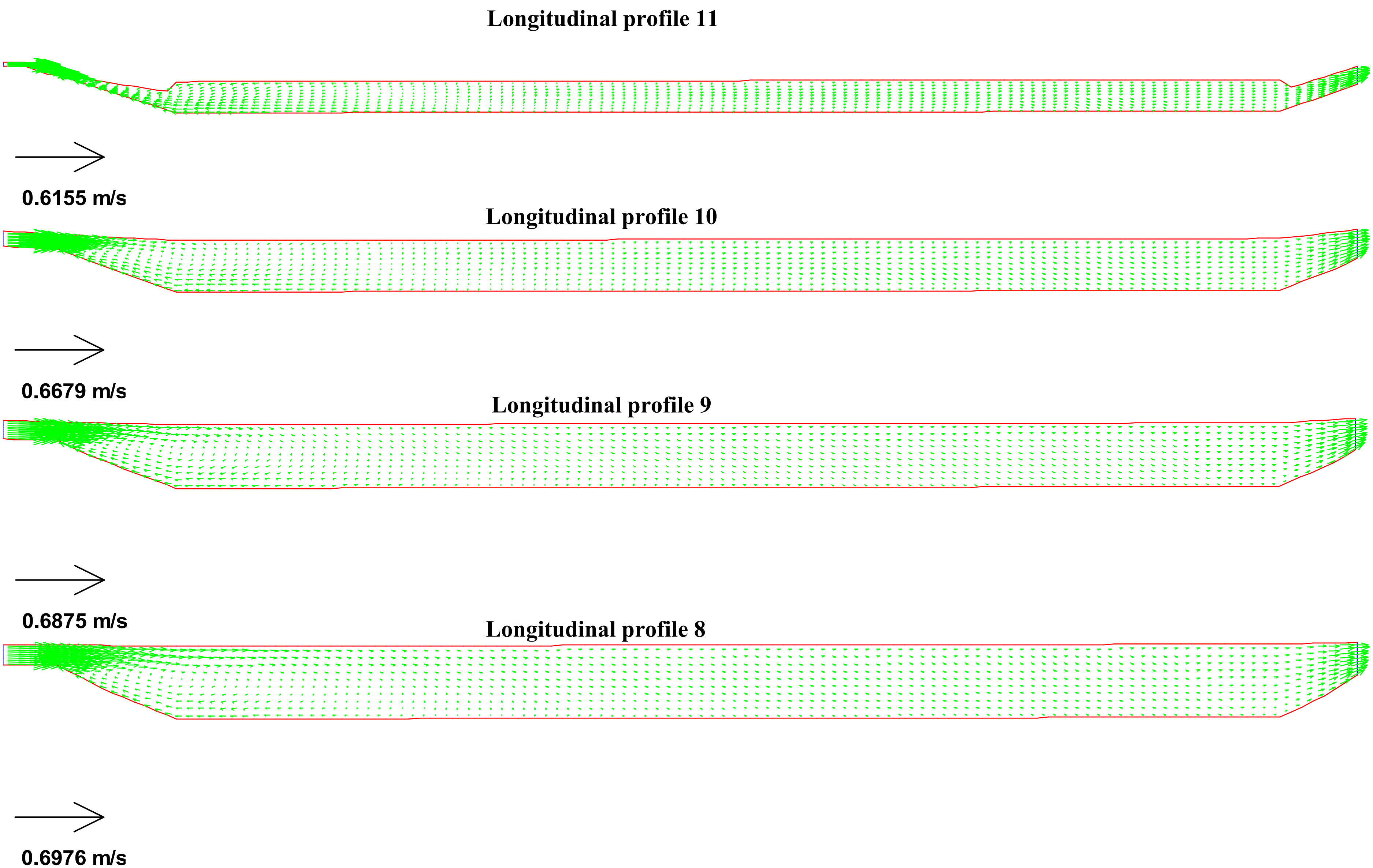

Velocity vector in X-Z plane

Annexure 5-7

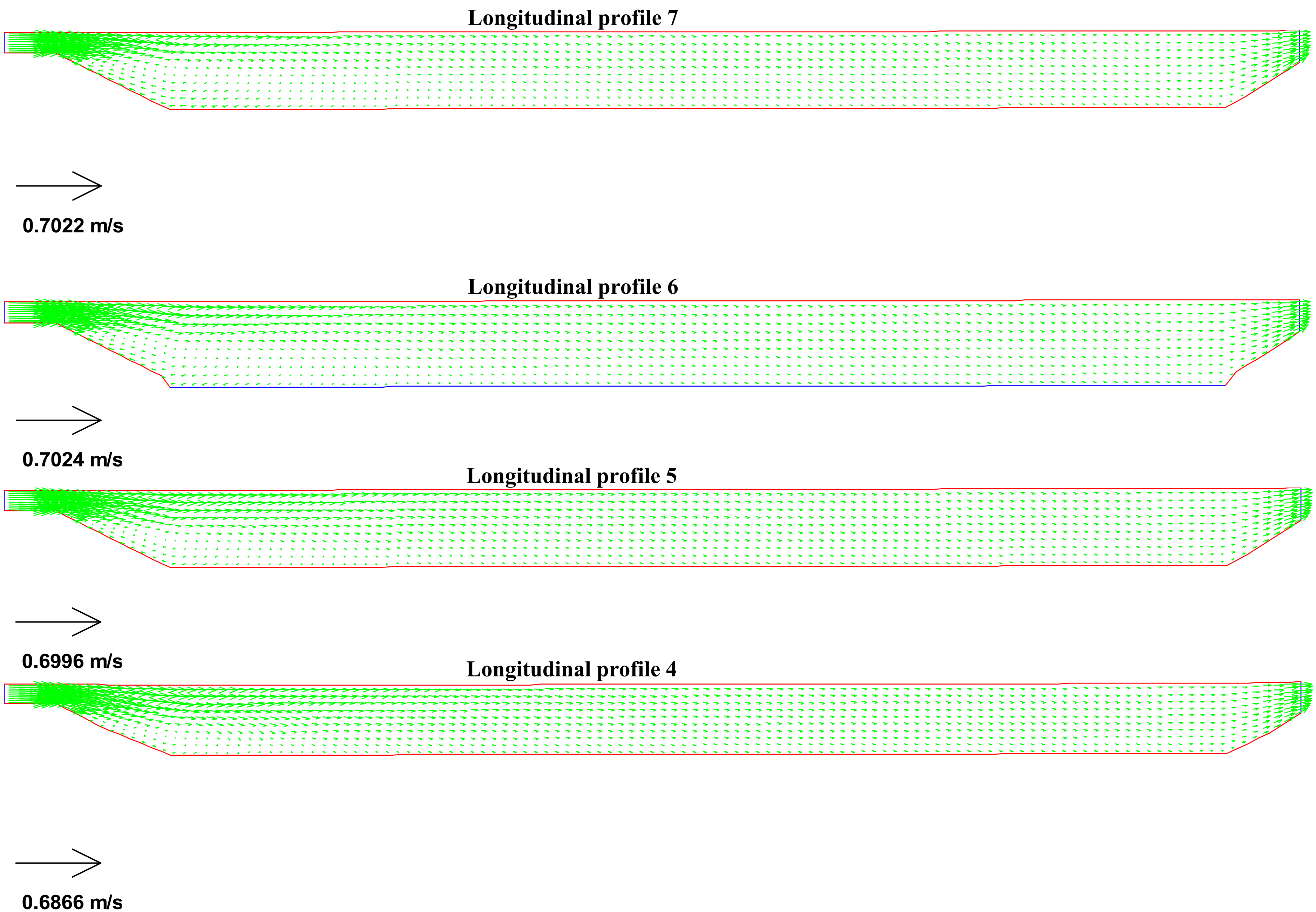

Velocity vector in X-Z plane

Annexure 5-7

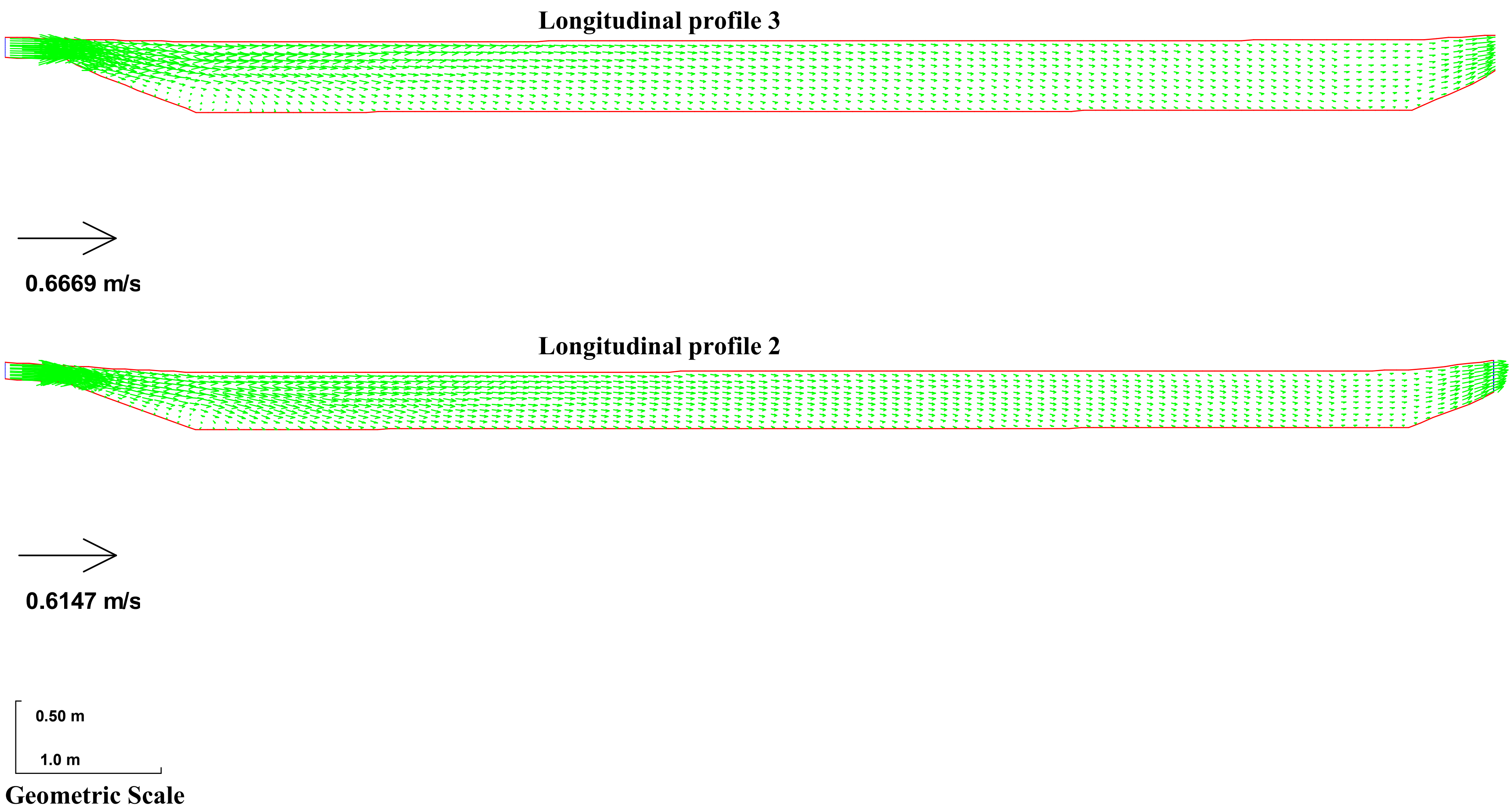

VELOCITY VECTOR IN LONGITUDINAL (X-Z) PLANE

Velocity vector in X-Z plane

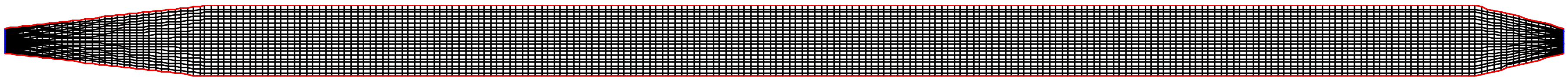

Plan

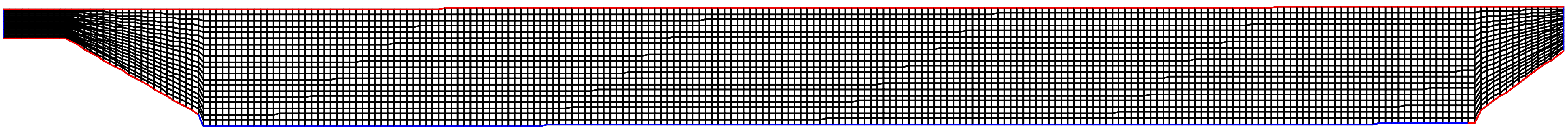

Sectional Elevation

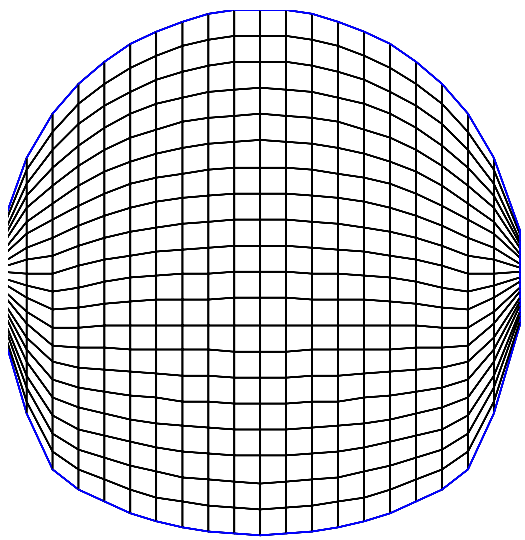

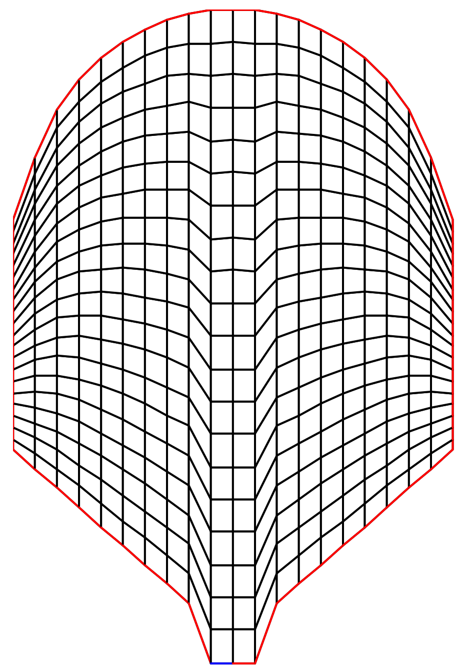

Cross section no. 1 and cross section no. 100

<u>Fine Grid in Plan, Longitudinal and cross-section</u>

Annexure 5-8

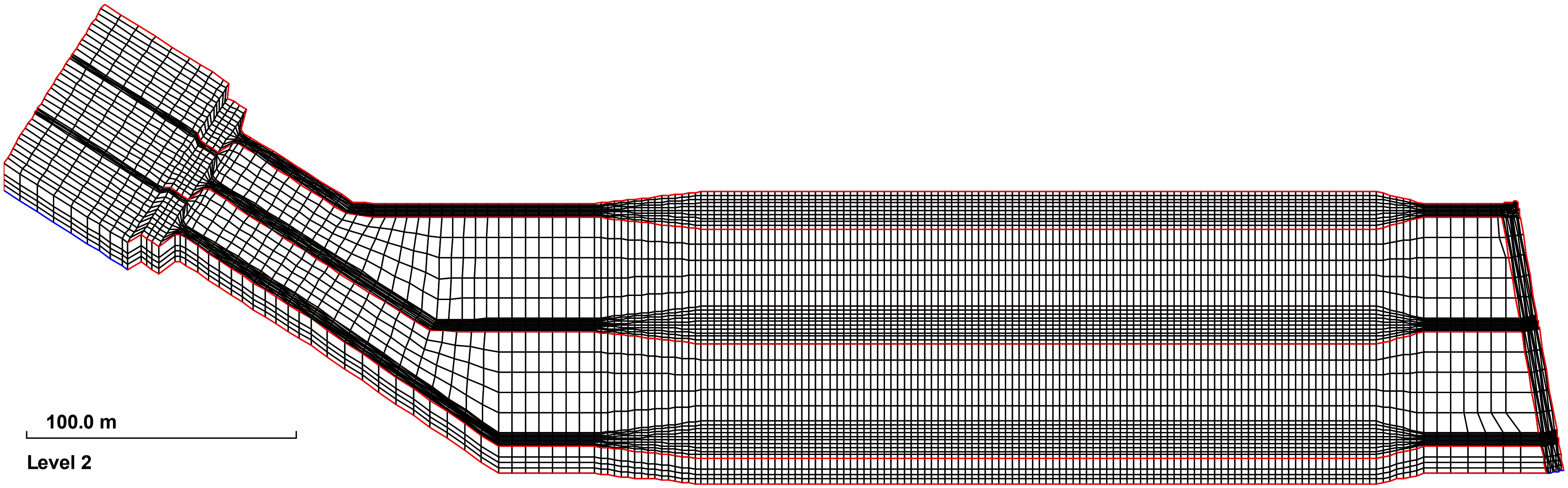

Desilting basin in plan

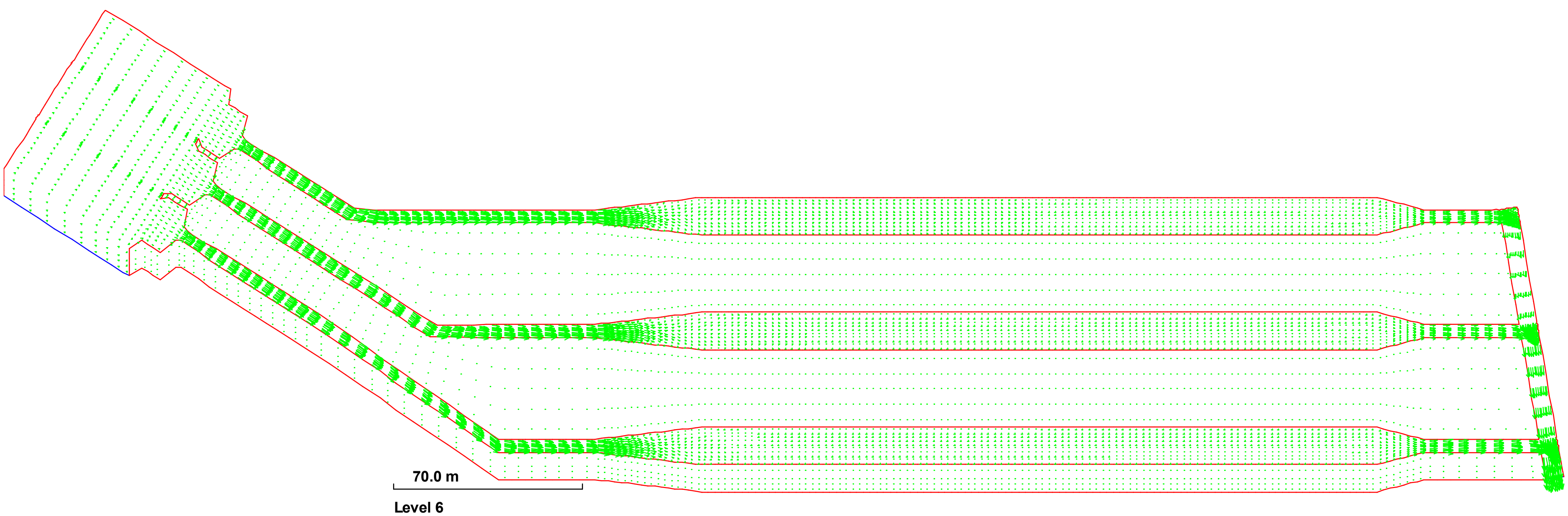

Velocity vector at mid level

Annexure 5-9

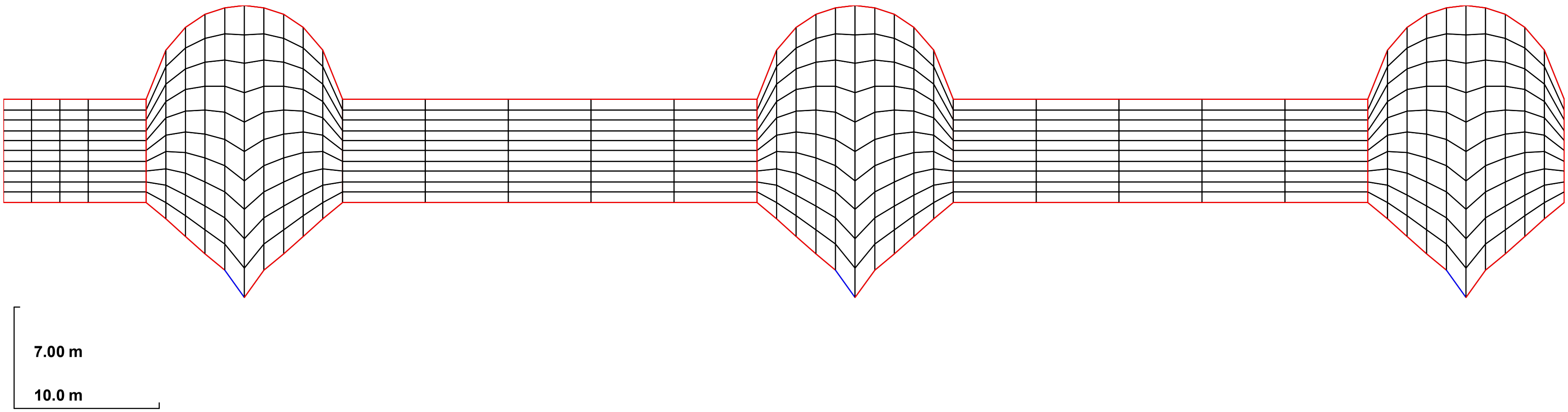

Cross-section no. 63

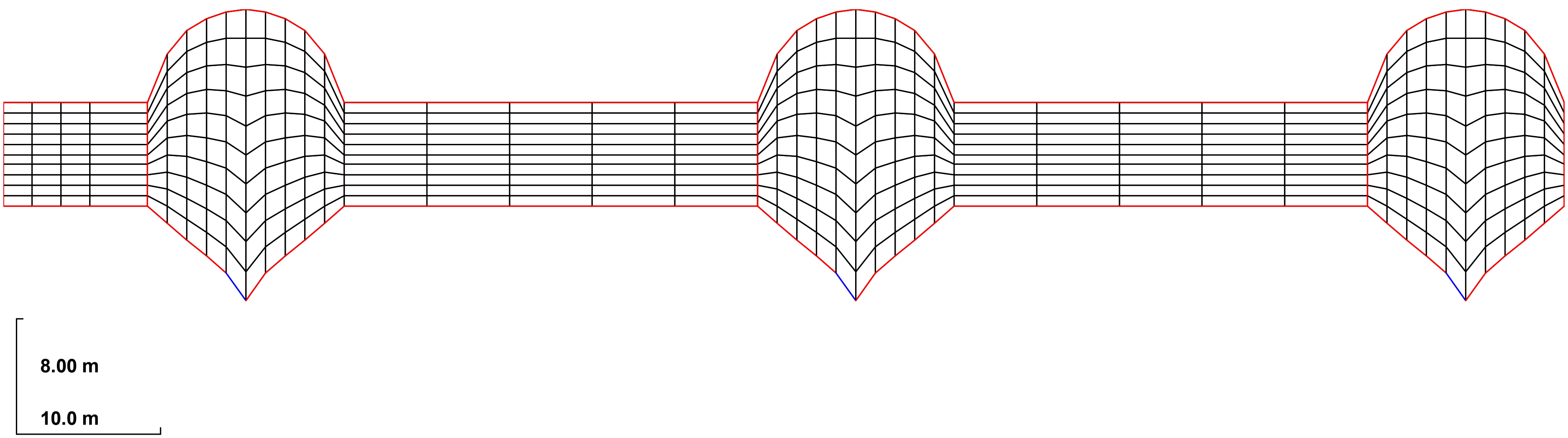

Cross-section no. 162

<u>Grid arrangement for three desilting basins in combination</u>

Annexure 5-10

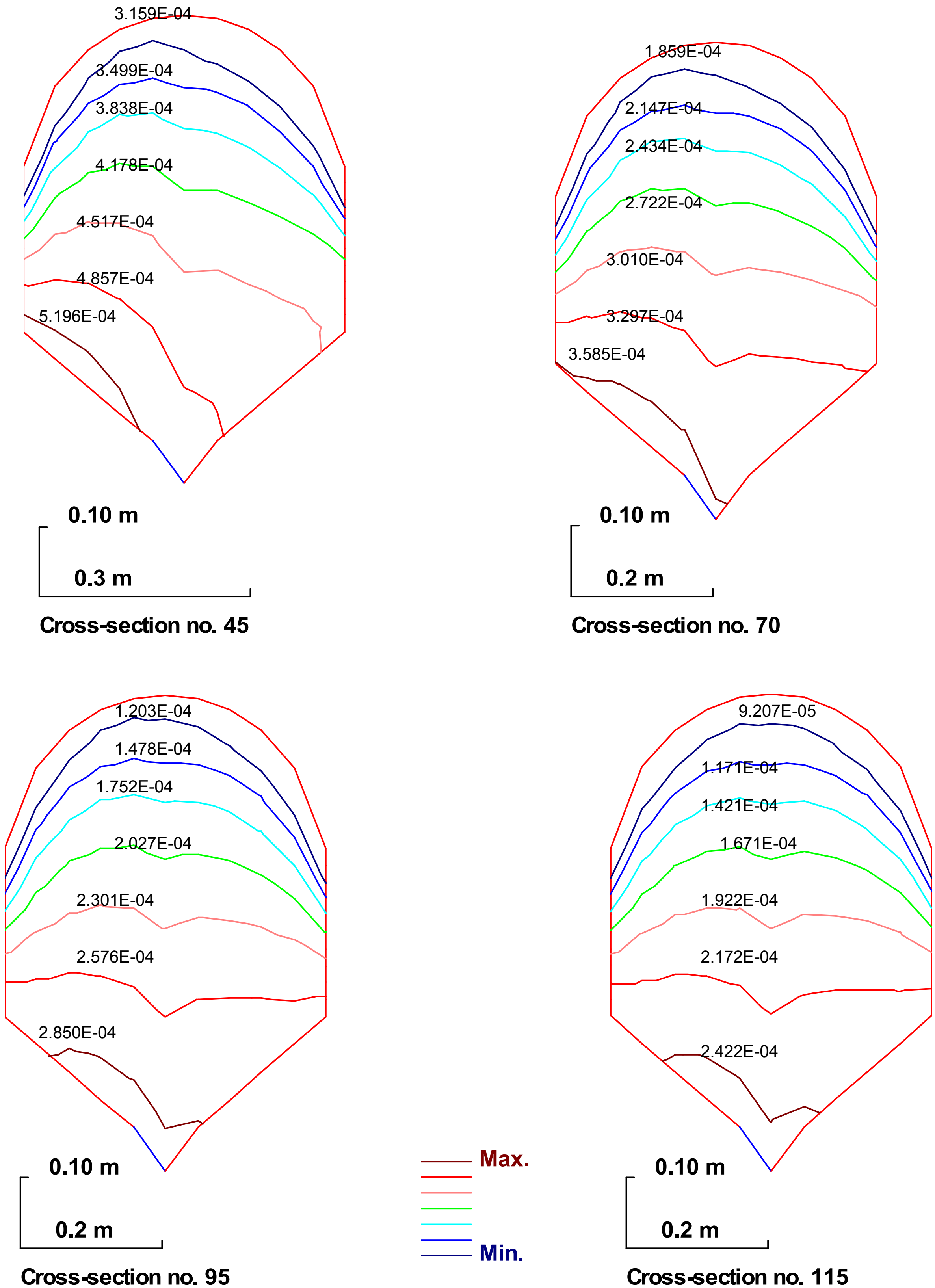

Sediment concentration profile at different cross section

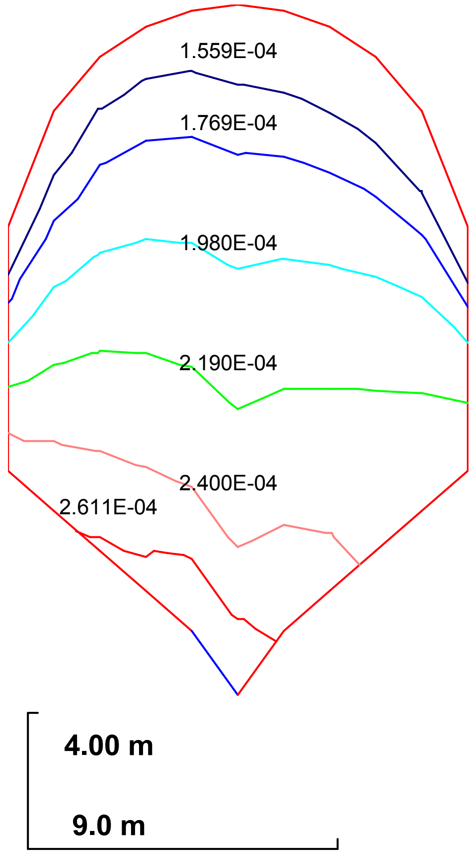

Cross-section no. 45

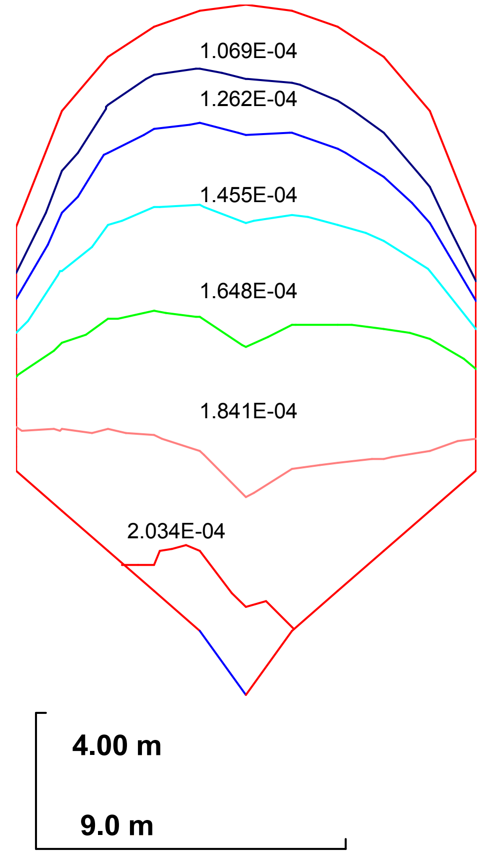

Cross-section no. 70

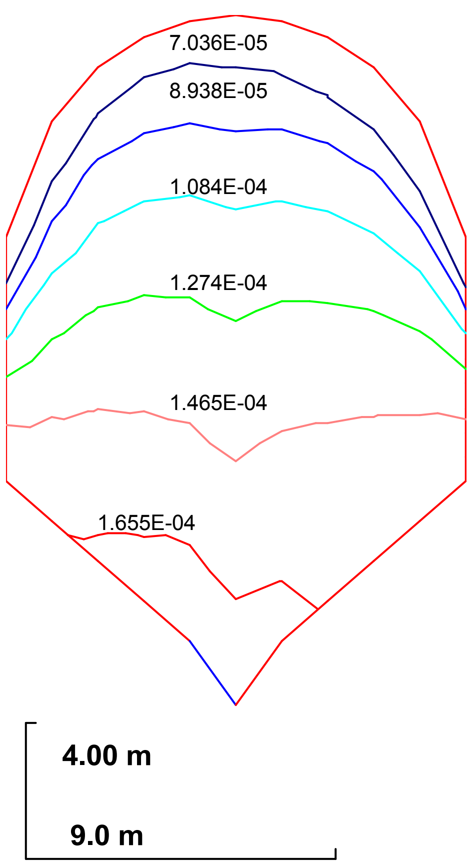

Cross-section no. 95

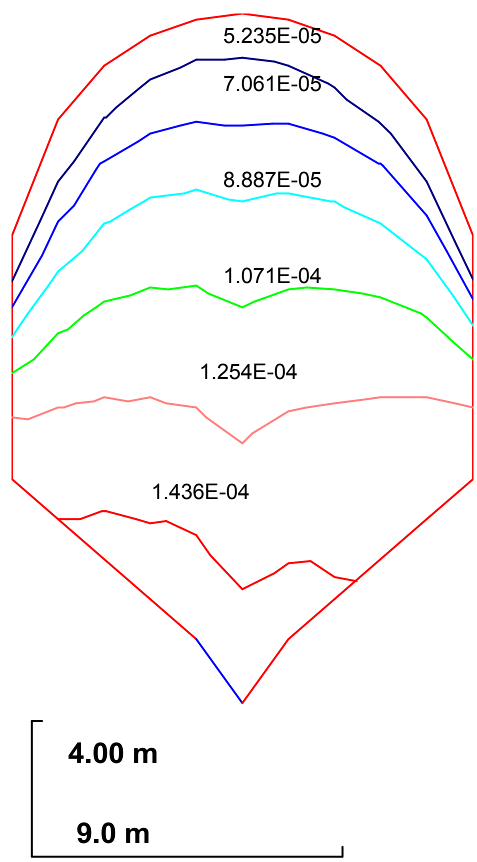

Cross-section no. 115

Sediment concentration profile at different cross sections for prototype

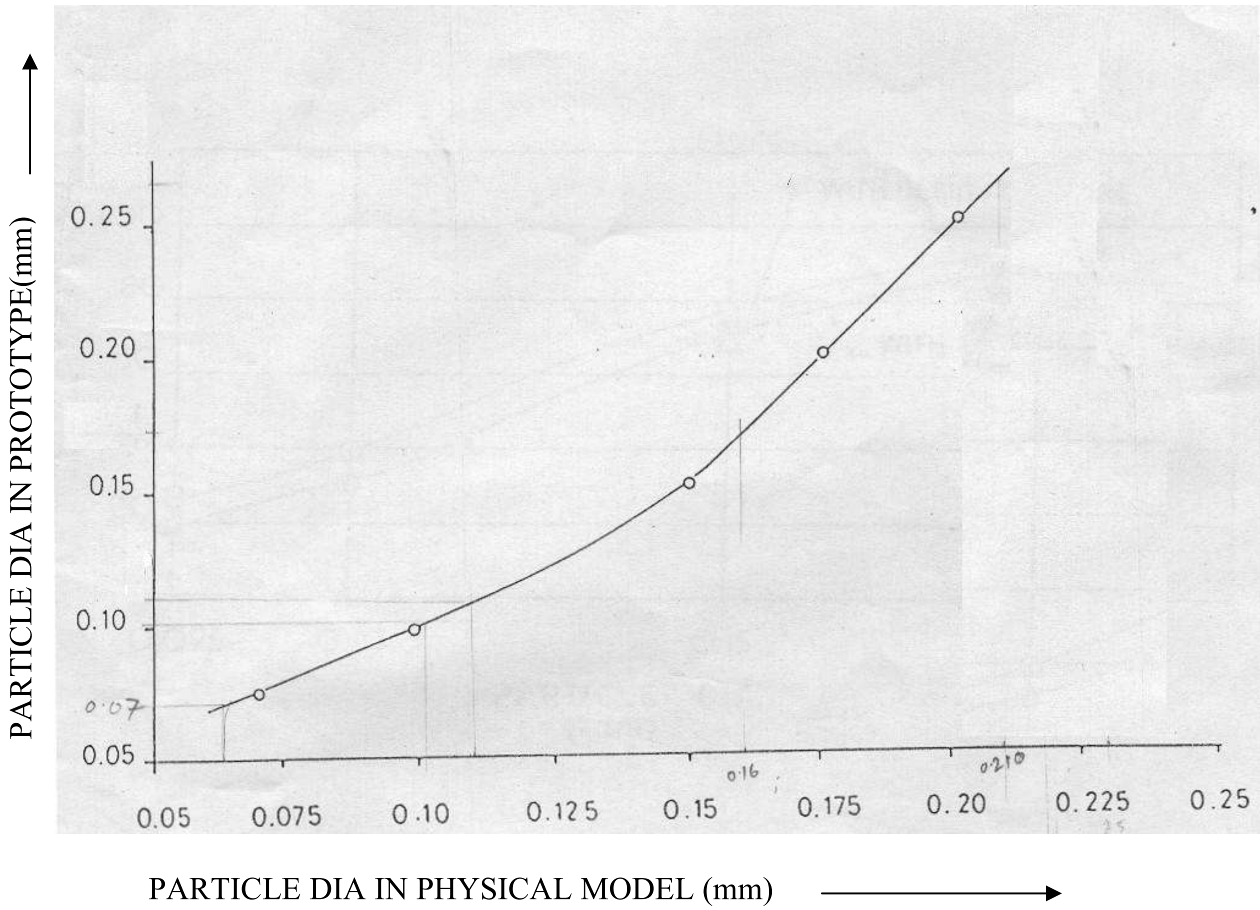

RELATIONSHIP BETWEEN PARTICLE SIZE IN PROTO TYPE AND MODEL
TALA H.E. PROJECT, BHUTAN

Ref: (1) Technical Report no. 3804, july 2001, Hydraulic Model studies for desilting basin, THEP, Bhutan(Report no.2), CWPRS, Pune

CONTROL FILE

```
T         tala hep bhutan     data set for model not pt
F 1 D
f 2 w               waterflow calculation
F 2 RIS         automatic
F 11 1.32 0.047          density of sediment and  shield coefiicient
F 4 0.5 500 .0001       relaxation, iterations, convergence criteria
F 33 5 100      time step and number of inner iterations
F 37 1             initiation of time dependent calculations
F 68 2
G 1 124 11 11 4     grid and array sizes
G 3 0 10 20 30 40 50 60 70 80 90 100     vertical grid distribution
G 7 0 1 2 11 2 11 0 0 0.011563 1.0 0.0 0.0             inflow
G 7 1 -1 2 11 2 11 0 0 0.009636 1.0 0.0 0.0            outflow
G 7 1 3  18 117  6 6 0 0 0.001927 0.0 0.0 1.0          flushing flow
G 8 18 117 2 11 2 11 0.0557 0.0 0.0
G 21 1 2 2 11 2 11
G 21 1 124 2 11 2 11
W 4 3 0 2 18 117 6 6
I 1 0.002222   inflowing sediments in kg/s
I 2 0.002222
I 3 0.002222
I 4 0.002222
N 0 1 0.25
N 0 2 0.25
N 0 3 0.25
N 0 4 0.25
S 4 0.000063  0.000716         sediment fraction nr, size, fallvelo,
S 3 0.000110  0.00210
S 2 0.000160  0.00426
S 1 0.000210  0.00697
B 0 0 0 0 0
W 1 80.000000 0.011563 1.000000
W 2 3 1 62 124
K 1 3600 60000
K 2 0 0
K 3 0.2 0.2 0.2 0.05 0.2 0.2
```

Co-ordinates for Grid					
Grid		Co-ordinates			
i	j	x	y	Z_{bottom}	Z_{top}
1	1	0	0.150	1.398	1.431
1	2	0	0.167	1.353	1.463
1	3	0	0.183	1.343	1.480
1	4	0	0.199	1.337	1.489
1	5	0	0.216	1.334	1.494
1	6	0	0.232	1.333	1.496
1	7	0	0.248	1.334	1.494
1	8	0	0.265	1.337	1.489
1	9	0	0.281	1.343	1.480
1	10	0	0.297	1.353	1.463
1	11	0	0.314	1.398	1.431
2	1	0.083	0.141	1.398	1.431
2	2	0.083	0.159	1.345	1.460
2	3	0.083	0.177	1.340	1.478
2	4	0.083	0.196	1.336	1.489
2	5	0.083	0.214	1.334	1.494
2	6	0.083	0.232	1.333	1.496
2	7	0.083	0.250	1.334	1.494
2	8	0.083	0.269	1.336	1.489
2	9	0.083	0.287	1.340	1.478
2	10	0.083	0.305	1.345	1.460
2	11	0.083	0.323	1.398	1.431
3	1	0.167	0.131	1.398	1.431
3	2	0.167	0.152	1.342	1.457
3	3	0.167	0.172	1.338	1.477
3	4	0.167	0.192	1.335	1.488
3	5	0.167	0.212	1.334	1.494
3	6	0.167	0.232	1.333	1.496
3	7	0.167	0.252	1.334	1.494
3	8	0.167	0.272	1.335	1.488
3	9	0.167	0.293	1.338	1.477
3	10	0.167	0.313	1.342	1.457
3	11	0.167	0.333	1.398	1.431
4	1	0.250	0.122	1.370	1.403
4	2	0.250	0.144	1.339	1.451
4	3	0.250	0.166	1.337	1.474
4	4	0.250	0.188	1.335	1.487
4	5	0.250	0.210	1.334	1.494
4	6	0.250	0.232	1.333	1.497
4	7	0.250	0.254	1.334	1.494
4	8	0.250	0.276	1.335	1.487
4	9	0.250	0.298	1.337	1.474
4	10	0.250	0.320	1.339	1.451
4	11	0.250	0.342	1.370	1.403
5	1	0.333	0.112	1.342	1.375
5	2	0.333	0.136	1.336	1.446
5	3	0.333	0.160	1.335	1.472
5	4	0.333	0.184	1.334	1.486
5	5	0.333	0.208	1.334	1.494
5	6	0.333	0.232	1.333	1.497
5	7	0.333	0.256	1.334	1.494
5	8	0.333	0.280	1.334	1.486
5	9	0.333	0.304	1.335	1.472
5	10	0.333	0.328	1.336	1.446
5	11	0.333	0.352	1.342	1.375

Co-ordinates for Grid					
Grid		Co-ordinates			
i	j	x	y	Z_{bottom}	Z_{top}
6	1	0.408	0.104	1.334	1.367
6	2	0.408	0.129	1.334	1.440
6	3	0.408	0.155	1.334	1.469
6	4	0.408	0.181	1.334	1.485
6	5	0.408	0.206	1.334	1.494
6	6	0.408	0.232	1.334	1.497
6	7	0.408	0.258	1.334	1.494
6	8	0.408	0.283	1.334	1.485
6	9	0.408	0.309	1.334	1.469
6	10	0.408	0.335	1.334	1.440
6	11	0.408	0.360	1.334	1.367
7	1	0.491	0.094	1.307	1.341
7	2	0.491	0.122	1.299	1.436
7	3	0.491	0.149	1.292	1.467
7	4	0.491	0.177	1.292	1.485
7	5	0.491	0.205	1.292	1.494
7	6	0.491	0.232	1.292	1.497
7	7	0.491	0.260	1.292	1.494
7	8	0.491	0.287	1.292	1.485
7	9	0.491	0.315	1.292	1.467
7	10	0.491	0.342	1.299	1.436
7	11	0.491	0.370	1.307	1.341
8	1	0.575	0.085	1.281	1.309
8	2	0.575	0.114	1.267	1.432
8	3	0.575	0.144	1.253	1.465
8	4	0.575	0.173	1.250	1.484
8	5	0.575	0.203	1.250	1.494
8	6	0.575	0.232	1.250	1.497
8	7	0.575	0.262	1.250	1.494
8	8	0.575	0.291	1.250	1.484
8	9	0.575	0.321	1.253	1.465
8	10	0.575	0.350	1.267	1.432
8	11	0.575	0.380	1.281	1.309
9	1	0.658	0.075	1.255	1.296
9	2	0.658	0.107	1.237	1.428
9	3	0.658	0.138	1.218	1.464
9	4	0.658	0.169	1.209	1.483
9	5	0.658	0.201	1.209	1.494
9	6	0.658	0.232	1.209	1.497
9	7	0.658	0.264	1.209	1.494
9	8	0.658	0.295	1.209	1.483
9	9	0.658	0.326	1.218	1.464
9	10	0.658	0.358	1.237	1.428
9	11	0.658	0.389	1.255	1.296
10	1	0.741	0.066	1.229	1.284
10	2	0.741	0.099	1.207	1.424
10	3	0.741	0.132	1.185	1.462
10	4	0.741	0.166	1.167	1.483
10	5	0.741	0.199	1.167	1.494
10	6	0.741	0.232	1.167	1.497
10	7	0.741	0.265	1.167	1.494
10	8	0.741	0.299	1.167	1.483
10	9	0.741	0.332	1.185	1.462
10	10	0.741	0.365	1.207	1.424
10	11	0.741	0.399	1.229	1.284

Co-ordinates for Grid					
Grid		Co-ordinates			
i	j	x	y	Z_{bottom}	Z_{top}
11	1	0.825	0.056	1.202	1.271
11	2	0.825	0.091	1.178	1.420
11	3	0.825	0.126	1.153	1.460
11	4	0.825	0.162	1.128	1.482
11	5	0.825	0.197	1.126	1.494
11	6	0.825	0.232	1.126	1.498
11	7	0.825	0.267	1.126	1.494
11	8	0.825	0.303	1.128	1.482
11	9	0.825	0.338	1.153	1.460
11	10	0.825	0.373	1.178	1.420
11	11	0.825	0.408	1.202	1.271
12	1	0.908	0.047	1.176	1.259
12	2	0.908	0.084	1.149	1.416
12	3	0.908	0.121	1.121	1.458
12	4	0.908	0.158	1.094	1.481
12	5	0.908	0.195	1.084	1.494
12	6	0.908	0.232	1.084	1.498
12	7	0.908	0.269	1.084	1.494
12	8	0.908	0.306	1.094	1.481
12	9	0.908	0.343	1.121	1.458
12	10	0.908	0.381	1.149	1.416
12	11	0.908	0.418	1.176	1.259
13	1	0.991	0.037	1.150	1.247
13	2	0.991	0.076	1.120	1.412
13	3	0.991	0.115	1.090	1.456
13	4	0.991	0.154	1.060	1.480
13	5	0.991	0.193	1.043	1.494
13	6	0.991	0.232	1.043	1.498
13	7	0.991	0.271	1.043	1.494
13	8	0.991	0.310	1.060	1.480
13	9	0.991	0.349	1.090	1.456
13	10	0.991	0.388	1.120	1.412
13	11	0.991	0.427	1.150	1.247
14	1	1.075	0.027	1.124	1.234
14	2	1.075	0.068	1.091	1.408
14	3	1.075	0.109	1.059	1.454
14	4	1.075	0.150	1.027	1.480
14	5	1.075	0.191	1.001	1.494
14	6	1.075	0.232	1.001	1.498
14	7	1.075	0.273	1.001	1.494
14	8	1.075	0.314	1.027	1.480
14	9	1.075	0.355	1.059	1.454
14	10	1.075	0.396	1.091	1.408
14	11	1.075	0.437	1.124	1.234
15	1	1.158	0.018	1.098	1.222
15	2	1.158	0.061	1.063	1.404
15	3	1.158	0.104	1.028	1.452
15	4	1.158	0.146	0.994	1.479
15	5	1.158	0.189	0.960	1.494
15	6	1.158	0.232	0.960	1.498
15	7	1.158	0.275	0.960	1.494
15	8	1.158	0.318	0.994	1.479
15	9	1.158	0.361	1.028	1.452
15	10	1.158	0.403	1.063	1.404
15	11	1.158	0.446	1.098	1.222

Co-ordinates for Grid					
Grid		Co-ordinates			
i	j	x	y	Z_{bottom}	Z_{top}
16	1	1.241	0.008	1.071	1.209
16	2	1.241	0.053	1.034	1.400
16	3	1.241	0.098	0.997	1.450
16	4	1.241	0.143	0.960	1.478
16	5	1.241	0.187	0.924	1.493
16	6	1.241	0.232	0.918	1.498
16	7	1.241	0.277	0.924	1.493
16	8	1.241	0.322	0.960	1.478
16	9	1.241	0.366	0.997	1.450
16	10	1.241	0.411	1.034	1.400
16	11	1.241	0.456	1.071	1.209
17	1	1.315	0.000	1.048	1.283
17	2	1.315	0.046	1.009	1.396
17	3	1.315	0.093	0.970	1.449
17	4	1.315	0.139	0.932	1.478
17	5	1.315	0.186	0.893	1.493
17	6	1.315	0.232	0.832	1.498
17	7	1.315	0.279	0.893	1.493
17	8	1.315	0.325	0.932	1.478
17	9	1.315	0.371	0.970	1.449
17	10	1.315	0.418	1.009	1.396
17	11	1.315	0.464	1.048	1.283
18	1	1.398	0.000	1.048	1.283
18	2	1.398	0.046	1.010	1.396
18	3	1.398	0.093	0.971	1.449
18	4	1.398	0.139	0.932	1.478
18	5	1.398	0.186	0.893	1.494
18	6	1.398	0.232	0.832	1.498
18	7	1.398	0.279	0.893	1.494
18	8	1.398	0.325	0.932	1.478
18	9	1.398	0.371	0.971	1.449
18	10	1.398	0.418	1.010	1.396
18	11	1.398	0.464	1.048	1.283
19	1	1.481	0.000	1.049	1.284
19	2	1.481	0.046	1.010	1.396
19	3	1.481	0.093	0.971	1.449
19	4	1.481	0.139	0.932	1.478
19	5	1.481	0.186	0.893	1.494
19	6	1.481	0.232	0.832	1.499
19	7	1.481	0.279	0.893	1.494
19	8	1.481	0.325	0.932	1.478
19	9	1.481	0.371	0.971	1.449
19	10	1.481	0.418	1.010	1.396
19	11	1.481	0.464	1.049	1.284
20	1	1.565	0.000	1.049	1.284
20	2	1.565	0.046	1.010	1.396
20	3	1.565	0.093	0.971	1.449
20	4	1.565	0.139	0.932	1.478
20	5	1.565	0.186	0.893	1.494
20	6	1.565	0.232	0.832	1.499
20	7	1.565	0.279	0.893	1.494
20	8	1.565	0.325	0.932	1.478
20	9	1.565	0.371	0.971	1.449
20	10	1.565	0.418	1.010	1.396
20	11	1.565	0.464	1.049	1.284

Co-ordinates for Grid					
Grid		Co-ordinates			
i	j	x	y	Z_{bottom}	Z_{top}
21	1	1.648	0.000	1.049	1.284
21	2	1.648	0.046	1.010	1.397
21	3	1.648	0.093	0.971	1.449
21	4	1.648	0.139	0.932	1.478
21	5	1.648	0.186	0.893	1.494
21	6	1.648	0.232	0.832	1.499
21	7	1.648	0.279	0.893	1.494
21	8	1.648	0.325	0.932	1.478
21	9	1.648	0.371	0.971	1.449
21	10	1.648	0.418	1.010	1.397
21	11	1.648	0.464	1.049	1.284
22	1	1.731	0.000	1.049	1.284
22	2	1.731	0.046	1.010	1.397
22	3	1.731	0.093	0.971	1.449
22	4	1.731	0.139	0.932	1.478
22	5	1.731	0.186	0.893	1.494
22	6	1.731	0.232	0.832	1.499
22	7	1.731	0.279	0.893	1.494
22	8	1.731	0.325	0.932	1.478
22	9	1.731	0.371	0.971	1.449
22	10	1.731	0.418	1.010	1.397
22	11	1.731	0.464	1.049	1.284
23	1	1.815	0.000	1.049	1.284
23	2	1.815	0.046	1.010	1.397
23	3	1.815	0.093	0.971	1.449
23	4	1.815	0.139	0.932	1.479
23	5	1.815	0.186	0.893	1.494
23	6	1.815	0.232	0.833	1.499
23	7	1.815	0.279	0.893	1.494
23	8	1.815	0.325	0.932	1.479
23	9	1.815	0.371	0.971	1.449
23	10	1.815	0.418	1.010	1.397
23	11	1.815	0.464	1.049	1.284
24	1	1.898	0.000	1.049	1.284
24	2	1.898	0.046	1.010	1.397
24	3	1.898	0.093	0.971	1.450
24	4	1.898	0.139	0.933	1.479
24	5	1.898	0.186	0.894	1.494
24	6	1.898	0.232	0.833	1.499
24	7	1.898	0.279	0.894	1.494
24	8	1.898	0.325	0.933	1.479
24	9	1.898	0.371	0.971	1.450
24	10	1.898	0.418	1.010	1.397
24	11	1.898	0.464	1.049	1.284
25	1	1.981	0.000	1.049	1.284
25	2	1.981	0.046	1.011	1.397
25	3	1.981	0.093	0.972	1.450
25	4	1.981	0.139	0.933	1.479
25	5	1.981	0.186	0.894	1.494
25	6	1.981	0.232	0.833	1.499
25	7	1.981	0.279	0.894	1.494
25	8	1.981	0.325	0.933	1.479
25	9	1.981	0.371	0.972	1.450
25	10	1.981	0.418	1.011	1.397
25	11	1.981	0.464	1.049	1.284

Co-ordinates for Grid					
Grid		Co-ordinates			
i	j	x	y	Z_{bottom}	Z_{top}
26	1	2.065	0.000	1.050	1.285
26	2	2.065	0.046	1.011	1.397
26	3	2.065	0.093	0.972	1.450
26	4	2.065	0.139	0.933	1.479
26	5	2.065	0.186	0.894	1.495
26	6	2.065	0.232	0.833	1.500
26	7	2.065	0.279	0.894	1.495
26	8	2.065	0.325	0.933	1.479
26	9	2.065	0.371	0.972	1.450
26	10	2.065	0.418	1.011	1.397
26	11	2.065	0.464	1.050	1.285
27	1	2.148	0.000	1.050	1.285
27	2	2.148	0.046	1.011	1.397
27	3	2.148	0.093	0.972	1.450
27	4	2.148	0.139	0.933	1.479
27	5	2.148	0.186	0.894	1.495
27	6	2.148	0.232	0.833	1.500
27	7	2.148	0.279	0.894	1.495
27	8	2.148	0.325	0.933	1.479
27	9	2.148	0.371	0.972	1.450
27	10	2.148	0.418	1.011	1.397
27	11	2.148	0.464	1.050	1.285
28	1	2.231	0.000	1.050	1.285
28	2	2.231	0.046	1.011	1.398
28	3	2.231	0.093	0.972	1.450
28	4	2.231	0.139	0.933	1.479
28	5	2.231	0.186	0.894	1.495
28	6	2.231	0.232	0.833	1.500
28	7	2.231	0.279	0.894	1.495
28	8	2.231	0.325	0.933	1.479
28	9	2.231	0.371	0.972	1.450
28	10	2.231	0.418	1.011	1.398
28	11	2.231	0.464	1.050	1.285
29	1	2.315	0.000	1.050	1.285
29	2	2.315	0.046	1.011	1.398
29	3	2.315	0.093	0.972	1.450
29	4	2.315	0.139	0.933	1.479
29	5	2.315	0.186	0.894	1.495
29	6	2.315	0.232	0.833	1.500
29	7	2.315	0.279	0.894	1.495
29	8	2.315	0.325	0.933	1.479
29	9	2.315	0.371	0.972	1.450
29	10	2.315	0.418	1.011	1.398
29	11	2.315	0.464	1.050	1.285
30	1	2.398	0.000	1.050	1.285
30	2	2.398	0.046	1.011	1.398
30	3	2.398	0.093	0.972	1.450
30	4	2.398	0.139	0.933	1.480
30	5	2.398	0.186	0.894	1.495
30	6	2.398	0.232	0.833	1.500
30	7	2.398	0.279	0.894	1.495
30	8	2.398	0.325	0.933	1.480
30	9	2.398	0.371	0.972	1.450
30	10	2.398	0.418	1.011	1.398
30	11	2.398	0.464	1.050	1.285

Co-ordinates for Grid					
Grid		Co-ordinates			
i	j	x	y	Z_{bottom}	Z_{top}
31	1	2.481	0.000	1.050	1.285
31	2	2.481	0.046	1.011	1.398
31	3	2.481	0.093	0.972	1.450
31	4	2.481	0.139	0.934	1.480
31	5	2.481	0.186	0.895	1.495
31	6	2.481	0.232	0.834	1.500
31	7	2.481	0.279	0.895	1.495
31	8	2.481	0.325	0.934	1.480
31	9	2.481	0.371	0.972	1.450
31	10	2.481	0.418	1.011	1.398
31	11	2.481	0.464	1.050	1.285
32	1	2.565	0.000	1.050	1.285
32	2	2.565	0.046	1.011	1.398
32	3	2.565	0.093	0.973	1.451
32	4	2.565	0.139	0.934	1.480
32	5	2.565	0.186	0.895	1.495
32	6	2.565	0.232	0.834	1.500
32	7	2.565	0.279	0.895	1.495
32	8	2.565	0.325	0.934	1.480
32	9	2.565	0.371	0.973	1.451
32	10	2.565	0.418	1.011	1.398
32	11	2.565	0.464	1.050	1.285
33	1	2.648	0.000	1.051	1.286
33	2	2.648	0.046	1.012	1.398
33	3	2.648	0.093	0.973	1.451
33	4	2.648	0.139	0.934	1.480
33	5	2.648	0.186	0.895	1.496
33	6	2.648	0.232	0.834	1.501
33	7	2.648	0.279	0.895	1.496
33	8	2.648	0.325	0.934	1.480
33	9	2.648	0.371	0.973	1.451
33	10	2.648	0.418	1.012	1.398
33	11	2.648	0.464	1.051	1.286
34	1	2.731	0.000	1.051	1.286
34	2	2.731	0.046	1.012	1.398
34	3	2.731	0.093	0.973	1.451
34	4	2.731	0.139	0.934	1.480
34	5	2.731	0.186	0.895	1.496
34	6	2.731	0.232	0.834	1.501
34	7	2.731	0.279	0.895	1.496
34	8	2.731	0.325	0.934	1.480
34	9	2.731	0.371	0.973	1.451
34	10	2.731	0.418	1.012	1.398
34	11	2.731	0.464	1.051	1.286
35	1	2.815	0.000	1.051	1.286
35	2	2.815	0.046	1.012	1.399
35	3	2.815	0.093	0.973	1.451
35	4	2.815	0.139	0.934	1.480
35	5	2.815	0.186	0.895	1.496
35	6	2.815	0.232	0.834	1.501
35	7	2.815	0.279	0.895	1.496
35	8	2.815	0.325	0.934	1.480
35	9	2.815	0.371	0.973	1.451
35	10	2.815	0.418	1.012	1.399
35	11	2.815	0.464	1.051	1.286

Co-ordinates for Grid					
Grid		Co-ordinates			
i	j	x	y	Z_{bottom}	Z_{top}
36	1	2.898	0.000	1.051	1.286
36	2	2.898	0.046	1.012	1.399
36	3	2.898	0.093	0.973	1.451
36	4	2.898	0.139	0.934	1.480
36	5	2.898	0.186	0.895	1.496
36	6	2.898	0.232	0.834	1.501
36	7	2.898	0.279	0.895	1.496
36	8	2.898	0.325	0.934	1.480
36	9	2.898	0.371	0.973	1.451
36	10	2.898	0.418	1.012	1.399
36	11	2.898	0.464	1.051	1.286
37	1	2.981	0.000	1.051	1.286
37	2	2.981	0.046	1.012	1.399
37	3	2.981	0.093	0.973	1.451
37	4	2.981	0.139	0.934	1.481
37	5	2.981	0.186	0.895	1.496
37	6	2.981	0.232	0.834	1.501
37	7	2.981	0.279	0.895	1.496
37	8	2.981	0.325	0.934	1.481
37	9	2.981	0.371	0.973	1.451
37	10	2.981	0.418	1.012	1.399
37	11	2.981	0.464	1.051	1.286
38	1	3.065	0.000	1.051	1.286
38	2	3.065	0.046	1.012	1.399
38	3	3.065	0.093	0.973	1.451
38	4	3.065	0.139	0.934	1.481
38	5	3.065	0.186	0.896	1.496
38	6	3.065	0.232	0.835	1.501
38	7	3.065	0.279	0.896	1.496
38	8	3.065	0.325	0.934	1.481
38	9	3.065	0.371	0.973	1.451
38	10	3.065	0.418	1.012	1.399
38	11	3.065	0.464	1.051	1.286
39	1	3.148	0.000	1.051	1.286
39	2	3.148	0.046	1.012	1.399
39	3	3.148	0.093	0.974	1.452
39	4	3.148	0.139	0.935	1.481
39	5	3.148	0.186	0.896	1.496
39	6	3.148	0.232	0.835	1.501
39	7	3.148	0.279	0.896	1.496
39	8	3.148	0.325	0.935	1.481
39	9	3.148	0.371	0.974	1.452
39	10	3.148	0.418	1.012	1.399
39	11	3.148	0.464	1.051	1.286
40	1	3.231	0.000	1.052	1.287
40	2	3.231	0.046	1.013	1.399
40	3	3.231	0.093	0.974	1.452
40	4	3.231	0.139	0.935	1.481
40	5	3.231	0.186	0.896	1.497
40	6	3.231	0.232	0.835	1.502
40	7	3.231	0.279	0.896	1.497
40	8	3.231	0.325	0.935	1.481
40	9	3.231	0.371	0.974	1.452
40	10	3.231	0.418	1.013	1.399
40	11	3.231	0.464	1.052	1.287

Co-ordinates for Grid					
Grid		Co-ordinates			
i	j	x	y	Z_{bottom}	Z_{top}
41	1	3.315	0.000	1.052	1.287
41	2	3.315	0.046	1.013	1.399
41	3	3.315	0.093	0.974	1.452
41	4	3.315	0.139	0.935	1.481
41	5	3.315	0.186	0.896	1.497
41	6	3.315	0.232	0.835	1.502
41	7	3.315	0.279	0.896	1.497
41	8	3.315	0.325	0.935	1.481
41	9	3.315	0.371	0.974	1.452
41	10	3.315	0.418	1.013	1.399
41	11	3.315	0.464	1.052	1.287
42	1	3.398	0.000	1.052	1.287
42	2	3.398	0.046	1.013	1.399
42	3	3.398	0.093	0.974	1.452
42	4	3.398	0.139	0.935	1.481
42	5	3.398	0.186	0.896	1.497
42	6	3.398	0.232	0.835	1.502
42	7	3.398	0.279	0.896	1.497
42	8	3.398	0.325	0.935	1.481
42	9	3.398	0.371	0.974	1.452
42	10	3.398	0.418	1.013	1.399
42	11	3.398	0.464	1.052	1.287
43	1	3.481	0.000	1.052	1.287
43	2	3.481	0.046	1.013	1.400
43	3	3.481	0.093	0.974	1.452
43	4	3.481	0.139	0.935	1.481
43	5	3.481	0.186	0.896	1.497
43	6	3.481	0.232	0.835	1.502
43	7	3.481	0.279	0.896	1.497
43	8	3.481	0.325	0.935	1.481
43	9	3.481	0.371	0.974	1.452
43	10	3.481	0.418	1.013	1.400
43	11	3.481	0.464	1.052	1.287
44	1	3.565	0.000	1.052	1.287
44	2	3.565	0.046	1.013	1.400
44	3	3.565	0.093	0.974	1.452
44	4	3.565	0.139	0.935	1.481
44	5	3.565	0.186	0.896	1.497
44	6	3.565	0.232	0.835	1.502
44	7	3.565	0.279	0.896	1.497
44	8	3.565	0.325	0.935	1.481
44	9	3.565	0.371	0.974	1.452
44	10	3.565	0.418	1.013	1.400
44	11	3.565	0.464	1.052	1.287
45	1	3.648	0.000	1.052	1.287
45	2	3.648	0.046	1.013	1.400
45	3	3.648	0.093	0.974	1.452
45	4	3.648	0.139	0.935	1.482
45	5	3.648	0.186	0.897	1.497
45	6	3.648	0.232	0.836	1.502
45	7	3.648	0.279	0.897	1.497
45	8	3.648	0.325	0.935	1.482
45	9	3.648	0.371	0.974	1.452
45	10	3.648	0.418	1.013	1.400
45	11	3.648	0.464	1.052	1.287

Co-ordinates for Grid					
Grid		Co-ordinates			
i	j	x	y	Z_{bottom}	Z_{top}
46	1	3.731	0.000	1.052	1.287
46	2	3.731	0.046	1.013	1.400
46	3	3.731	0.093	0.975	1.453
46	4	3.731	0.139	0.936	1.482
46	5	3.731	0.186	0.897	1.497
46	6	3.731	0.232	0.836	1.502
46	7	3.731	0.279	0.897	1.497
46	8	3.731	0.325	0.936	1.482
46	9	3.731	0.371	0.975	1.453
46	10	3.731	0.418	1.013	1.400
46	11	3.731	0.464	1.052	1.287
47	1	3.815	0.000	1.053	1.288
47	2	3.815	0.046	1.014	1.400
47	3	3.815	0.093	0.975	1.453
47	4	3.815	0.139	0.936	1.482
47	5	3.815	0.186	0.897	1.498
47	6	3.815	0.232	0.836	1.503
47	7	3.815	0.279	0.897	1.498
47	8	3.815	0.325	0.936	1.482
47	9	3.815	0.371	0.975	1.453
47	10	3.815	0.418	1.014	1.400
47	11	3.815	0.464	1.053	1.288
48	1	3.898	0.000	1.053	1.288
48	2	3.898	0.046	1.014	1.400
48	3	3.898	0.093	0.975	1.453
48	4	3.898	0.139	0.936	1.482
48	5	3.898	0.186	0.897	1.498
48	6	3.898	0.232	0.836	1.503
48	7	3.898	0.279	0.897	1.498
48	8	3.898	0.325	0.936	1.482
48	9	3.898	0.371	0.975	1.453
48	10	3.898	0.418	1.014	1.400
48	11	3.898	0.464	1.053	1.288
49	1	3.981	0.000	1.053	1.288
49	2	3.981	0.046	1.014	1.400
49	3	3.981	0.093	0.975	1.453
49	4	3.981	0.139	0.936	1.482
49	5	3.981	0.186	0.897	1.498
49	6	3.981	0.232	0.836	1.503
49	7	3.981	0.279	0.897	1.498
49	8	3.981	0.325	0.936	1.482
49	9	3.981	0.371	0.975	1.453
49	10	3.981	0.418	1.014	1.400
49	11	3.981	0.464	1.053	1.288
50	1	4.065	0.000	1.053	1.288
50	2	4.065	0.046	1.014	1.401
50	3	4.065	0.093	0.975	1.453
50	4	4.065	0.139	0.936	1.482
50	5	4.065	0.186	0.897	1.498
50	6	4.065	0.232	0.836	1.503
50	7	4.065	0.279	0.897	1.498
50	8	4.065	0.325	0.936	1.482
50	9	4.065	0.371	0.975	1.453
50	10	4.065	0.418	1.014	1.401
50	11	4.065	0.464	1.053	1.288

Co-ordinates for Grid					
Grid		Co-ordinates			
i	j	x	y	Z_{bottom}	Z_{top}
51	1	4.148	0.000	1.053	1.288
51	2	4.148	0.046	1.014	1.401
51	3	4.148	0.093	0.975	1.453
51	4	4.148	0.139	0.936	1.482
51	5	4.148	0.186	0.897	1.498
51	6	4.148	0.232	0.836	1.503
51	7	4.148	0.279	0.897	1.498
51	8	4.148	0.325	0.936	1.482
51	9	4.148	0.371	0.975	1.453
51	10	4.148	0.418	1.014	1.401
51	11	4.148	0.464	1.053	1.288
52	1	4.231	0.000	1.053	1.288
52	2	4.231	0.046	1.014	1.401
52	3	4.231	0.093	0.975	1.453
52	4	4.231	0.139	0.936	1.483
52	5	4.231	0.186	0.898	1.498
52	6	4.231	0.232	0.837	1.503
52	7	4.231	0.279	0.898	1.498
52	8	4.231	0.325	0.936	1.483
52	9	4.231	0.371	0.975	1.453
52	10	4.231	0.418	1.014	1.401
52	11	4.231	0.464	1.053	1.288
53	1	4.315	0.000	1.053	1.288
53	2	4.315	0.046	1.014	1.401
53	3	4.315	0.093	0.975	1.454
53	4	4.315	0.139	0.937	1.483
53	5	4.315	0.186	0.898	1.498
53	6	4.315	0.232	0.837	1.503
53	7	4.315	0.279	0.898	1.498
53	8	4.315	0.325	0.937	1.483
53	9	4.315	0.371	0.975	1.454
53	10	4.315	0.418	1.014	1.401
53	11	4.315	0.464	1.053	1.288
54	1	4.398	0.000	1.053	1.288
54	2	4.398	0.046	1.015	1.401
54	3	4.398	0.093	0.976	1.454
54	4	4.398	0.139	0.937	1.483
54	5	4.398	0.186	0.898	1.499
54	6	4.398	0.232	0.837	1.503
54	7	4.398	0.279	0.898	1.499
54	8	4.398	0.325	0.937	1.483
54	9	4.398	0.371	0.976	1.454
54	10	4.398	0.418	1.015	1.401
54	11	4.398	0.464	1.053	1.288
55	1	4.481	0.000	1.054	1.289
55	2	4.481	0.046	1.015	1.401
55	3	4.481	0.093	0.976	1.454
55	4	4.481	0.139	0.937	1.483
55	5	4.481	0.186	0.898	1.499
55	6	4.481	0.232	0.837	1.504
55	7	4.481	0.279	0.898	1.499
55	8	4.481	0.325	0.937	1.483
55	9	4.481	0.371	0.976	1.454
55	10	4.481	0.418	1.015	1.401
55	11	4.481	0.464	1.054	1.289

Co-ordinates for Grid					
Grid		Co-ordinates			
i	j	x	y	Z_{bottom}	Z_{top}
56	1	4.565	0.000	1.054	1.289
56	2	4.565	0.046	1.015	1.401
56	3	4.565	0.093	0.976	1.454
56	4	4.565	0.139	0.937	1.483
56	5	4.565	0.186	0.898	1.499
56	6	4.565	0.232	0.837	1.504
56	7	4.565	0.279	0.898	1.499
56	8	4.565	0.325	0.937	1.483
56	9	4.565	0.371	0.976	1.454
56	10	4.565	0.418	1.015	1.401
56	11	4.565	0.464	1.054	1.289
57	1	4.648	0.000	1.054	1.289
57	2	4.648	0.046	1.015	1.402
57	3	4.648	0.093	0.976	1.454
57	4	4.648	0.139	0.937	1.483
57	5	4.648	0.186	0.898	1.499
57	6	4.648	0.232	0.837	1.504
57	7	4.648	0.279	0.898	1.499
57	8	4.648	0.325	0.937	1.483
57	9	4.648	0.371	0.976	1.454
57	10	4.648	0.418	1.015	1.402
57	11	4.648	0.464	1.054	1.289
58	1	4.731	0.000	1.054	1.289
58	2	4.731	0.046	1.015	1.402
58	3	4.731	0.093	0.976	1.454
58	4	4.731	0.139	0.937	1.483
58	5	4.731	0.186	0.898	1.499
58	6	4.731	0.232	0.837	1.504
58	7	4.731	0.279	0.898	1.499
58	8	4.731	0.325	0.937	1.483
58	9	4.731	0.371	0.976	1.454
58	10	4.731	0.418	1.015	1.402
58	11	4.731	0.464	1.054	1.289
59	1	4.815	0.000	1.054	1.289
59	2	4.815	0.046	1.015	1.402
59	3	4.815	0.093	0.976	1.454
59	4	4.815	0.139	0.937	1.484
59	5	4.815	0.186	0.898	1.499
59	6	4.815	0.232	0.838	1.504
59	7	4.815	0.279	0.898	1.499
59	8	4.815	0.325	0.937	1.484
59	9	4.815	0.371	0.976	1.454
59	10	4.815	0.418	1.015	1.402
59	11	4.815	0.464	1.054	1.289
60	1	4.898	0.000	1.054	1.289
60	2	4.898	0.046	1.015	1.402
60	3	4.898	0.093	0.976	1.455
60	4	4.898	0.139	0.938	1.484
60	5	4.898	0.186	0.899	1.499
60	6	4.898	0.232	0.838	1.504
60	7	4.898	0.279	0.899	1.499
60	8	4.898	0.325	0.938	1.484
60	9	4.898	0.371	0.976	1.455
60	10	4.898	0.418	1.015	1.402
60	11	4.898	0.464	1.054	1.289

Co-ordinates for Grid					
Grid		Co-ordinates			
i	j	x	y	Z_{bottom}	Z_{top}
61	1	4.981	0.000	1.054	1.289
61	2	4.981	0.046	1.016	1.402
61	3	4.981	0.093	0.977	1.455
61	4	4.981	0.139	0.938	1.484
61	5	4.981	0.186	0.899	1.499
61	6	4.981	0.232	0.838	1.504
61	7	4.981	0.279	0.899	1.499
61	8	4.981	0.325	0.938	1.484
61	9	4.981	0.371	0.977	1.455
61	10	4.981	0.418	1.016	1.402
61	11	4.981	0.464	1.054	1.289
62	1	5.065	0.000	1.055	1.290
62	2	5.065	0.046	1.016	1.402
62	3	5.065	0.093	0.977	1.455
62	4	5.065	0.139	0.938	1.484
62	5	5.065	0.186	0.899	1.500
62	6	5.065	0.232	0.838	1.505
62	7	5.065	0.279	0.899	1.500
62	8	5.065	0.325	0.938	1.484
62	9	5.065	0.371	0.977	1.455
62	10	5.065	0.418	1.016	1.402
62	11	5.065	0.464	1.055	1.290
63	1	5.148	0.000	1.055	1.290
63	2	5.148	0.046	1.016	1.402
63	3	5.148	0.093	0.977	1.455
63	4	5.148	0.139	0.938	1.484
63	5	5.148	0.186	0.899	1.500
63	6	5.148	0.232	0.838	1.505
63	7	5.148	0.279	0.899	1.500
63	8	5.148	0.325	0.938	1.484
63	9	5.148	0.371	0.977	1.455
63	10	5.148	0.418	1.016	1.402
63	11	5.148	0.464	1.055	1.290
64	1	5.231	0.000	1.055	1.290
64	2	5.231	0.046	1.016	1.403
64	3	5.231	0.093	0.977	1.455
64	4	5.231	0.139	0.938	1.484
64	5	5.231	0.186	0.899	1.500
64	6	5.231	0.232	0.838	1.505
64	7	5.231	0.279	0.899	1.500
64	8	5.231	0.325	0.938	1.484
64	9	5.231	0.371	0.977	1.455
64	10	5.231	0.418	1.016	1.403
64	11	5.231	0.464	1.055	1.290
65	1	5.315	0.000	1.055	1.290
65	2	5.315	0.046	1.016	1.403
65	3	5.315	0.093	0.977	1.455
65	4	5.315	0.139	0.938	1.484
65	5	5.315	0.186	0.899	1.500
65	6	5.315	0.232	0.838	1.505
65	7	5.315	0.279	0.899	1.500
65	8	5.315	0.325	0.938	1.484
65	9	5.315	0.371	0.977	1.455
65	10	5.315	0.418	1.016	1.403
65	11	5.315	0.464	1.055	1.290

Co-ordinates for Grid					
Grid		Co-ordinates			
i	j	x	y	Z_{bottom}	Z_{top}
66	1	5.398	0.000	1.055	1.290
66	2	5.398	0.046	1.016	1.403
66	3	5.398	0.093	0.977	1.455
66	4	5.398	0.139	0.938	1.485
66	5	5.398	0.186	0.899	1.500
66	6	5.398	0.232	0.838	1.505
66	7	5.398	0.279	0.899	1.500
66	8	5.398	0.325	0.938	1.485
66	9	5.398	0.371	0.977	1.455
66	10	5.398	0.418	1.016	1.403
66	11	5.398	0.464	1.055	1.290
67	1	5.481	0.000	1.055	1.290
67	2	5.481	0.046	1.016	1.403
67	3	5.481	0.093	0.977	1.455
67	4	5.481	0.139	0.939	1.485
67	5	5.481	0.186	0.900	1.500
67	6	5.481	0.232	0.839	1.505
67	7	5.481	0.279	0.900	1.500
67	8	5.481	0.325	0.939	1.485
67	9	5.481	0.371	0.977	1.455
67	10	5.481	0.418	1.016	1.403
67	11	5.481	0.464	1.055	1.290
68	1	5.565	0.000	1.055	1.290
68	2	5.565	0.046	1.016	1.403
68	3	5.565	0.093	0.978	1.456
68	4	5.565	0.139	0.939	1.485
68	5	5.565	0.186	0.900	1.500
68	6	5.565	0.232	0.839	1.505
68	7	5.565	0.279	0.900	1.500
68	8	5.565	0.325	0.939	1.485
68	9	5.565	0.371	0.978	1.456
68	10	5.565	0.418	1.016	1.403
68	11	5.565	0.464	1.055	1.290
69	1	5.648	0.000	1.056	1.291
69	2	5.648	0.046	1.017	1.403
69	3	5.648	0.093	0.978	1.456
69	4	5.648	0.139	0.939	1.485
69	5	5.648	0.186	0.900	1.501
69	6	5.648	0.232	0.839	1.506
69	7	5.648	0.279	0.900	1.501
69	8	5.648	0.325	0.939	1.485
69	9	5.648	0.371	0.978	1.456
69	10	5.648	0.418	1.017	1.403
69	11	5.648	0.464	1.056	1.291
70	1	5.731	0.000	1.056	1.291
70	2	5.731	0.046	1.017	1.403
70	3	5.731	0.093	0.978	1.456
70	4	5.731	0.139	0.939	1.485
70	5	5.731	0.186	0.900	1.501
70	6	5.731	0.232	0.839	1.506
70	7	5.731	0.279	0.900	1.501
70	8	5.731	0.325	0.939	1.485
70	9	5.731	0.371	0.978	1.456
70	10	5.731	0.418	1.017	1.403
70	11	5.731	0.464	1.056	1.291

Co-ordinates for Grid					
Grid		Co-ordinates			
i	j	x	y	Z_{bottom}	Z_{top}
71	1	5.815	0.000	1.056	1.291
71	2	5.815	0.046	1.017	1.404
71	3	5.815	0.093	0.978	1.456
71	4	5.815	0.139	0.939	1.485
71	5	5.815	0.186	0.900	1.501
71	6	5.815	0.232	0.839	1.506
71	7	5.815	0.279	0.900	1.501
71	8	5.815	0.325	0.939	1.485
71	9	5.815	0.371	0.978	1.456
71	10	5.815	0.418	1.017	1.404
71	11	5.815	0.464	1.056	1.291
72	1	5.898	0.000	1.056	1.291
72	2	5.898	0.046	1.017	1.404
72	3	5.898	0.093	0.978	1.456
72	4	5.898	0.139	0.939	1.485
72	5	5.898	0.186	0.900	1.501
72	6	5.898	0.232	0.839	1.506
72	7	5.898	0.279	0.900	1.501
72	8	5.898	0.325	0.939	1.485
72	9	5.898	0.371	0.978	1.456
72	10	5.898	0.418	1.017	1.404
72	11	5.898	0.464	1.056	1.291
73	1	5.981	0.000	1.056	1.291
73	2	5.981	0.046	1.017	1.404
73	3	5.981	0.093	0.978	1.456
73	4	5.981	0.139	0.939	1.486
73	5	5.981	0.186	0.900	1.501
73	6	5.981	0.232	0.839	1.506
73	7	5.981	0.279	0.900	1.501
73	8	5.981	0.325	0.939	1.486
73	9	5.981	0.371	0.978	1.456
73	10	5.981	0.418	1.017	1.404
73	11	5.981	0.464	1.056	1.291
74	1	6.065	0.000	1.056	1.291
74	2	6.065	0.046	1.017	1.404
74	3	6.065	0.093	0.978	1.456
74	4	6.065	0.139	0.939	1.486
74	5	6.065	0.186	0.901	1.501
74	6	6.065	0.232	0.840	1.506
74	7	6.065	0.279	0.901	1.501
74	8	6.065	0.325	0.939	1.486
74	9	6.065	0.371	0.978	1.456
74	10	6.065	0.418	1.017	1.404
74	11	6.065	0.464	1.056	1.291
75	1	6.148	0.000	1.056	1.291
75	2	6.148	0.046	1.017	1.404
75	3	6.148	0.093	0.979	1.457
75	4	6.148	0.139	0.940	1.486
75	5	6.148	0.186	0.901	1.501
75	6	6.148	0.232	0.840	1.506
75	7	6.148	0.279	0.901	1.501
75	8	6.148	0.325	0.940	1.486
75	9	6.148	0.371	0.979	1.457
75	10	6.148	0.418	1.017	1.404
75	11	6.148	0.464	1.056	1.291

Co-ordinates for Grid					
Grid		Co-ordinates			
i	j	x	y	Z_{bottom}	Z_{top}
76	1	6.231	0.000	1.057	1.292
76	2	6.231	0.046	1.018	1.404
76	3	6.231	0.093	0.979	1.457
76	4	6.231	0.139	0.940	1.486
76	5	6.231	0.186	0.901	1.502
76	6	6.231	0.232	0.840	1.507
76	7	6.231	0.279	0.901	1.502
76	8	6.231	0.325	0.940	1.486
76	9	6.231	0.371	0.979	1.457
76	10	6.231	0.418	1.018	1.404
76	11	6.231	0.464	1.057	1.292
77	1	6.315	0.000	1.057	1.292
77	2	6.315	0.046	1.018	1.404
77	3	6.315	0.093	0.979	1.457
77	4	6.315	0.139	0.940	1.486
77	5	6.315	0.186	0.901	1.502
77	6	6.315	0.232	0.840	1.507
77	7	6.315	0.279	0.901	1.502
77	8	6.315	0.325	0.940	1.486
77	9	6.315	0.371	0.979	1.457
77	10	6.315	0.418	1.018	1.404
77	11	6.315	0.464	1.057	1.292
78	1	6.398	0.000	1.057	1.292
78	2	6.398	0.046	1.018	1.404
78	3	6.398	0.093	0.979	1.457
78	4	6.398	0.139	0.940	1.486
78	5	6.398	0.186	0.901	1.502
78	6	6.398	0.232	0.840	1.507
78	7	6.398	0.279	0.901	1.502
78	8	6.398	0.325	0.940	1.486
78	9	6.398	0.371	0.979	1.457
78	10	6.398	0.418	1.018	1.404
78	11	6.398	0.464	1.057	1.292
79	1	6.481	0.000	1.057	1.292
79	2	6.481	0.046	1.018	1.405
79	3	6.481	0.093	0.979	1.457
79	4	6.481	0.139	0.940	1.486
79	5	6.481	0.186	0.901	1.502
79	6	6.481	0.232	0.840	1.507
79	7	6.481	0.279	0.901	1.502
79	8	6.481	0.325	0.940	1.486
79	9	6.481	0.371	0.979	1.457
79	10	6.481	0.418	1.018	1.405
79	11	6.481	0.464	1.057	1.292
80	1	6.565	0.000	1.057	1.292
80	2	6.565	0.046	1.018	1.405
80	3	6.565	0.093	0.979	1.457
80	4	6.565	0.139	0.940	1.486
80	5	6.565	0.186	0.901	1.502
80	6	6.565	0.232	0.840	1.507
80	7	6.565	0.279	0.901	1.502
80	8	6.565	0.325	0.940	1.486
80	9	6.565	0.371	0.979	1.457
80	10	6.565	0.418	1.018	1.405
80	11	6.565	0.464	1.057	1.292

Co-ordinates for Grid					
Grid		Co-ordinates			
i	j	x	y	Z_{bottom}	Z_{top}
81	1	6.648	0.000	1.057	1.292
81	2	6.648	0.046	1.018	1.405
81	3	6.648	0.093	0.979	1.457
81	4	6.648	0.139	0.940	1.487
81	5	6.648	0.186	0.902	1.502
81	6	6.648	0.232	0.841	1.507
81	7	6.648	0.279	0.902	1.502
81	8	6.648	0.325	0.940	1.487
81	9	6.648	0.371	0.979	1.457
81	10	6.648	0.418	1.018	1.405
81	11	6.648	0.464	1.057	1.292
82	1	6.731	0.000	1.057	1.292
82	2	6.731	0.046	1.018	1.405
82	3	6.731	0.093	0.980	1.458
82	4	6.731	0.139	0.941	1.487
82	5	6.731	0.186	0.902	1.502
82	6	6.731	0.232	0.841	1.507
82	7	6.731	0.279	0.902	1.502
82	8	6.731	0.325	0.941	1.487
82	9	6.731	0.371	0.980	1.458
82	10	6.731	0.418	1.018	1.405
82	11	6.731	0.464	1.057	1.292
83	1	6.815	0.000	1.058	1.293
83	2	6.815	0.046	1.019	1.405
83	3	6.815	0.093	0.980	1.458
83	4	6.815	0.139	0.941	1.487
83	5	6.815	0.186	0.902	1.503
83	6	6.815	0.232	0.841	1.508
83	7	6.815	0.279	0.902	1.503
83	8	6.815	0.325	0.941	1.487
83	9	6.815	0.371	0.980	1.458
83	10	6.815	0.418	1.019	1.405
83	11	6.815	0.464	1.058	1.293
84	1	6.898	0.000	1.058	1.293
84	2	6.898	0.046	1.019	1.405
84	3	6.898	0.093	0.980	1.458
84	4	6.898	0.139	0.941	1.487
84	5	6.898	0.186	0.902	1.503
84	6	6.898	0.232	0.841	1.508
84	7	6.898	0.279	0.902	1.503
84	8	6.898	0.325	0.941	1.487
84	9	6.898	0.371	0.980	1.458
84	10	6.898	0.418	1.019	1.405
84	11	6.898	0.464	1.058	1.293
85	1	6.981	0.000	1.058	1.293
85	2	6.981	0.046	1.019	1.405
85	3	6.981	0.093	0.980	1.458
85	4	6.981	0.139	0.941	1.487
85	5	6.981	0.186	0.902	1.503
85	6	6.981	0.232	0.841	1.508
85	7	6.981	0.279	0.902	1.503
85	8	6.981	0.325	0.941	1.487
85	9	6.981	0.371	0.980	1.458
85	10	6.981	0.418	1.019	1.405
85	11	6.981	0.464	1.058	1.293

Co-ordinates for Grid					
Grid		Co-ordinates			
i	j	x	y	Z_{bottom}	Z_{top}
86	1	7.065	0.000	1.058	1.293
86	2	7.065	0.046	1.019	1.406
86	3	7.065	0.093	0.980	1.458
86	4	7.065	0.139	0.941	1.487
86	5	7.065	0.186	0.902	1.503
86	6	7.065	0.232	0.841	1.508
86	7	7.065	0.279	0.902	1.503
86	8	7.065	0.325	0.941	1.487
86	9	7.065	0.371	0.980	1.458
86	10	7.065	0.418	1.019	1.406
86	11	7.065	0.464	1.058	1.293
87	1	7.148	0.000	1.058	1.293
87	2	7.148	0.046	1.019	1.406
87	3	7.148	0.093	0.980	1.458
87	4	7.148	0.139	0.941	1.487
87	5	7.148	0.186	0.902	1.503
87	6	7.148	0.232	0.841	1.508
87	7	7.148	0.279	0.902	1.503
87	8	7.148	0.325	0.941	1.487
87	9	7.148	0.371	0.980	1.458
87	10	7.148	0.418	1.019	1.406
87	11	7.148	0.464	1.058	1.293
88	1	7.231	0.000	1.058	1.293
88	2	7.231	0.046	1.019	1.406
88	3	7.231	0.093	0.980	1.458
88	4	7.231	0.139	0.941	1.488
88	5	7.231	0.186	0.903	1.503
88	6	7.231	0.232	0.842	1.508
88	7	7.231	0.279	0.903	1.503
88	8	7.231	0.325	0.941	1.488
88	9	7.231	0.371	0.980	1.458
88	10	7.231	0.418	1.019	1.406
88	11	7.231	0.464	1.058	1.293
89	1	7.315	0.000	1.058	1.293
89	2	7.315	0.046	1.019	1.406
89	3	7.315	0.093	0.980	1.459
89	4	7.315	0.139	0.942	1.488
89	5	7.315	0.186	0.903	1.503
89	6	7.315	0.232	0.842	1.508
89	7	7.315	0.279	0.903	1.503
89	8	7.315	0.325	0.942	1.488
89	9	7.315	0.371	0.980	1.459
89	10	7.315	0.418	1.019	1.406
89	11	7.315	0.464	1.058	1.293
90	1	7.398	0.000	1.058	1.293
90	2	7.398	0.046	1.020	1.406
90	3	7.398	0.093	0.981	1.459
90	4	7.398	0.139	0.942	1.488
90	5	7.398	0.186	0.903	1.504
90	6	7.398	0.232	0.842	1.508
90	7	7.398	0.279	0.903	1.504
90	8	7.398	0.325	0.942	1.488
90	9	7.398	0.371	0.981	1.459
90	10	7.398	0.418	1.020	1.406
90	11	7.398	0.464	1.058	1.293

Co-ordinates for Grid					
Grid		Co-ordinates			
i	j	x	y	Z_{bottom}	Z_{top}
91	1	7.481	0.000	1.059	1.294
91	2	7.481	0.046	1.020	1.406
91	3	7.481	0.093	0.981	1.459
91	4	7.481	0.139	0.942	1.488
91	5	7.481	0.186	0.903	1.504
91	6	7.481	0.232	0.842	1.509
91	7	7.481	0.279	0.903	1.504
91	8	7.481	0.325	0.942	1.488
91	9	7.481	0.371	0.981	1.459
91	10	7.481	0.418	1.020	1.406
91	11	7.481	0.464	1.059	1.294
92	1	7.565	0.000	1.059	1.294
92	2	7.565	0.046	1.020	1.406
92	3	7.565	0.093	0.981	1.459
92	4	7.565	0.139	0.942	1.488
92	5	7.565	0.186	0.903	1.504
92	6	7.565	0.232	0.842	1.509
92	7	7.565	0.279	0.903	1.504
92	8	7.565	0.325	0.942	1.488
92	9	7.565	0.371	0.981	1.459
92	10	7.565	0.418	1.020	1.406
92	11	7.565	0.464	1.059	1.294
93	1	7.648	0.000	1.059	1.294
93	2	7.648	0.046	1.020	1.407
93	3	7.648	0.093	0.981	1.459
93	4	7.648	0.139	0.942	1.488
93	5	7.648	0.186	0.903	1.504
93	6	7.648	0.232	0.842	1.509
93	7	7.648	0.279	0.903	1.504
93	8	7.648	0.325	0.942	1.488
93	9	7.648	0.371	0.981	1.459
93	10	7.648	0.418	1.020	1.407
93	11	7.648	0.464	1.059	1.294
94	1	7.731	0.000	1.059	1.294
94	2	7.731	0.046	1.020	1.407
94	3	7.731	0.093	0.981	1.459
94	4	7.731	0.139	0.942	1.488
94	5	7.731	0.186	0.903	1.504
94	6	7.731	0.232	0.842	1.509
94	7	7.731	0.279	0.903	1.504
94	8	7.731	0.325	0.942	1.488
94	9	7.731	0.371	0.981	1.459
94	10	7.731	0.418	1.020	1.407
94	11	7.731	0.464	1.059	1.294
95	1	7.815	0.000	1.059	1.294
95	2	7.815	0.046	1.020	1.407
95	3	7.815	0.093	0.981	1.459
95	4	7.815	0.139	0.942	1.489
95	5	7.815	0.186	0.903	1.504
95	6	7.815	0.232	0.843	1.509
95	7	7.815	0.279	0.903	1.504
95	8	7.815	0.325	0.942	1.489
95	9	7.815	0.371	0.981	1.459
95	10	7.815	0.418	1.020	1.407
95	11	7.815	0.464	1.059	1.294
96	1	7.898	0.000	1.059	1.294
96	2	7.898	0.046	1.020	1.407
96	3	7.898	0.093	0.981	1.460
96	4	7.898	0.139	0.943	1.489
96	5	7.898	0.186	0.904	1.504
96	6	7.898	0.232	0.843	1.509
96	7	7.898	0.279	0.904	1.504
96	8	7.898	0.325	0.943	1.489
96	9	7.898	0.371	0.981	1.460
96	10	7.898	0.418	1.020	1.407
96	11	7.898	0.464	1.059	1.294
97	1	7.981	0.000	1.059	1.294
97	2	7.981	0.046	1.021	1.407
97	3	7.981	0.093	0.982	1.460
97	4	7.981	0.139	0.943	1.489
97	5	7.981	0.186	0.904	1.504
97	6	7.981	0.232	0.843	1.509
97	7	7.981	0.279	0.904	1.504
97	8	7.981	0.325	0.943	1.489
97	9	7.981	0.371	0.982	1.460
97	10	7.981	0.418	1.021	1.407
97	11	7.981	0.464	1.059	1.294
98	1	8.065	0.000	1.060	1.295
98	2	8.065	0.046	1.021	1.407
98	3	8.065	0.093	0.982	1.460
98	4	8.065	0.139	0.943	1.489
98	5	8.065	0.186	0.904	1.505
98	6	8.065	0.232	0.843	1.510
98	7	8.065	0.279	0.904	1.505
98	8	8.065	0.325	0.943	1.489
98	9	8.065	0.371	0.982	1.460
98	10	8.065	0.418	1.021	1.407
98	11	8.065	0.464	1.060	1.295
99	1	8.148	0.000	1.060	1.295
99	2	8.148	0.046	1.021	1.407
99	3	8.148	0.093	0.982	1.460
99	4	8.148	0.139	0.943	1.489
99	5	8.148	0.186	0.904	1.505
99	6	8.148	0.232	0.843	1.510
99	7	8.148	0.279	0.904	1.505
99	8	8.148	0.325	0.943	1.489
99	9	8.148	0.371	0.982	1.460
99	10	8.148	0.418	1.021	1.407
99	11	8.148	0.464	1.060	1.295
100	1	8.231	0.000	1.060	1.295
100	2	8.231	0.046	1.021	1.408
100	3	8.231	0.093	0.982	1.460
100	4	8.231	0.139	0.943	1.489
100	5	8.231	0.186	0.904	1.505
100	6	8.231	0.232	0.843	1.510
100	7	8.231	0.279	0.904	1.505
100	8	8.231	0.325	0.943	1.489
100	9	8.231	0.371	0.982	1.460
100	10	8.231	0.418	1.021	1.408
100	11	8.231	0.464	1.060	1.295

Co-ordinates for Grid					
Grid		Co-ordinates			
i	j	x	y	Z_{bottom}	Z_{top}
101	1	8.315	0.000	1.060	1.295
101	2	8.315	0.046	1.021	1.408
101	3	8.315	0.093	0.982	1.460
101	4	8.315	0.139	0.943	1.489
101	5	8.315	0.186	0.904	1.505
101	6	8.315	0.232	0.843	1.510
101	7	8.315	0.279	0.904	1.505
101	8	8.315	0.325	0.943	1.489
101	9	8.315	0.371	0.982	1.460
101	10	8.315	0.418	1.021	1.408
101	11	8.315	0.464	1.060	1.295
102	1	8.398	0.000	1.060	1.295
102	2	8.398	0.046	1.021	1.408
102	3	8.398	0.093	0.982	1.460
102	4	8.398	0.139	0.943	1.490
102	5	8.398	0.186	0.904	1.505
102	6	8.398	0.232	0.843	1.510
102	7	8.398	0.279	0.904	1.505
102	8	8.398	0.325	0.943	1.490
102	9	8.398	0.371	0.982	1.460
102	10	8.398	0.418	1.021	1.408
102	11	8.398	0.464	1.060	1.295
103	1	8.481	0.000	1.060	1.295
103	2	8.481	0.046	1.021	1.408
103	3	8.481	0.093	0.982	1.460
103	4	8.481	0.139	0.944	1.490
103	5	8.481	0.186	0.905	1.505
103	6	8.481	0.232	0.844	1.510
103	7	8.481	0.279	0.905	1.505
103	8	8.481	0.325	0.944	1.490
103	9	8.481	0.371	0.982	1.460
103	10	8.481	0.418	1.021	1.408
103	11	8.481	0.464	1.060	1.295
104	1	8.565	0.000	1.060	1.295
104	2	8.565	0.046	1.021	1.408
104	3	8.565	0.093	0.983	1.461
104	4	8.565	0.139	0.944	1.490
104	5	8.565	0.186	0.905	1.505
104	6	8.565	0.232	0.844	1.510
104	7	8.565	0.279	0.905	1.505
104	8	8.565	0.325	0.944	1.490
104	9	8.565	0.371	0.983	1.461
104	10	8.565	0.418	1.021	1.408
104	11	8.565	0.464	1.060	1.295
105	1	8.648	0.000	1.061	1.296
105	2	8.648	0.046	1.022	1.408
105	3	8.648	0.093	0.983	1.461
105	4	8.648	0.139	0.944	1.490
105	5	8.648	0.186	0.905	1.506
105	6	8.648	0.232	0.844	1.511
105	7	8.648	0.279	0.905	1.506
105	8	8.648	0.325	0.944	1.490
105	9	8.648	0.371	0.983	1.461
105	10	8.648	0.418	1.022	1.408
105	11	8.648	0.464	1.061	1.296

Co-ordinates for Grid					
Grid		Co-ordinates			
i	j	x	y	Z_{bottom}	Z_{top}
106	1	8.731	0.000	1.061	1.296
106	2	8.731	0.046	1.022	1.408
106	3	8.731	0.093	0.983	1.461
106	4	8.731	0.139	0.944	1.490
106	5	8.731	0.186	0.905	1.506
106	6	8.731	0.232	0.844	1.511
106	7	8.731	0.279	0.905	1.506
106	8	8.731	0.325	0.944	1.490
106	9	8.731	0.371	0.983	1.461
106	10	8.731	0.418	1.022	1.408
106	11	8.731	0.464	1.061	1.296
107	1	8.815	0.000	1.061	1.296
107	2	8.815	0.046	1.022	1.409
107	3	8.815	0.093	0.983	1.461
107	4	8.815	0.139	0.944	1.490
107	5	8.815	0.186	0.905	1.506
107	6	8.815	0.232	0.844	1.511
107	7	8.815	0.279	0.905	1.506
107	8	8.815	0.325	0.944	1.490
107	9	8.815	0.371	0.983	1.461
107	10	8.815	0.418	1.022	1.409
107	11	8.815	0.464	1.061	1.296
108	1	8.898	0.000	1.061	1.296
108	2	8.898	0.046	1.022	1.409
108	3	8.898	0.093	0.983	1.461
108	4	8.898	0.139	0.944	1.490
108	5	8.898	0.186	0.905	1.506
108	6	8.898	0.232	0.844	1.511
108	7	8.898	0.279	0.905	1.506
108	8	8.898	0.325	0.944	1.490
108	9	8.898	0.371	0.983	1.461
108	10	8.898	0.418	1.022	1.409
108	11	8.898	0.464	1.061	1.296
109	1	8.981	0.000	1.061	1.296
109	2	8.981	0.046	1.022	1.409
109	3	8.981	0.093	0.983	1.461
109	4	8.981	0.139	0.944	1.491
109	5	8.981	0.186	0.905	1.506
109	6	8.981	0.232	0.844	1.511
109	7	8.981	0.279	0.905	1.506
109	8	8.981	0.325	0.944	1.491
109	9	8.981	0.371	0.983	1.461
109	10	8.981	0.418	1.022	1.409
109	11	8.981	0.464	1.061	1.296
110	1	9.065	0.000	1.061	1.296
110	2	9.065	0.046	1.022	1.409
110	3	9.065	0.093	0.983	1.461
110	4	9.065	0.139	0.944	1.491
110	5	9.065	0.186	0.906	1.506
110	6	9.065	0.232	0.845	1.511
110	7	9.065	0.279	0.906	1.506
110	8	9.065	0.325	0.944	1.491
110	9	9.065	0.371	0.983	1.461
110	10	9.065	0.418	1.022	1.409
110	11	9.065	0.464	1.061	1.296

Co-ordinates for Grid							Co-ordinates for Grid					
Grid		Co-ordinates					Grid		Co-ordinates			
i	j	x	y	Z_{bottom}	Z_{top}		i	j	x	y	Z_{bottom}	Z_{top}
111	1	9.148	0.000	1.061	1.296		116	1	9.565	0.000	1.062	1.297
111	2	9.148	0.046	1.022	1.409		116	2	9.565	0.046	1.023	1.410
111	3	9.148	0.093	0.984	1.462		116	3	9.565	0.093	0.984	1.462
111	4	9.148	0.139	0.945	1.491		116	4	9.565	0.139	0.945	1.491
111	5	9.148	0.186	0.906	1.506		116	5	9.565	0.186	0.906	1.507
111	6	9.148	0.232	0.845	1.511		116	6	9.565	0.232	0.845	1.512
111	7	9.148	0.279	0.906	1.506		116	7	9.565	0.279	0.906	1.507
111	8	9.148	0.325	0.945	1.491		116	8	9.565	0.325	0.945	1.491
111	9	9.148	0.371	0.984	1.462		116	9	9.565	0.371	0.984	1.462
111	10	9.148	0.418	1.022	1.409		116	10	9.565	0.418	1.023	1.410
111	11	9.148	0.464	1.061	1.296		116	11	9.565	0.464	1.062	1.297
112	1	9.231	0.000	1.062	1.297		117	1	9.648	0.000	1.062	1.297
112	2	9.231	0.046	1.023	1.409		117	2	9.648	0.046	1.023	1.410
112	3	9.231	0.093	0.984	1.462		117	3	9.648	0.093	0.984	1.462
112	4	9.231	0.139	0.945	1.491		117	4	9.648	0.139	0.945	1.492
112	5	9.231	0.186	0.906	1.507		117	5	9.648	0.186	0.907	1.507
112	6	9.231	0.232	0.845	1.512		117	6	9.648	0.232	0.846	1.512
112	7	9.231	0.279	0.906	1.507		117	7	9.648	0.279	0.907	1.507
112	8	9.231	0.325	0.945	1.491		117	8	9.648	0.325	0.945	1.492
112	9	9.231	0.371	0.984	1.462		117	9	9.648	0.371	0.984	1.462
112	10	9.231	0.418	1.023	1.409		117	10	9.648	0.418	1.023	1.410
112	11	9.231	0.464	1.062	1.297		117	11	9.648	0.464	1.062	1.297
113	1	9.315	0.000	1.062	1.297		118	1	9.731	0.021	1.091	1.239
113	2	9.315	0.046	1.023	1.409		118	2	9.731	0.064	1.055	1.420
113	3	9.315	0.093	0.984	1.462		118	3	9.731	0.106	1.020	1.467
113	4	9.315	0.139	0.945	1.491		118	4	9.731	0.148	0.985	1.494
113	5	9.315	0.186	0.906	1.507		118	5	9.731	0.190	0.949	1.508
113	6	9.315	0.232	0.845	1.512		118	6	9.731	0.232	0.948	1.512
113	7	9.315	0.279	0.906	1.507		118	7	9.731	0.274	0.949	1.508
113	8	9.315	0.325	0.945	1.491		118	8	9.731	0.316	0.985	1.494
113	9	9.315	0.371	0.984	1.462		118	9	9.731	0.359	1.020	1.467
113	10	9.315	0.418	1.023	1.409		118	10	9.731	0.401	1.055	1.420
113	11	9.315	0.464	1.062	1.297		118	11	9.731	0.443	1.091	1.239
114	1	9.398	0.000	1.062	1.297		119	1	9.815	0.043	1.119	1.266
114	2	9.398	0.046	1.023	1.409		119	2	9.815	0.081	1.088	1.429
114	3	9.398	0.093	0.984	1.462		119	3	9.815	0.118	1.056	1.472
114	4	9.398	0.139	0.945	1.491		119	4	9.815	0.156	1.024	1.496
114	5	9.398	0.186	0.906	1.507		119	5	9.815	0.194	1.000	1.508
114	6	9.398	0.232	0.845	1.512		119	6	9.815	0.232	1.000	1.513
114	7	9.398	0.279	0.906	1.507		119	7	9.815	0.270	1.000	1.508
114	8	9.398	0.325	0.945	1.491		119	8	9.815	0.308	1.024	1.496
114	9	9.398	0.371	0.984	1.462		119	9	9.815	0.346	1.056	1.472
114	10	9.398	0.418	1.023	1.409		119	10	9.815	0.384	1.088	1.429
114	11	9.398	0.464	1.062	1.297		119	11	9.815	0.422	1.119	1.266
115	1	9.481	0.000	1.062	1.297		120	1	9.898	0.064	1.148	1.292
115	2	9.481	0.046	1.023	1.410		120	2	9.898	0.098	1.120	1.439
115	3	9.481	0.093	0.984	1.462		120	3	9.898	0.131	1.092	1.477
115	4	9.481	0.139	0.945	1.491		120	4	9.898	0.165	1.063	1.498
115	5	9.481	0.186	0.906	1.507		120	5	9.898	0.199	1.052	1.509
115	6	9.481	0.232	0.845	1.512		120	6	9.898	0.232	1.052	1.513
115	7	9.481	0.279	0.906	1.507		120	7	9.898	0.266	1.052	1.509
115	8	9.481	0.325	0.945	1.491		120	8	9.898	0.299	1.063	1.498
115	9	9.481	0.371	0.984	1.462		120	9	9.898	0.333	1.092	1.477
115	10	9.481	0.418	1.023	1.410		120	10	9.898	0.367	1.120	1.439
115	11	9.481	0.464	1.062	1.297		120	11	9.898	0.400	1.148	1.292

Co-ordinates for Grid					
Grid		Co-ordinates			
i	j	x	y	Z_{bottom}	Z_{top}
121	1	9.981	0.085	1.176	1.319
121	2	9.981	0.115	1.152	1.449
121	3	9.981	0.144	1.127	1.482
121	4	9.981	0.173	1.104	1.500
121	5	9.981	0.203	1.104	1.510
121	6	9.981	0.232	1.104	1.513
121	7	9.981	0.261	1.104	1.510
121	8	9.981	0.291	1.104	1.500
121	9	9.981	0.320	1.127	1.482
121	10	9.981	0.349	1.152	1.449
121	11	9.981	0.379	1.176	1.319
122	1	10.065	0.107	1.205	1.346
122	2	10.065	0.132	1.184	1.458
122	3	10.065	0.157	1.163	1.486
122	4	10.065	0.182	1.157	1.502
122	5	10.065	0.207	1.157	1.510
122	6	10.065	0.232	1.157	1.513
122	7	10.065	0.257	1.157	1.510
122	8	10.065	0.282	1.157	1.502
122	9	10.065	0.307	1.163	1.486
122	10	10.065	0.332	1.184	1.458
122	11	10.065	0.357	1.205	1.346
123	1	10.148	0.128	1.234	1.372
123	2	10.148	0.149	1.216	1.468
123	3	10.148	0.170	1.209	1.491
123	4	10.148	0.191	1.209	1.504
123	5	10.148	0.211	1.209	1.511
123	6	10.148	0.232	1.209	1.513
123	7	10.148	0.253	1.209	1.511
123	8	10.148	0.274	1.209	1.504
123	9	10.148	0.294	1.209	1.491
123	10	10.148	0.315	1.216	1.468
123	11	10.148	0.336	1.234	1.372
124	1	10.231	0.150	1.263	1.400
124	2	10.231	0.167	1.263	1.478
124	3	10.231	0.183	1.263	1.496
124	4	10.231	0.199	1.263	1.506
124	5	10.231	0.216	1.263	1.511
124	6	10.231	0.232	1.263	1.513
124	7	10.231	0.248	1.263	1.511
124	8	10.231	0.265	1.263	1.506
124	9	10.231	0.281	1.263	1.496
124	10	10.231	0.297	1.263	1.478
124	11	10.231	0.314	1.263	1.400